Progress Report

July 1, 1996 through December 31, 1996

NASA-UVA LIGHT AEROSPACE ALLOY AND STRUCTURES TECHNOLOGY PROGRAM (LA^2ST)

NASA-LaRC Grant NAG-1-745

Submitted to:

National Aeronautics and Space Administration
Langley Research Center
Hampton, Virginia 23681-0001

Attention:

Mr. Neil Price
Grants Officer
MS 126

For Review by:

Mr. Dennis L. Dicus
Grant Monitor
Metallic Materials Branch, MS 188A

Submitted by:

Richard P. Gangloff
Professor
Edgar A. Starke, Jr.
University Professor

Department of Materials Science and Engineering
School of Engineering and Applied Science
University of Virginia

Report No. UVA/528266/MS97/121
February 1997

SCHOOL OF
ENGINEERING
& APPLIED SCIENCE

University of Virginia
Thornton Hall
Charlottesville, VA 22903

UNIVERSITY OF VIRGINIA
School of Engineering and Applied Science

The University of Virginia's School of Engineering and Applied Science has an undergraduate enrollment of approximately 1,500 students with a graduate enrollment of approximately 600. There are 160 faculty members, a majority of whom conduct research in addition to teaching.

Research is a vital part of the educational program and interests parallel academic specialties. These range from the classical engineering disciplines of Chemical, Civil, Electrical, and Mechanical and Aerospace to newer, more specialized fields of Applied Mechanics, Biomedical Engineering, Systems Engineering, Materials Science, Nuclear Engineering and Engineering Physics, Applied Mathematics and Computer Science. Within these disciplines there are well equipped laboratories for conducting highly specialized research. All departments offer the doctorate; Biomedical and Materials Science grant only graduate degrees. In addition, courses in the humanities are offered within the School.

The University of Virginia (which includes approximately 2,000 faculty and a total of full-time student enrollment of about 17,000), also offers professional degrees under the schools of Architecture, Law, Medicine, Nursing, Commerce, Business Administration, and Education. In addition, the College of Arts and Sciences houses departments of Mathematics, Phyics, Chemistry and others relevant to the engineering research program. The School of Engineering and Applied Science is an integral part of this University community which provides opportunities for interdisciplinary work in pursuit of the basic goals of education, research, and public service.

NASA-UVA LIGHT AEROSPACE ALLOY AND STRUCTURES TECHNOLOGY PROGRAM

LA^2ST

Program Directors:

Edgar A. Starke, Jr.
Richard P. Gangloff

Co-principal Investigators:

Robert G. Kelly
John R. Scully
Gary J. Shiflet
Glenn E. Stoner
John A. Wert

NASA-LaRC Grant Monitor:

Dennis L. Dicus

SEAS Report No. UVA/528266/MSE97/121
February 1997

Copy No.____

TABLE OF CONTENTS

TABLE OF CONTENTS (continued)

NASA-UVa LIGHT AEROSPACE ALLOY AND STRUCTURES TECHNOLOGY PROGRAM *(LA²ST)*

Executive Summary

The NASA-UVa Light Aerospace Alloy and Structures Technology (LA^2ST) Program was initiated in 1986 and continues with a high level of activity. Projects are being conducted by graduate students and faculty advisors in the Department of Materials Science and Engineering at the University of Virginia. This work is funded by the NASA-Langley Research Center under Grant NAG-1-745. Here, we report on progress achieved between July 1 and December 31, 1996.

The objective of the LA^2ST Program is to conduct interdisciplinary graduate student research on the performance of next generation, light-weight aerospace alloys, composites and thermal gradient structures in collaboration with NASA-Langley researchers. Specific technical objectives are presented for each research project. We generally aim to produce relevant data and basic understanding of material mechanical response, environmental/corrosion behavior, and microstructure; new monolithic and composite alloys; advanced processing methods; new solid and fluid mechanics analyses; measurement and modeling advances; and a pool of educated graduate students for aerospace technologies.

The accomplishments presented in this report are summarized as follows.

- Three research areas are being actively investigated, including: (1) Mechanical and Environmental Degradation Mechanisms in Advanced Light Metals, (2) Aerospace Materials Science, and (3) Mechanics of Materials for Light Aerospace Structures.
- Eleven research projects are being conducted by 8 Ph.D. and 2 M.S. level graduate students, 2 post doctoral fellows and 7 faculty members. Each project is planned and executed in conjunction with a specific branch and technical monitor at NASA-LaRC.
- One undergraduate was recruited to conduct research in the Metallic Materials Branch at NASA- LaRC during the Summer of 1996. No undergraduates are currently participating in LA^2ST research at UVa.

- Collective accomplishments between July and December of 1996 include: 8 journal or proceedings publications, 1 NASA progress report, 6 presentations at national technical meetings. The LA^{2}ST totals since 1986 are 125 publications (83 archival journal or book publications), 24 Ph.D. dissertations or M.S. theses, 122 external technical presentations, 20 NASA progress reports, and 4 NASA Contractor Reports. Since 1986, 36 graduate students, including 33 citizens of the United States, have been involved with LA^{2}ST research; 24 have received the M.S. or Ph.D. degree. Six post-doctoral research associates have participated in LA^{2}ST research. A total of 13 different faculty have worked on the LA^{2}ST program.

Summary of Recent Results

Research on the elevated temperature fracture toughness of advanced Al-Cu-Mg-Ag alloys establishes that C416 (a low Cu variant of AA2519+Mg+Ag) exhibits superior initiation and growth toughnesses, due to a lower volume fraction of large undissolved Al_2Cu constituents. SEM fractography and modeling of particle/matrix decohesion suggest that void nucleation at dipsersoids is repressed at elevated temperatures. The fracture strain of AA2519+Mg+Ag rises with temperature because reduced void nucleation at dispersoids at elevated temperatures delays void-sheet coalescence and enables strain accumulation through void growth. (Project #1)

Research on the transition from localized corrosion to the initiation of stress corrosion cracking in AA2096 revealed a susceptibility to SCC in underaged 4, 6, and 8 hours tempers exposed to alternate immersion in 0.6 M NaCl. Investigation of the differing corrosion characteristics and morphology of AA2096 in these susceptible tempers exposed to alternate immersion compared to pre-exposure testing in $NaCl/CO_2$ is ongoing. Measurement of repassivation potentials revealed higher E_{RP} for AA2096 T3 compared to underaged tempers but no statistical differences between the various underaged tempers. Galvanostatic/potentiostatic experiments used to "dial-in" pit sizes revealed that it is likely that any loss in breaking load strength in tensile specimens pre-exposed to $NaCl/CO_2$ is solely due to the formation of the pit and not due to SCC. (Project #2)

Windows of SCC susceptibility are being defined for AA 2096 in various tempers. AA 2096 extrusions resist SCC in the T3 and underaged 12 hours and T8 tempers in alternate immersion SCC testing. In contrast, a window of SCC susceptibility is observed in the 4 to 8 h underaged conditions when isothermally aged at 160°C. In contrast, careful examination of AA 2090 reveals susceptibility in both underaged and T8 tempers. (Project #3)

Results to date indicate that the occluded solution that develops inside riveted joints on aircraft contain a wide variety of ionic species, leaving open to question the applicability to life prediction of corrosion test results in simple sodium chloride solutions. (Project #5)

Comprehensive compression and texture tests have been completed for multiple directions in several regions of the three extrusions. In all regions, the yield anisotropy is accurately predicted by the inclusion models and the given texture. A strong understanding of the role that matrix and precipitate effects play in the total plastic anisotropy of aluminum alloys has been achieved. (Project #6)

Research on time-cycle-dependent environmental fatigue in 7000-series aluminum alloys demonstrated that chromate addition to NaCl solution eliminated beneficial corrosion-product induced crack closure at low loading frequencies, but reduced substantially fatigue crack propagation rates for 7075-T651 and T7351 (S-L orientation) stressed at intermediate frequencies where closure was less important. A new adjusted compliance ratio method reduced scatter, associated with the global offset-method to measure closure load, but yielded closure levels that were inconsistent with predictions of Newman's plasticity model at Paris-regime ΔK/low R conditions. (Project #8)

INTRODUCTION

Background

In 1986 the Metallic Materials Branch in the Materials Division of the NASA-Langley Research Center initiated sponsorship of graduate student engineering and scientific research in the Department of Materials Science and Engineering at the University of Virginia[1]. This work

emphasized the mechanical and corrosion behavior of light aerospace alloys, particularly Al-Li-Cu based compositions, in aggressive aerospace environments[2-4].

In the Fall of 1988, the scope of this program increased to incorporate research on the development and processing of advanced aerospace materials[5]. Additional funding was provided by the Metallic Materials and Mechanics of Materials Branches at NASA-LaRC. In early 1989 the program was further enhanced to include interdisciplinary work on solid mechanics and thermal structures, with funding from several Divisions within the Structures Directorate at NASA-LaRC[6]. The Departments of Civil Engineering (Applied Mechanics Program) and Mechanical and Aerospace Engineering participated in this expanded program. With this growth, the NASA-UVa Light Aerospace Alloy and Structures Technology Program (or LA^{2}ST Program) was formed within the School of Engineering and Applied Science at UVa.

Since 1989, the LA^{2}ST program has operated with full participation from 6 to 13 faculty and 10 to 15 graduate students, yearly, as outlined in the last 13 progress reports[7-21] and seven grant renewal proposals[22-28]. Seven 2-day Grant Review Meetings have been held in July at the Langley Research Center, with over 25 faculty and graduate students from UVa participating at each meeting[9,11,13,15,17,19,21]. Since 1990, undergraduate engineering students have been involved in research projects at both NASA-LaRC and UVa.

In October of 1991, E.A. Starke proposed a substantial enhancement to the base LA^{2}ST Program[30,31]. The objective of this supplement was to involve UVa faculty with engineering scientists from aluminum alloy producers and airframe manufacturers in a broad research program to develop aluminum alloys and composites for elevated temperature High Speed Civil Transport applications. This research began in January of 1992 and the results are separately reported. The LA^{2}ST and HSCT activities were merged in 1995[27], however, the progress report for the HSCT component of the program is being published separately from this report.

Problem and Needs

Future aerospace structures require high performance light alloys and metal matrix composites with associated processing and fabrication techniques; new structural design methods and concepts with experimental evaluations; component reliability/ durability/damage tolerance

prediction procedures; and a pool of masters and doctoral level engineers and scientists. Work on advanced materials and structures must be interdisciplinary and integrated. The thermal and chemical effects of aerospace environments on light metals and composites are particularly important to material performance. Nationally, academic efforts in these areas are limited. The NASA-UVa LA^{2}ST Program addresses these needs.

LA^{2}ST Program

As detailed in the original proposal[6] and affirmed in the most recent renewal[29], faculty from the Departments of Materials Science and Engineering, Mechanical and Aerospace Engineering, and Civil Engineering and Applied Mechanics at UVa have participated in the LA^{2}ST research and education program focused on high performance, light weight, aerospace alloys and structures. We aim to develop long term and interdisciplinary collaborations between graduate students, UVa faculty, and NASA-Langley researchers.

Our research efforts are producing basic understanding of materials performance, new monolithic and composite alloys, advanced processing methods, solid and fluid mechanics analyses, measurement advances, and new methods for modeling material microstructure and properties. A major product of the LA^{2}ST program is graduate students with interdisciplinary education and research experience in materials science, mechanics and mathematics. These advances should enable various NASA technologies.

The scope of the LA^{2}ST Program is broad. Three research areas are being investigated, including:

- Mechanical and Environmental Degradation Mechanisms in Advanced Light Metals and Composites,
- Aerospace Materials Science,
- Mechanics of Materials for Light Aerospace Structures.

Eleven research projects within these areas were active during this report period, and six are reported here. Three, which are concerned with the HSCT are reported under separate cover. These projects involve seven faculty, and ten graduate students. Eighty pct of the graduate

students are currently at the doctoral level (8 of 10), nine of ten are citizens of the United, and two are conducting all research at the Langley Research Center. In each case the research provides the basis for the thesis or dissertation requirement of graduate studies at the University of Virginia. Each project is developed in conjunction with a specific LaRC researcher. Research is conducted at either UVa or LaRC, and under the guidance of UVa faculty and NASA staff. Participating students and faculty are closely identified with a NASA-LaRC branch.

Technology Transfer

Method for Increasing the Corrosion Resistance of Aluminum and Aluminum Alloys. U.S. Patent # 5,266,356. (Patent re-issued October 1996). Inventors: Roudolph G. Buchheit and Glenn E. Stoner.

This invention was the outcome of research sponsored by the UVA-NASA Grant concerning the mechanism of stress corrosion cracking of advanced aluminum lithium alloys. The research accidentally led to the discovery that under certain circumstances, the presence of lithium ions, carbon dioxide (or carbonates) and an elevated pH environment led to the formation of a precipitate/coating on the aluminum alloy which was extremely protective. The main application for this coating (a form of conversion coating) is to provide a non-toxic alternative to chromate coatings which have health and environmental consequences in the areas of metal finishing. This is especially true in the aerospace industry where metal finishing for corrosion control is responsible for up to 90% of the pollution in that industry. The invention has been the subject of ongoing research at Sandia National Laboratory and the University of Virginia. Sponsors include DOE Inventions Program at UVA and DARPA at UVA and Sandia. Sandia has also provided considerable funding for use inside that agency for programs related to National Defense. The invention is currently Licensed through the Virginia Center for Innovative Technology (CIT) to Clariant Corporation of Charlotte, NC. Clariant Corporation is also a participant in the current DARPA program. It is anticipated that the coating system will be marketed as a chromate free conversion coating for aluminum alloys used in architectural, automotive, beverage container, and aerospace applications.

Corrosion Processes in Aging Aircraft - Robert G. Kelly

In order to develop life prediction strategies for aging aircraft, the corrosion processes occurring in occluded regions such as lap splice joints must be characterized and modeled. The characterization of the corrosive solutions that develop inside these regions during service is a necessary first step. Cooperative work between NASA/LaRC and UVa is aimed at developing such an understanding. NASA/LaRC personnel are collecting samples which are analyzed at UVa for the corrosive species. Once the types of species present and their relative concentrations are determined, a coordinated experimental and modeling approach will be used to develop more accurate estimations of aircraft service life. These results will have important applications in both the civilian and military fleets.

Organization of Progress Report

This progress report first provides LA^{2}ST Program administrative information including statistics on the productivity of faculty and graduate student participants, a history of current and graduated students, refereed or archival publications, and a list of ongoing projects with NASA and UVa advisors.

Six sections summarize the technical accomplishments of each research project, emphasizing the period from July 1 to December 31, 1996. Each section contains a brief narrative of objective, recent progress, conclusions and immediate milestones. Appendices I through III document grant-sponsored publications, conference participation and citations of all LA^{2}ST Progress Reports produced since 1986.

References

1. R.P. Gangloff, G.E. Stoner and M.R. Louthan, Jr., "Environment Assisted Degradation Mechanisms in Al-Li Alloys", University of Virginia, Proposal No. MS-NASA/LaRC-3545-87, October, 1986.

2. R.P. Gangloff, G.E. Stoner and R.E. Swanson, "Environment Assisted Degradation Mechanisms in Al-Li Alloys", University of Virginia, Report No. UVA/528266/MS88 /101, January, 1988.

3. R.P. Gangloff, G.E. Stoner and R.E. Swanson, "Environment Assisted Degradation Mechanisms in Advanced Light Metals", University of Virginia, Report No. UVA/528266/MS88/102, June, 1988.

4. R.P. Gangloff, G.E. Stoner and R.E. Swanson, "Environment Assisted Degradation Mechanisms in Advanced Light Metals", University of Virginia, Report No. UVA/528266/MS89/103, January, 1989.

5. T.H. Courtney, R.P. Gangloff, G.E. Stoner and H.G.F. Wilsdorf, "The NASA-UVa Light Alloy Technology Program", University of Virginia, Proposal No. MS NASA/LaRC-3937-88, March, 1988.

6. R.P. Gangloff, "NASA-UVa Light Aerospace Alloy and Structures Technology Program", University of Virginia, Proposal No. MS NASA/LaRC-4278-89, January, 1989.

7. R.P. Gangloff, "NASA-UVa Light Aerospace Alloy and Structures Technology Program", University of Virginia, Report No. UVA/528266/MS90/104, August, 1989.

8. R.P. Gangloff, "NASA-UVa Light Aerospace Alloy and Structures Technology Program", University of Virginia, Report No. UVA/528266/MS90/105, December, 1989.

9. R.P. Gangloff, "NASA-UVa Light Aerospace Alloy and Structures Technology Program", UVa Report No. UVA/528266/MS90/106, June, 1990.

10. R.P. Gangloff, "NASA-UVa Light Aerospace Alloy and Structures Technology Program", UVa Report No. UVA/528266/MS91/107, January, 1991.

11. R.P. Gangloff, "NASA-UVa Light Aerospace Alloy and Structures Technology Program", UVa Report No. UVA/528266/MS91/108, July, 1991.

12. R.P. Gangloff, "NASA-UVa Light Aerospace Alloy and Structures Technology Program", UVa Report No. UVA/528266/MS92/109, January, 1992.

13. R.P. Gangloff, "NASA-UVa Light Aerospace Alloy and Structures Technology Program", UVa Report No. UVA/528266/MS93/111, July, 1992.

14. R.P. Gangloff, "NASA-UVa Light Aerospace Alloy and Structures Technology Program", UVa Report No. UVA/528266/MSE93/112, March, 1993.

15. R.P. Gangloff, "NASA-UVa Light Aerospace Alloy and Structures Technology Program", UVa Report No. UVA/528266/MSE93/113, July, 1993.

16. R.P. Gangloff, "NASA-UVa Light Aerospace Alloy and Structures Technology Program", UVa Report No. UVA/528266/MSE93/114, March, 1994.

17. R.P. Gangloff, "NASA-UVa Light Aerospace Alloy and Structures Technology Program," UVA Report No. UVA/528266/MSE94/116, July, 1994.

18. E.A. Starke, Jr. and R.P. Gangloff, "NASA-UVa Light Aerospace Alloy and Structures Technology Program", UVa Report No. UVA/528266/MSE94/117, March, 1995.

19. R.P. Gangloff, and E.A. Starke, Jr., "NASA-UVa Light Aerospace Alloy and Structures Technology Program", UVa Report No. UVA/528266/MS95/118, July, 1995.

20. R.P. Gangloff, and E.A. Starke, Jr., "NASA-UVa Light Aerospace Alloy and Structures Technology Program", UVa Report No. UVA/528266/MS95/119, January, 1996.

21. R.P. Gangloff, and E.A. Starke, Jr., "NASA-UVa Light Aerospace Alloy and Structures Technology Program", UVa Report No. UVA/528266/MS96/120, June, 1996.

22. R.P. Gangloff, "NASA-UVa Light Aerospace Alloy and Structures Technology Program", University of Virginia, Proposal No. MS- NASA/LaRC-4512-90, November, 1989.

23. R.P. Gangloff, "NASA-UVa Light Aerospace Alloy and Structures Technology Program", University of Virginia, Proposal No. MS- NASA/LaRC-4841-91, September, 1990.

24. R.P. Gangloff, "NASA-UVa Light Aerospace Alloy and Structures Technology Program", University of Virginia, Proposal No. MS- NASA/LaRC-5219-92, October, 1991.

25. R.P. Gangloff, "NASA-UVa Light Aerospace Alloy and Structures Technology Program", University of Virginia, Proposal No. MSE- NASA/LaRC-5691-93, November, 1992.

26. R.P. Gangloff, "NASA-UVa Light Aerospace Alloy and Structures Technology Program", Proposal No. MSE-NASA/LaRC-6074-94, University of Virginia, Charlottesville, VA, November, 1993.

27 R. P. Gangloff and E. A. Starke, Jr., "NASA-UVa Light Aerospace Alloy and Structures Technology Program", Proposal No. MSE-NASA/LaRC-6478-95, University of Virginia, Charlottesville, VA, November, 1994.

28. R.P. Gangloff and E.A. Starke, Jr., "NASA-UVA Light Aerospace Alloy and Structures Technology Program", Proposal No. MSE-NASA/LaRC-6855-96, University of Virginia, Charlottesville, VA, October, 1995.

29. R.P. Gangloff and E.A. Starke, Jr., "NASA-UVA Light Aerospace Alloy and Structures Technology Program", Proposal No. MSE-NASA/LaRC-7272-97, University of Virginia, Charlottesville, VA, October, 1996.

30. R.P. Gangloff, E.A. Starke, Jr., J.M. Howe and F.E. Wawner, "NASA-UVa Light Aerospace Alloy and Structures Technology Program: Supplement on Aluminum Based Materials for High Speed Aircraft", University of Virginia, Proposal No. MS NASA/LaRC-5215-92, October, 1991.

31. R.P. Gangloff, E.A. Starke, Jr., J.M. Howe and F.E. Wawner, "NASA-UVa Light Aerospace Alloy and Structures Technology Program: Supplement on Aluminum Based Materials for High Speed Aircraft", University of Virginia, Proposal No. MSE NASA/LaRC-5691-93, November, 1992.

SUMMARY STATISTICS

Table I documents the numbers of students and faculty who have participated in the LA^{2}ST Program, both during this reporting period and since program inception in 1986. Academic and research accomplishments are indicated by the degrees awarded, publications and presentations. Graduate students and research associates who participated in the LA^{2}ST Program are named in Tables II and III, respectively.

TABLE I: LA^{2}ST Program Statistics

	Current 7/1/96 to 12/31/96	Cumulative 1986 to 12/31/96
PhD Students--UVa:	7	23
--NASA-LaRC:	1	1
MS Students--UVa:	1	10
--NASA:	1	1
--VPI:	0	1
Undergraduates--UVa:	0	9
--NASA-LaRC:	1	16
Faculty--UVa:	7	13
--VPI:	0	1
Research Associates--UVa:	1	7
Ph.D. Awarded:	0	17
M.S. Awarded:	0	7
Employers--NASA:	0	4
--Federal:	0	4
--University:	0	1
--Industry:	0	8
--Next degree:	0	5
Publications:	8	125

TABLE I: LA²ST Program Statistics (continued)

	Current 7/1/96 to 12/31/96	Cumulative 1986 to 12/31/96
Presentations:	6	122
Dissertations/Theses:	0	24
NASA Reports:	1	24

TABLE II

GRADUATE STUDENT PARTICIPATION IN THE NASA-UVa LA²ST PROGRAM

June, 1996

POS #	GRADUATE STUDENT EMPLOYER	ENTERED PROGRAM	DEGREE COMPLETED	LANGLEY RESIDENCY	RESEARCH TOPIC	UVa/NASA-LaRC ADVISORS
1.	R. S. Piascik NASA-Langley	6/86	Ph.D. 10/89		Damage Localization Mechanisms in Corrosion Fatigue of Aluminum-Lithium Alloys	R. P. Gangloff D. L. Dicus
2.	J. P. Moran NIST	9/88	Ph.D. 12/89		An Investigation of the Localized Corrosion and Stress Corrosion Cracking Behavior of Alloy 2090	G. E. Stoner W. B. Lisagor
3.	R. G. Buchheit Sandia National Laboratories	6/87	Ph.D. 12/90		Measurements and Mechanisms of Localized Aqueous Corrosion in Aluminum-Lithium Alloys	G. E. Stoner D. L. Dicus
4.	D. B. Gundel Ph.D.-UVa	9/88	M.S. 12/90		Investigation of the Reaction Kinetics Between SiC Fibers and Titanium Matrix Composites	F. E. Wawner W. B. Brewer
5.	F. Rivet (VPI)	9/88	M.S. 12/90		Deformation and Fracture of Aluminum-Lithium Alloys: The Effect of Dissolved Hydrogen	R. E. Swanson (VPI) D. L. Dicus
6.	C. Copper Ph.D.-UVa	4/89	M.S. 12/90		Design of Cryogenic Tanks for Space Vehicles	W. D. Pilkey J. K. Haviland D. R. Rummler M.J. Shuart
7.	J. A. Wagner NASA-Langley	6/87	Ph.D.	PhD Research @ LaRC	Temperature Effects on the Deformation and Fracture of Al-Li-Cu-In Alloys	R. P. Gangloff W. B. Lisagor J. C. Newman
8.	W. C. Porr, Jr. David Taylor Naval Ship R&DC	1/88	Ph.D. 6/92		Elevated Temperature Facture of an Advanced Powder Metallurgy Aluminum Alloy	R. P. Gangloff C. E. Harris
9.	J. B. Parse Consultant	9/88	Ph.D. 6/92		Quantitative Characterization of the Spatial Distribution of Particles in Materials	J. A. Wert D. R. Tenney
10.	D. C. Slavik Knolls Atomic Power Lab	9/89	Ph.D. 6/93		Environment Enhanced Fatigue of Advanced Aluminum Alloys and Composites	R. P. Gangloff D. L. Dicus

TABLE II (continued)
GRADUATE STUDENT PARTICIPATION IN THE NASA-UVa LA²ST PROGRAM
(continued)

POS #	GRADUATE STUDENT EMPLOYER	ENTERED PROGRAM	DEGREE COMPLETED	LANGLEY RESIDENCY	RESEARCH TOPIC	UVa/NASA-LaRC ADVISORS
11.	C. L. Lach NASA-Langley	9/89	M.S.	MS Research @LaRC	Effect of Temperature on the Fracture Toughness of Weldalite™ 049	R. P. Gangloff W. B. Lisagor
12.	R. J. Kilmer General Motors	11/89	Ph.D. 9/93		Effect of Zn Additions on the Environmental Stability of Alloy 8090	G. E. Stoner W.B. Lisagor
13.	M. F. Coyle Pennsylvania State Univ. York Campus, Mech. Eng.	12/89	Ph.D. 5/95		Visoplastic Response of High Temperature Structures	E. A. Thornton J. H. Starnes, Jr.
14.	C. J. Lissenden University of Kentucky; Engineering Mechanics	9/90	Ph.D. 6/93		Inelastic Response of Metal Matrix Composites Under Biaxial Loading	C. T. Herakovich M. J. Pindera W. S. Johnson
15.	C. Cooper AMP Incorporated	1/91	Ph.D. 6/93		Shell Structures Analytical Modeling	W. D. Pilkey J. K. Haviland M. Shuart J. Stroud
16.	Douglas Wall Babcock & Wilcox	4/91	Ph.D. 1/96		Measurements and Mechanisms of Localized Corrosion in Al-Li-Cu Alloys	G. E. Stoner D. L. Dicus
17.	S. W. Smith NASA-LaRC	4/91	Ph.D. 5/95		Hydrogen Interactions with Al-Li Alloys	J. R. Scully W. B. Lisagor
18.	D. B. Gundel Wright Laboratories US Air Force	4/91	Ph.D. 9/94		Effect of Thermal Exposure on the Mechanical Properties of Titanium/ SiC Composites	F. E. Wawner W. B. Brewer
19.	K. McCarthy	5/91	M.S. 6/93 (Nonthesis)		Shell Structures Analytical Modeling	W. D. Pilkey M. J. Shuart J. Stroud
20.	M. Lyttle	12/91	M.S. 12/93		Superplasticity in Al-Li-Cu Alloys	J. A. Wert T. T. Bales
21.	T. Johnson NASA-LaRC	12/91	Ph.D. 6/93	(NASA Minority Grantee)	Shell Structures Analytical Modeling	W. D. Pilkey M. J. Shuart J. Stroud

TABLE II (continued)
GRADUATE STUDENT PARTICIPATION IN THE NASA-UVa LA²ST PROGRAM
(continued)

POS #	GRADUATE STUDENT EMPLOYER	ENTERED PROGRAM	DEGREE COMPLETED	LANGLEY RESIDENCY	RESEARCH TOPIC	UVa/NASA-LaRC ADVISORS
22.	S. T. Pride Rohm and Haas	12/91	Ph.D. 6/94	(NASA Minority Grantee)	Metastable Pitting of Al Alloys	J. R. Scully D. L. Dicus
23.	M. A. Rowley	1/92	M.S. 12/93	(UVa AEP Sponsored)	Viscoplasticity of Metals	E. A. Thornton J. H. Starnes, Jr.
24.	M. J. Haynes	9/92	M.S./Ph.D. 5/94		Elevated Temperature Fracture of Advanced	R. P. Gangloff W.B. Lisagor
25.	M. Mason Allied Signal	9/92	M.S. 11/94		Environmental Effects in Fatigue Life Prediction	R. P. Gangloff R. S. Piascik
26.	H. J. Koenigsmann UVa	6/93	Ph.D. 5/96		Precipitation Hardening and Microstructural Stability in Al-Si-Ge-Cu	E.A. Starke, Jr. W.B. Lisagor
27.	E. Richey PhD-UVa	9/93	M.S. 5/95		Computer Modeling of Environmental Fatigue Crack Propagation	R.P. Gangloff R.S. Piascik
28.	M. Lyttle	1/94	Ph.D.		Wide-Panel Aluminum Alloy Extrusions	J.A. Wert W.B. Lisagor
29.	Z. Gasem	1/94	Ph.D.		Time-Dependent Environmental Fatigue in 7000-Series Al Alloys	R.P. Gangloff R.S. Piascik
30.	S. P. Hayes	9/94	Ph.D.		Temperature and Hydrogen-Effects on Fracture in Ti Alloys	R.P. Gangloff W. Brewer
31.	S. M. Kazanjian	12/94	Ph.D.		Temperature and Microstructure Effects on Fracture in Ti Alloys	E.A. Starke, Jr. D.L. Dicus
32.	R. D. Schroedter, III Customer Management Services	6/93	Ph.D. 1/96		Damage Evolution in Polymeric Composites	C.T. Herakovich C.E. Harris
33.	K. L. Eklund	8/95	Ph.D. (left program 11/96)		Metallurgical Factors Controlling SCC in A2096 and C155	J.R. Scully M.S. Domack

TABLE II (continued)
GRADUATE STUDENT PARTICIPATION IN THE NASA-UVa LA²ST PROGRAM
(continued)

34.	B.J. Connolly	1/96	Ph.D.	Localized Corrosion and Stress Corrosion Crack Initation in Advanced Al-Li-Cu Alloys	G. Stoner J.R. Scully M.S. Domack
35.	L.A. Pawlick	12/96	Ph.D.	Metallurgical Factors Controlling Stress Corrosion Cracking in AA2096 and C155	J.R. Scully M. Domack W.B. Lisagor
36.	K.S. Lewis	8/96	M.S.	Determination of the Corrosive Species Found Within Aircraft Lap-Splice Joints	R.G. Kelly R.S. Piascik

TABLE III

Post-Doctoral Research Associate Participation
in NASA-UVA LA²ST Program
June, 1996

Pos #	Research Assoc.	Tenure	Research	Supervisor
1.	Yang Leng	3/89 to 12/91	Elevated Temperature Deformation and Fracture of PM AL Alloys and Composites	R. P. Gangloff
2.	Farshad Mizadeh	7/89 to 12/91	Deformation of Metal Matrix Composites	C. T. Herakovich Marek-Jerzy Pindera
3.	A. K. Mukhopadhyay	6/91 to 6/92	Aluminum Alloy Development	E. A. Starke, Jr.
4.	Sang-Shik Kim	12/91 to 2/94	Environmental Fatigue Life Prediction	R. P. Gangloff
5.	B. Skrotzki	1/95 to 9/95	Mechanical Property Anisotropy	E. A. Starke, Jr. G. J. Shiflet
6.	H. Hargarter	8/95	Mechanical Property Anisotropy	E. A. Starke, Jr. G. J. Shiflet
			Temperature and Microstructure Effects on Fracture in Ti Alloys	E. A. Starke, Jr.
7.	M. Inman	5/96	Localized Solution Chemistry in Al Alloys	R.G. Kelly

GRANT PUBLICATIONS: (REFEREED JOURNALS, ARCHIVAL VOLUMES AND NASA CONTRACTOR REPORTS)

The following papers are based on research conducted under LA^{2}ST Program support, and are published in the referred or archival literature.

83. Bin Wu, J.R. Scully, A.S. Mikhailov, J.L. Hudson, "Cooperative Stochastic Behavior in Localized Corrosion: I. Model", submitted to J. Electrochem. Soc., August 1996.

82. T.T. Lunt, S.T. Pride, J.R. Scully, A.S. Mikhailov, J.L. Hudson, "Cooperative Stochastic Behavior in Localized Corrosion: II. Experiments", submitted to J. Electrochem. Soc., August 1996.

81. R.J. Kilmer, S.W. Smith, J.R. Scully, and G.E. Stoner, "Effect of Aging Time on Aqueous Stress Corrosion and Internal Hydrogen Embrittlement in Al-Li-Cu Alloys" submitted to Metall. Trans., September, 1996.

80. G.S. Frankel, J.R. Scully, C.V. Jahnes, "Repassivation of Pits in Aluminum Thin Films," J. Electrochem. Soc., 143(6), pp. 1843-1840, (1996).

79. H.J. Koenigsmann, and E.A. Starke, Jr., "Cavity Nucleation and Growth in an Al-Si-Ge Alloy," Scripta Metallurgica et Materialia, Vol. 35, pp. 1205-1209 (1996).

78. M.J. Haynes and R.P. Gangloff, "Elevated Temperature Fracture Toughness of Al-Cu-Mg-Ag Sheet: Characterization and Modeling", Metallurgical and Materials Transactions A, in review (1997).

77. M. T. Lyttle and J. A. Wert, "The Plastic Anisotropy of an Al-Li-Cu-Zr Alloy Extrusion in Unidirectional Deformation", Metallurgical Transactions A, 27A, p. 3503 (1996).

76. G.S. Frankel, J.R. Scully, C.V. Jahnes, "Repassivation of Pits in Aluminum Thin Films", in Critical Factors in Localized Corrosion II, P.M. Natishan, R.G. Kelly, G.S. Frankel and R.C. Newman, eds., The Electrochemical Society, PV 95-15, p. 30 (1996).

75. R.J. Kilmer, S.W. Smith, J.P. Moran, J.R. Scully, "The Effect of Microstructure on Hydrogen Assisted Fracture and Stress Corrosion Cracking Behavior in Al-Li-Cu Alloys", submitted to Metall. Trans. A, (1996) July.

74. C.J. Lissenden, and C.T. Herkovich, "Interfacial Debonding in Laminated Titanium Matrix Composites," Mechanics of Materials, Elsivier Publishing, in press (1996).

73. H.J. Koenigsmann, E.A. Starke, Jr., and P.E. Allaire, "Finite Element/Experimental Analysis of Cavity Nucleation in an Al-Si-Ge Alloy," Acta Metallurgica et Materialia, Vol. 44, pp. 3069-2075 (1996).

72. B. Skrotzki, G.J. Shiflet, and E.A. Starke, Jr. On the Effect of Stress on Nucleation and Growth of Precipitates in an Al-Cu-Mg-Ag Alloy, Metallurgical Transactions A, Vol. 27A, pp. 3431-3444 (1996).

71. B. Skrotzki, H. Hargarter and E.A. Starke, Jr. Microstructural stability under creep conditions of two Al-Cu-Mg-Ag Alloys, Proceedings of the 5th International Conference on Aluminum Alloys, July 1-5, Grenoble, France, pp. 1245-1250 (1996).

70. M.J. Haynes and Richard P. Gangloff, "High Resolution R-Curve Characterization of the Fracture Toughness of Thin Sheet Aluminum Alloys", Journal of Testing and Evaluation, Vol. 25, pp. 82-98 (1997).

69. M.J. Haynes, Brian P. Somerday, Cynthia L. Lach and Richard P. Gangloff, "Micromechanical Modeling of Temperature-Dependent Initiation Fracture Toughness in Advanced Aluminum Alloys", in 27th National Symposium on Fatigue and Fracture Mechanics, ASTM STP, R.S. Piascik, R.P. Gangloff, N.E. Dowling and J.C. Newman, eds., ASTM, Philadelphia, PA, pp. 165-190 (1997).

68. H. J. Koenigsmann and E. A. Starke, Jr., "Cavity Nucleation and Fracture in an Al-Si-Ge Alloy", submitted to Proceedings of the 5th International Conference on Aluminum Alloys, July 1-5, Grenoble, France, pp. 1479-1484 (1996).

67. C.J. Lissenden, B. A. Lerch, and C. T. Herakovich, "Response of SiC/Ti Under Combined Loading - Part III: Microstructural Evaluation", J. Composite Materials, Vol. 30, No. 1, pp. 84-108 (1996).

66. D.C. Slavik and Richard P. Gangloff, "Environment and Microstructure Effects on Fatigue Crack Facet Orientation in an Al-Li-Cu-Zr Alloy", Acta Metallurgica et Materialia, Vol 44, pp. 3515-3534 (1996).

65. R.S. Piascik and R. P. Gangloff, "Modeling Environment-Enhanced Fatigue Crack Growth in Al-Li-Cu-Zr," in Hydrogen Effects on Material Behavior, A. W. Thompson and N.R. Moody, eds., TMS-AIME, Warrendale, PA, pp. 409-433 (1996).

64. J.R. Scully, Co-editor *"Electrochemical Noise-Application to Analysis and Interpretation of Corrosion Data,"* American Society for Testing of Materials Special Technical Publication, STP 1277, J. Kearns, J.R. Scully, P.R. Roberge, D.L. Reichert, and J.L. Dawson, eds., Philadelphia, PA (1996).

63. S.T. Pride, J.R. Scully and J.L. Hudson, "Analysis of Electrochemical Noise from Metastable Pitting in Al, Aged Al-2%Cu and AA 2024-T3," in Electrochemical Noise Methods in Corrosion ASTM STP, 1277, ASTM, Philadelphia, PA, pp. 307-331 (1996).

62. S. W. Smith and J. R. Scully, "Hydrogen Trapping and Its Correlation to the Hydrogen Embrittlement Susceptibility of Al-Li-Cu-Zr Alloys," in TMS Hydrogen Effects on Materials Behavior, N. R. Moody and A. W. Thompson, eds., TMS-AIME, Warrendale, PA, p. 131 (1996).

63. B. Skrotzki, E.A. Starke, and G.J. Shiflet, "Alterung einer Al-Cu-Mg-Ag-Legierung unter äußerer Spannung," Hauptversammlung 1995 der Deutschen Gesellschaft für Materialkunde e.V., Bochum, Germany, June (1995).

62. J.A. Wert and M.T. Lyttle, "Microstructure Evolution During High-Temperature Deformation of Aluminum Alloys", 16th Riso International Symposium on Microstructural and Crystallographic Aspects of Recrystallization, N. Hansen, D. Juul Jensen, Y.L. Liu and B. Ralph (eds), Riso National Laboratory, Roskilde, Denmark, pp.589-594 (1995).

61. J.R. Scully, S.T. Pride, H.S. Scully, J.L. Hudson, "Some Correlations Between Metastable Pitting and Pit Stabilization in Metals" Electrochemical Society Localized Corrosion II Symposia Proceedings, P. Natishan, R. Newman, G. Frankel, R. Kelly, eds. Electrochemical Soc. Proceedings, Vol. 95-15 (1996).

60. B. Skrotzki, E. A. Starke and G. J. Shiflet, "The Effect of Stress on Nucleation and Growth of Precipitates in Al-Cu-Mg-X Alloys", Proc. of the 2nd International Conference on Microstructure and Mechanical Properties of Aging Materials, TMS-AIME, Warrendale, PA, in press (1996).

59. P.N. Kalu and J.A. Wagner, " A Microtexture Investigation of the Fracture Behavior of Al- Li Alloy 2090", Lightweight Alloys for Aerospace Applications III, TMS-AIME, Warrendale, PA, in press (1996).

58. H.J. Koenigsmann and E.A. Starke, Jr., "Fracture Behavior in Al-Si-Ge Alloys", in Proceedings of the 2nd International Conference on Microstructures and Mechanical Properties of Aging Materials, TMS-AIME, Warrendale, PA, in press (1996).

57. S.S. Kim, M. J. Haynes and R.P. Gangloff, "Localized Deformation Control of Elevated Temperature Fracture in Submicron Grain Aluminum with Dispersoids", Materials Science and Engineering A, Vol. 203, pp. 256-271 (1995).

56. E.A. Thornton and J.D. Kolenski, "Viscoplastic Response of Structures with Intense Local Heating", Journal of Aerospace Engineering, in press (1996).

55. C.J. Lissenden, C. T. Herakovich, and M-J. Pindera, "Response of SiC/Ti Under Combined Loading - Part II: Room Temperature Creep Effects", J. Composite Materials, Vol. 29, No. 10, pp. 1403-1417 (1995).

54. C.J. Lissenden, C. T. Herakovich, and M-J. Pindera, "Response of SiC/Ti Under Combined Loading - Part I: Theory and Experiment for Imperfect Bonding", J. Composite Materials, Vol. 29, No. 2, pp. 130-155 (1995).

53. E.A. Thornton, M.F. Coyle, and R.N. McLeod, "Experimental Study of Plate Buckling Induced by Spatial Temperature Gradients," Journal of Thermal Stresses, in press (1996).

52. C.J. Lissenden, C. T. Herakovich, and M-J. Pindera, "Inelastic Deformation of TMC Under Multiaxial Loading" in Life Prediction Methodology for Titanium Matrix Composites, ASTM STP, W.S. Johnson, ed., ASTM, Philadelphia, PA, in press (1996).

51. R.G. Buchheit, F.D. Wall, G.E. Stoner and J.P. Moran, "Anodic Dissolution-Based Mechanism for the Rapid Cracking, Preexposure Phenomenon Demonstrated by Aluminum-Lithium-Copper Alloys", Corrosion, Vol. 51, pp. 417-428 (1995).

50. C.J. Lissenden and C.T. Herakovich, "Numerical Modelling of Damage Development and Viscoplasticity in Metal Matrix Composites," Computer Methods in Applied Mechanics and Engineering, Vol. 126, pp. 289-303 (1995).

49. J. R. Scully, "Electrochemical Tests," in Manual on Corrosion Tests; Application and Interpretation, R. Baboian, ed., ASTM, Philadelphia, PA, pp. 75-90 (1995).

48. R.P. Gangloff, "Corrosion Fatigue Cracking", in Manual on Corrosion Tests: Application and Interpretation, R. Baboian, ed., ASTM, Philadelphia, PA, pp. 253-271 (1995).

47. B. Skrotzki, E. A. Starke and G. J. Shiflet, "Effect of Texture and Precipitates on Mechanical Property Anisotropy of Al-Cu-Mg-X Alloys", Proc. of the 4th International Conference on Aluminum Alloys, Vol. II, EMAS, Warley Heath, UK p. 40 (1994).

46. R.G. Buchheit, G.E. Stoner and G.J. Shiflet, "Corrosion Properties of a Rapidly Solidified $Al_{90}Fe_5Gd_5$ Alloy", J. Electrochem. Soc., in revision (1996).

45. M.E. Mason and R. P. Gangloff, "Modeling Time-Dependent Corrosion Fatigue Crack Propagation in 7000 Series Aluminum Alloys," in FAA/NASA International Symposium on Advanced Structural Integrity Methods for Airframe Durability and Damage Tolerance, C. E. Harris, ed., NASA Conference Publication 3274, Part 1, NASA-Langley Research Center, Hampton, VA, pp. 441-462 (1994).

44. J. M. Duva, J. Aboudi, and C. T. Herakovich, "A Probabilistic Micromechanics Model for Damaged Composites", Damage Mechanics in Composites, D. H. Allen and J.W. Ju, eds., ASME, AMD-Vol. 185, pp. 1-20 (1994).

43. C.J. Lisssenden and C.T. Herakovich, "Modelling Interfacial Debonding in Titanium Matrix Composites", in Inelasticity and Micromechanics of Metal Matrix Composites,

G.Z. Voyiadjis and J.W. Jue, eds., Elsevier, Studies in Applied Mechanics 41, Amsterdam, pp. 239-260 (1994).

42. J. Aboudi, F. Mirzadeh, and C.T. Herakovich, "Response of Metal Matrix Laminates with Temperature Dependent Properties," J. Composites Technology & Research, Vol. 16, No. 1, pp. 68-76 (1994).

41. C.J. Lissenden, M-J. Pindera, and C.T. Herakovich, "Stiffness Degradation of SiC/Ti Tubes Subjected to Biaxial Loading," J. Composite Science & Technology, Vol. 10, pp. 23-36 (1994).

40. S.T. Pride, J.R. Scully and J.L. Hudson, "Metastable Pitting of Aluminum and Criteria for the Transition to Stable Pit Growth," Journal of the Electrochemical Society, Vol. 141, No. 11, p. 3028 (1994).

39. C.J. Lissenden, C. T. Herakovich, and M-J. Pindera, "Damage Induced Room Temperature Creep of Titanium Matrix Composites", Durability of Composite Materials, R. C. Wetherhold, ed., ASME MD-Vol. 51, pp. 39-50 (1994).

38. H.J. Koenigsmann and E.A. Starke, Jr., "Microstructural Stability and Fracture Behavior in Al-Si-Ge Alloys", Proceedings of the 4th International Conference on Aluminum Alloys - Their Physical and Mechanical Properties, T.H. Sanders, Jr. and E.A. Starke, Jr., eds., Atlanta, GA, Vol. II, pp. 24-31 (1994).

37. M.T. Lyttle and J.A. Wert, "Modeling of Continuous Recrystallization in Aluminum Alloys," Journal of Materials Science, Vol. 29, pp. 3342-3350 (1994).

36. E. Richey, III, A.W. Wilson, J.M. Pope, and R.P. Gangloff, "Computer Modeling the Fatigue Crack Growth Rate Behavior of Metals in Corrosive Environments", NASA CR194982, NASA-Langley Research Center, Hampton, VA (1994).

35. R.G. Buchheit, J.P. Moran and G.E. Stoner, "The Electrochemical Behavior of the T1 (Al2CuLi) Intermetallic Compound and Its Role in Localized Corrosion of Al-3Cu-2Li Alloys", Corrosion, Vol. 50, pp. 120-130 (1994).

34. D. Gundel, P. Taylor and F. Wawner, "The Fabrication of Thin Oxide Coatings on Ceramic Fibers by a Sol-Gel Technique", Journal of Materials Science, Vol. 29, pp. 1795-1800 (1994).

33. M.T. Lyttle and J.A. Wert, "Simulative Modeling of Continuous Recrystallization of Aluminum Alloys", in Advances in Hot Deformation Textures and Microstructures, J.J. Jonas, T.R. Bieler and K.J. Bowman, eds., TMS-AIME, Warrendale, PA, pp. 373-383 (1994).

32. R.P. Gangloff, R.S. Piascik, D.L. Dicus and J.C. Newman, "Fatigue Crack Propagation in Aerospace Aluminum Alloys", Journal of Aircraft, Vol. 31, pp. 720-729 (1994).

31. W.C. Porr, Jr. and R.P. Gangloff, "Elevated Temperature Fracture of RS/PM Alloy 8009: Part I-Fracture Mechanics Behavior", Metall. Trans. A, Vol. 25A, pp. 365-379 (1994).

30. J.R. Scully, T. O. Knight, R. G. Buchheit, and D. E. Peebles, "Electrochemical Characteristics of the Al_2Cu, Al_3Ta and Al_3Zr Intermetallic Phases and Their Relevancy to the Localized Corrosion of Al Alloys," Corrosion Science, Vol. 35, pp. 185-195 (1993).

29. E.A. Thornton, "Thermal Buckling of Plates and Shells," Applied Mechanics Reviews, Vol. 46, No. 10, pp. 485-506 (1993).

28. R.P. Gangloff and Sang Shik Kim, "Environment Enhanced Fatigue Crack Propagation in Metals: Inputs to Fracture Mechanics Life Prediction", NASA CR-191538, NASA-Langley Research Center, Hampton, VA (1993).

27. R.S. Piascik and R.P. Gangloff, "Environmental Fatigue of an Al-Li-Cu Alloy: Part II - Microscopic Hydrogen Cracking Processes", Metall. Trans. A, Vol. 24A, pp. 2751-2762 (1993).

26. D.C. Slavik, J.A. Wert and R.P. Gangloff, "Determining Fracture Facet Crystallography Using Electron Back Scatter Patterns and Quantitative Tilt Fractography", Journal of Materials Research, Vol. 8, pp. 2482-2491 (1993).

25. D.C. Slavik, C.P. Blankenship, Jr., E.A. Starke, Jr. and R.P. Gangloff, "Intrinsic Fatigue Crack Growth Rates for Al-Li-Cu-Mg Alloys in Vacuum", Metall. Trans. A, Vol. 24A, pp. 1807-1817 (1993).

24. D. Gundel and F. Wawner, "The Influence of Defects on the Response of Titanium/SiC Fiber Composites to Thermal Exposure", Composites Engineering, Vol. 4, No. 1, pp. 47-65 (1993).

23. J.B. Parse and J.A. Wert, "A Geometrical Description of Particle Distributions in Materials", Modeling and Simulation in Materials Science and Engineering, Vol. 1, pp. 275-296 (1993).

22. D.C. Slavik and R.P. Gangloff, "Microscopic Processes of Environmental Fatigue Crack Propagation in Al-Li-Cu Alloy 2090", in Fatigue '93, Vol. II, J.-P. Bailon and J.I. Dickson, eds., EMAS, West Midlands, UK, pp. 757-765 (1993).

21. C.J. Lissenden, M-J. Pindera and C.T. Herakovich, "Response of SiC/Ti Tubes Under Biaxial Loading in the Presence of Damage," Damage Mechanics in Composites, D.H. Allen and D.C. Lagoudas, Eds., ASME- AMD-Vol. 150, AD-Vol. 132, pp. 73-90 (1992).

20. J.S. Hidde, and C.T. Herakovich, "Inelastic Response of Hybrid Composite Laminates," Journal of Composite Materials, Vol. 26, No. 1 (1992).

19. J.A. Wagner and R.P. Gangloff, "Fracture Toughness of Al-Li-Cu-In Alloys", Scripta Metallurgica et Materialia, Vol. 26, pp. 1779-1784 (1992).

18. R.G. Buchheit, Jr., J.P. Moran, F.D. Wall, and G.E. Stoner, "Rapid Anodic Dissolution Based SCC of 2090 (Al-Li-Cu) by Isolated Pit Solutions," Parkins Symposium on Fundamental Aspects of Stress Corrosion Cracking, S.M. Bruemmer, E.I. Meletis, R.H. Jones, W.W. Gerberich, F.P. Ford and R.W. Staehle, eds., TMS-AIME, Warrendale, PA, p. 141 (1992).

17. J.P. Moran, R.G. Buchheit, Jr., and G.E. Stoner, "Mechanisms of SCC of Alloy 2090 (Al-Li- Cu) - A Comparison of Interpretations from Static and Slow Strain Rate Techniques", Parkins Symposium on Fundamental Aspects of Stress Corrosion Cracking, S.M. Bruemmer, E.I. Meletis, R.H. Jones, W.W. Gerberich, F.P. Ford and R.W. Staehle, eds., TMS-AIME, Warrendale, PA, p. 159 (1992).

16. R.J. Kilmer, T.J. Witters and G.E. Stoner, "Effect of Zn Additions on the Precipitation Events and Implications to Stress Corrosion Cracking Behavior in Al-Li-Cu-Mg-Zn Alloys", Proceedings of the Sixth International Al-Li Conference, M. Peters and P.J. Winkler, eds., DGM Informationsgesellschaft, Verlag, pp. 755-760 (1992).

15. C.T. Herakovich and J.S. Hidde, "Response of Metal Matrix Composites with Imperfect Bonding", Ultramicroscopy, Vol. 40, pp. 215-228 (1992).

14. R.P. Gangloff, D.C. Slavik, R.S. Piascik and R.H. Van Stone, "Direct Current Electrical Potential Measurement of the Growth of Small Fatigue Cracks", in Small Crack Test Methods, ASTM STP 1149, J.M. Larsen and J.E. Allison, eds., ASTM, Philadelphia, PA, pp. 116-168 (1992).

13. R.G. Buchheit, Jr., F.D. Wall, G.E. Stoner and J.P. Moran, "Stress Corrosion Cracking of Al- Li-Cu-Zr Alloy 2090 in Aqueous Cl- and Mixed Cl-/CO3-2 Environments", CORROSION/91, Paper No. 99, NACE, Houston, TX (1991).

12. R.J. Kilmer and G.E. Stoner, "The Effect of Trace Additions of Zn on the Precipitation Behavior of Alloy 8090 During Artificial Aging", Proceedings, Light Weight Alloys for Aerospace Applications II, E.W. Lee, ed., TMS-AIME, Warrendale, PA, pp. 3-15 (1991).

11. W.C. Porr, Jr., Anthony Reynolds, Yang Leng and R.P. Gangloff, "Elevated Temperature Cracking of RSP Aluminum Alloy 8009: Characterization of the Environmental Effect", Scripta Metallurgica et Materialia, Vol. 25, pp. 2627-2632 (1991).

10. J. Aboudi, J.S. Hidde and C.T. Herakovich, "Thermo-Mechanical Response Predictions for Metal Matrix Composites", in Mechanics of Composites at Elevated and Cryogenic Temperatures, S.N. Singhal, W.F. Jones and C.T. Herakovich, eds., ASME AMD, Vol. 118, pp. 1-18 (1991). Also, Science & Engineering of Composite Materials, Vol. 2, No. 3, pp. 151-170 (1993).

9. R.S. Piascik and R.P. Gangloff, "Environmental Fatigue of an Al-Li-Cu Alloy: Part I - Intrinsic Crack Propagation Kinetics in Hydrogenous Environments", Metallurgical Transactions A, Vol. 22A, pp. 2415-2428 (1991).

8. W.C. Porr, Jr., Y. Leng, and R.P. Gangloff, "Elevated Temperature Fracture Toughness of P/M Al-Fe-V-Si", in Low Density, High Temperature Powder Metallurgy Alloys, W.E. Frazier, M.J. Koczak, and P.W. Lee, eds., TMS- AIME, Warrendale, PA, pp. 129-155 (1991).

7. Y. Leng, William C. Porr, Jr. and Richard P. Gangloff, "Time Dependent Crack Growth in P/M Al-Fe-V-Si at Elevated Temperatures", Scripta Metallurgica et Materialia, Vol. 25, pp. 895-900 (1991).

6. R.J. Kilmer and G.E. Stoner, "Effect of Zn Additions on Precipitation During Aging of Alloy 8090", Scripta Metallurgica et Materialia, Vol. 25, pp. 243-248 (1991).

5. D.B. Gundel and F.E. Wawner, "Interfacial Reaction Kinetics of Coated SiC Fibers", Scripta Metallurgica et Materialia, Vol. 25, pp. 437-441 (1991).

4. R.G. Buchheit, Jr., J.P. Moran and G.E. Stoner, "Localized Corrosion Behavior of Alloy 2090-The Role of Microstructural Heterogeneity", Corrosion, Vol. 46, pp. 610-617 (1990).

3. Y. Leng, W.C. Porr, Jr. and R.P. Gangloff, "Tensile Deformation of 2618 and Al-Fe-Si-V Aluminum Alloys at Elevated Temperatures", Scripta Metallurgica et Materialia, Vol. 24, pp. 2163-2168 (1990).

2. R.P. Gangloff, "Corrosion Fatigue Crack Propagation in Metals", in Environment Induced Cracking of Metals, R.P. Gangloff and M.B. Ives, eds., NACE, Houston, TX, pp. 55-109 (1990).

1. R.S. Piascik and R.P. Gangloff, "Aqueous Environment Effects on Intrinsic Corrosion Fatigue Crack Propagation in an Al-Li-Cu Alloy", in Environment Induced Cracking of Metals, R.P. Gangloff and M.B. Ives, eds., NACE, Houston, TX, pp. 233-239 (1990).

COMPLETED PROJECTS: (1986 to present reporting period)

1. DAMAGE LOCALIZATION MECHANISMS IN CORROSION FATIGUE OF ALUMINUM-LITHIUM ALLOYS
   Faculty Investigator: R.P. Gangloff
   Graduate Student: Robert S. Piascik
   Degree: PhD
   UVa Department: Materials Science and Engineering (MS&E)
   NASA-LaRC Contact: D. L. Dicus (Metallic Materials)
   Start Date: June, 1986
   Completion Date: November, 1989
   Employment: NASA-Langley Research Center

2. AN INVESTIGATION OF THE LOCALIZED CORROSION AND STRESS CORROSION CRACKING BEHAVIOR OF ALLOY 2090 (Al-Li-Cu)
   Faculty Investigator: Glenn E. Stoner
   Graduate Student: James P. Moran
   Degree: PhD
   UVa Department: MS&E
   NASA-LaRC Contact: W.B. Lisagor (Metallic Materials)
   Start Date: September, 1988
   Completion Date: December, 1989
   Co-Sponsor: ALCOA
   Employment: ALCOA Laboratories

3. MECHANISMS OF LOCALIZED CORROSION IN AL-LI-CU ALLOY 2090
   Faculty Investigator: G.E. Stoner
   Graduate Student: R.G. Buchheit
   Degree: PhD
   UVa Department: MS&E
   NASA-LaRC Contact: D.L. Dicus (Metallic Materials)
   Start Date: June, 1987
   Completion Date: December, 1990
   Cosponsor: Alcoa
   Employment: Sandia National Laboratories

4. DEFORMATION AND FRACTURE OF ALUMINUM-LITHIUM ALLOYS: THE EFFECT OF DISSOLVED HYDROGEN

Faculty Investigator: R.E. Swanson (VPI)
Graduate Student: Frederic C. Rivet
Degree: MS
VPI Department: Materials Engineering
NASA-LaRC Contact: D.L. Dicus (Metallic Materials)
Start Date: September, 1988
Completion Date: December, 1990
Employment: Not determined

5. INVESTIGATION OF THE REACTION KINETICS BETWEEN SiC FIBERS AND SELECTIVELY ALLOYED TITANIUM MATRIX COMPOSITES AND DETERMINATION OF THEIR MECHANICAL PROPERTIES

Faculty Investigator: F.E. Wawner
Graduate Student: Douglas B. Gundel
Degree: MS
UVa Department: MS&E
NASA-LaRC Contact: D.L. Dicus and W.B. Brewer (Metallic Materials)
Start Date: January, 1989
Completion Date: December, 1990
Employment: Graduate School, University of Virginia; PhD candidate on LA^{2}ST Program; Department of Materials Science

6. DESIGN OF CRYOGENIC TANKS FOR SPACE VEHICLES

Faculty Investigators: W.D. Pilkey and J.K. Haviland
Graduate Student: Charles Copper
Degree: MS
UVa Department: Mechanical and Aerospace Engineering (MAE)
NASA-LaRC Contact: D.R. Rummler (Structural Mechanics Division), R.C. Davis and M.J. Shuart (Aircraft Structures)
Start Date: April, 1989
Completion Date: December, 1990
Employment: Graduate School, University of Virginia; PhD candidate on NASA-Headquarters sponsored program; Department of Mechanical and Aerospace Engineering

7. ELEVATED TEMPERATURE FRACTURE OF AN ADVANCED RAPIDLY SOLIDIFIED, POWDER METALLURGY ALUMINUM ALLOY

Faculty Investigator: R.P. Gangloff
Graduate Student: William C. Porr, Jr.
Degree: PhD
UVa Department: MS&E
NASA-LaRC Contact: C.E. Harris (Mechanics of Materials)
Start Date: January, 1988
Completion Date: June, 1992
Employment: David Taylor Naval Ship R&D Center

8. QUANTITATIVE CHARACTERIZATION OF THE SPATIAL DISTRIBUTION OF PARTICLES IN MATERIALS: APPLICATION TO MATERIALS PROCESSING

Faculty Investigator: John A. Wert
Graduate Student: Joseph Parse
Degree: PhD
UVa Department: MS&E
NASA-LaRC Contact: D.R. Tenney (Materials Division)
Start Date: September, 1988
Completion Date: June, 1992
Employment: Private Consultant

9. ENVIRONMENTAL FATIGUE CRACK GROWTH AND CRACKING MECHANISMS IN Al-Li-Cu Alloy 2090

Faculty Investigator: R.P. Gangloff
Graduate Student: Donald C. Slavik
Degree: PhD
UVa Department: MS&E
NASA-LaRC Contact: D.L. Dicus (Metallic Materials)
Start Date: September, 1989
Completion Date: June, 1993
Employment: Knolls Atomic Power Laboratory

10. INELASTIC DEFORMATION OF METAL MATRIX COMPOSITES UNDER BIAXIAL LOADING

Faculty Investigators: Carl T. Herakovich and Marek-Jerzy Pindera
Graduate Student: Mr. Clifford J. Lissenden
Degree: PhD
UVa Department: Civil Engineering and the Applied Mechanics Program
NASA-LaRC Contact: W.S. Johnson (Mechanics of Materials)
Start Date: September, 1990
Completion Date: June, 1993
Employment: University of Kentucky, Department of Engineering Mechanics

11. EFFECT OF TEMPERATURE ON THE RESPONSE OF METALLIC SHELL STRUCTURES

Faculty Investigators: W.D. Pilkey and J.K. Haviland
Graduate Student: Karen McCarthy
Degree: MS (non-thesis)
Graduate Student: Theodore Johnson (NASA Minority Grantee)
Degree: PhD
Employment: NASA-LaRC
Graduate Student: Charles Copper
Degree: PhD
Employment: AMP Incorporated
UVa Department: MAE
NASA-LaRC Contact: M.J. Shuart and Jeffrey Stroud (Aircraft Structures)
Start Date: April, 1991
Completion Date: May, 1993

12. EFFECTS OF Zn ADDITIONS ON THE PRECIPITATION AND STRESS CORROSION CRACKING BEHAVIOR OF ALLOY 8090

Faculty Investigator: Glenn E. Stoner
Graduate Student: Raymond J. Kilmer
Degree: PhD
Department: MS&E
NASA-LaRC Contact: W.B. Lisagor (Metallic Materials)
Start Date: September, 1989
Completion Date: September, 1993
Cosponsor: Alcoa
Employment: General Motors

13. PROCESSING AND SUPERPLASTIC PROPERTIES OF WELDALITE™ SHEET

Faculty Investigator: John A. Wert
Graduate Student: Mark Lyttle
Degree: MS
Department: MS&E
NASA-LaRC Contact: T.T. Bales (Metallic Materials)
Start Date: September, 1991
Completion Date: December, 1993
Employment: Graduate School, University of Virginia; PhD Candidate in Materials Science and Engineering

14. METASTABLE PITTING OF Al ALLOYS AND CRITERIA FOR THE TRANSITION TO STABLE PITTING

Faculty Investigators: John R. Scully and J.L. Hudson
Graduate Student: Sheldon T. Pride
Degree: PhD
Department: Chemical Engineering
NASA-LaRC Contact: D.L. Dicus (Metallic Materials)
Start Date: September, 1991
Completion Date: May, 1994
Cosponsor: NASA Graduate Student Researchers Program, Under Represented Minority Emphasis
Employment: Rohm and Haas Chemical Company

15. THE EFFECT OF THERMAL EXPOSURE ON THE MECHANICAL PROPERTIES OF Ti-1100/SCS-6 COMPOSITES

Faculty Investigator: F.E. Wawner
Graduate Student: Douglas B. Gundel
Degree: PhD
UVa Department: MS&E
NASA-LaRC Contact: D.L. Dicus and W.B. Brewer (Metallic Materials)
Start Date: April, 1991
Completion Date: June, 1994
Employment: Wright Laboratories (WL/MLLM), US Air Force Materials Laboratory

16. ENVIRONMENTAL EFFECTS IN FATIGUE LIFE PREDICTION: MODELING ENVIRONMENTAL CRACK PROPAGATION IN LIGHT AEROSPACE ALLOYS

Faculty Investigator: R. P. Gangloff
Graduate Student: Mark E. Mason
Degree: MS
UVa Department: MS&E
NASA-LaRC Contact: R. S. Piascik (Mechanics of Materials)
Start Date: January, 1992
Completion Date: November, 1994
Employment: Allied-Signal; Hopewell, VA

17. ENVIRONMENTAL EFFECTS IN FATIGUE LIFE PREDICTION: MODELING ENVIRONMENTAL CRACK PROPAGATION IN LIGHT AEROSPACE ALLOYS

Faculty Investigator: R. P. Gangloff
Graduate Student: Edward Richey, III
Degree: MS
UVa Department: MANE
NASA-LaRC Contact: R. S. Piascik (Mechanics of Materials)
Start Date: September, 1993
Completion Date: May, 1995
Employment: Graduate School, University of Virginia; PhD Candidate in Materials Science and Engineering

18. HYDROGEN INTERACTIONS IN ALUMINUM-LITHIUM 2090 AND SELECTED MODEL ALLOYS

Faculty Investigator: John R. Scully
Graduate Student: Stephen W. Smith; PhD Candidate
UVa Department: MS&E
NASA-LaRC Contact: W.B. Lisagor and D.L. Dicus (Metallic Materials)
Start Date: April, 1991
Anticipated Completion Date: May, 1995
Cosponsor: Virginia CIT
Employment: NASA-LaRC

19. MECHANISMS OF LOCALIZED CORROSION IN ALLOYS 2090 AND 2095

Faculty Investigator: G.E. Stoner
Graduate Student: F.D. Wall
UVa Department: MS&E
NASA-LaRC Contact: M.S. Domack (Metallic Materials)
Start Date: April, 1991
Completion Date: January, 1996
Employment: Babcock & Wilcox

20. Al-Si-Ge-Cu ALLOY DEVELOPMENT
    Faculty Investigator: E.A. Starke, Jr.
    Graduate Student: H.J. Koenigsmann, Ph.D.
    UVa Department: Materials Science and Engineering
    NASA-LaRC Contact: W.B. Lisagor (Metallic Materials)
    Start Date: September, 1993
    Completion Date: May, 1996
    Employment: H-T Technologies

21. DAMAGE EVOLUTION IN POLYMERIC COMPOSITES
    Faculty Investigator: C.T. Herakovich
    Graduate Student: R.D. Schroedter, III
    UVa Department: Civil Engineering & Applied Mechanics
    NASA-LaRC Contact: C.E. Harris
    Start Date: June, 1993
    Completion Date: January, 1996
    Employment: Customer Management Services

22. EFFECTS OF TEXTURE AND PRECIPITATES ON MECHANICAL PROPERTY ANISOTROPY OF Al-Cu-Mg-X ALLOYS
    Faculty Investigators: E.A. Starke, Jr. and G.J. Shiflet
    Graduate Student: None
    Post Doctoral Research Associate: B. Skrotzki, H. Hargarter
    UVa Department: Materials Science and Engineering
    NASA-LaRC Contact: W.B. Lisagor
    Start Date: September, 1993
    Completion Date: December, 1996

ADMINISTRATIVE PROGRESS

Post Doctoral Participation

We currently have one Post-Doctoral, Hinrich Hargarter, participating in the program.

Graduate Student Recruitment

The LA^{2}ST Program has encountered no problems in recruiting the best graduate students entering the participating Departments at UVa, and in sufficient numbers to achieve our education and research objectives.

Undergraduate Research Participation

In April of 1990, the LA^{2}ST Program was increased in scope to include undergraduate engineering students. Four students worked at NASA-LaRC during the Summer of 1990, none were recruited for the 1991 program, and seven were successfully recruited to work at NASA-LaRC during the Summer of 1992. Each student was a rising senior in an engineering or science major closely related to aerospace materials and mechanics. Represented universities have included Harvard, Georgia Institute of Technology, Virginia Polytechnic Institute, Duke, the University of Missouri, California Polytechnical Institute, and North Carolina State University. Professor Glenn E. Stoner assumed responsibility for the 1993 Summer Undergraduate Program. In the summer of 1995, two students from the Pennsylvania State University and Duke University worked in the Metallic Materials Branch at NASA-LaRC. A graduating senior from Duke University participated in the program during the summer of 1996.

CURRENT PROJECTS

MECHANICAL AND ENVIRONMENTAL DEGRADATION MECHANISMS IN ADVANCED LIGHT METALS AND COMPOSITES

1. TIME-TEMPERATURE DEPENDENT FRACTURE IN ADVANCED WROUGHT INGOT METALLURGY, AND SPRAY DEPOSITED ALUMINUM ALLOYS
   - Faculty Investigator: R.P. Gangloff
   - Graduate Student: Michael J. Haynes; PhD (direct) candidate
   - UVa Department: MS&E
   - NASA-LaRC Contact: A. P. Reynolds (Metallic Materials)
   - Start Date: September, 1992
   - Completion Date: March, 1997
   - Project #1

2. CRYOGENIC TEMPERATURE EFFECTS ON THE DEFORMATION AND FRACTURE OF Al-Li-Cu-In ALLOYS
   - Faculty Investigator: R.P. Gangloff
   - Graduate Student: John A. Wagner; PhD candidate and NASA-LaRC employee
   - UVa Department: MS&E
   - NASA-LaRC Contacts: W.B. Lisagor (Metallic Materials) and J.C. Newman (Mechanics of Materials)
   - Start Date: June, 1987
   - Anticipated Completion Date: June, 1997
   - Project #2

3. EFFECTS OF AGING AND TEMPERATURE ON THE DUCTILE FRACTURE OF AA2095 AND AA2195
   - Faculty Investigator: R.P. Gangloff
   - Graduate Student: Cynthia L. Lach; MS candidate and NASA- LaRC employee
   - UVa Department: MS&E
   - NASA-LaRC Contacts: W.B. Lisagor (Metallic Materials)
   - Start Date: August, 1990
   - Anticipated Completion Date: June, 1997
   - Project #3

4. MECHANISMS OF LOCALIZED CORROSION AND STRESS CORROSION CRACK INITIATION IN ADVANCED Al-Li-Cu ALLOYS

Faculty Investigators: G.E. Stoner and J.R. Scully
Graduate Student: Brian J. Connolly; PhD candidate
UVa Department: MS&E
NASA-LaRC Contact: M. Domack
Start Date: May, 1996
Anticipated Completion Date: May, 1999
Project #4

5. METALLURGICAL FACTORS CONTROLLING STRESS CORROSION CRACKING IN AA2096 AND C155

Faculty Investigator: John R. Scully
Graduate Student: Leigh Ann Pawlick; PhD Candidate
UVa Department: MS&E
NASA-LaRC Contact: W.B. Lisagor and D.L. Dicus (Metallic Materials)
Start Date: May, 1997
Anticipated Completion Date: May, 1999
Cosponsor: Virginia CIT
Project #5

6a. MECHANISMS OF DEFORMATION AND FRACTURE IN HIGH STRENGTH TITANIUM ALLOYS: EFFECTS OF TEMPERATURE AND DISSOLVED HYDROGEN

Faculty Investigators: R. P. Gangloff
Graduate Student: Sean P. Hayes; PhD Candidate
UVa Department: MS&E
NASA-LaRC Contact: W. Brewer (Metallic Materials)
Start Date: September, 1994
Completion Date: September, 1997
Project #6a

6b. MECHANISMS OF DEFORMATION AND FRACTURE IN HIGH STRENGTH TITANIUM ALLOYS: EFFECTS OF TEMPERATURE AND MICROSTRUCTURE

Faculty Investigators: E. A. Starke, Jr.
Graduate Student: Susan M. Kazanjian, PhD Candidate
UVa Department: MS&E
NASA-LaRC Contact: To be determined (Metallic Materials)
Start Date: January, 1995
Completion Date: December, 1998
Project #6b

7. DETERMINATION OF THE CORROSIVE SPECIES FOUND WITHIN AIRCRAFT LAP-SPLICE JOINTS

Faculty Investigators: R.G. Kelly
Graduate Assistant: Karen S. Lewis, M.S. Candidate
UVa Department: Materials Science and Engineering
NASA-LaRC Contact: R.S. Piascik
Start Date: July, 1996
Completion Date: July, 1999
Project #7

AEROSPACE MATERIALS SCIENCE

8. EVALUATION OF WIDE-PANEL ALUMINUM ALLOY EXTRUSIONS

Faculty Investigator: John A. Wert
Graduate Student: Mark T. Lyttle, Ph.D. Candidate
UVa Department: Materials Science and Engineering
NASA-LaRC Contact: T. T. Bales (Metallic Materials)
Start Date: January, 1994
Completion Date: May, 1997
Project #8

9. EFFECTS OF TEXTURE AND PRECIPITATES ON MECHANICAL PROPERTY ANISOTROPY OF Al-Cu-Mg-X ALLOYS

Faculty Investigators: E.A. Starke, Jr. and G.J. Shiflet
Graduate Student: None
Post Doctoral Research Associate: B. Skrotzki, H. Hargarter
UVa Department: Materials Science and Engineering
NASA-LaRC Contact: W.B. Lisagor
Start Date: January, 1995
Completion Date: To be determined
Project #9

MECHANICS OF MATERIALS FOR LIGHT AEROSPACE STRUCTURES

10. FREQUENCY-DEPENDENT FATIGUE CRACK PROPAGATION IN 7000 SERIES ALUMINUM ALLOYS IN AN AGGRESSIVE ENVIRONMENT

Faculty Investigator: R.P. Gangloff
Graduate Student: Z. Gasem, Ph.D. Candidate
UVa Department: MS&E
NASA-LaRC Contact: R.S. Piascik (Mechanics of Materials)
Start Date: January, 1992
Anticipated Completion Date: December, 1997
Project #11

RESEARCH PROGRESS AND PLANS (July 1 to December 31, 1996)

Research progress, recorded during the period from July 1, 1996 to December 31, 1996, is summarized for each project in the following sections. The standard format includes the program objective, recent progress, conclusions, and immediate milestones.

Project #1: TIME-TEMPERATURE DEPENDENT FRACTURE IN ADVANCED ALUMINUM ALLOYS

Faculty Investigator:	Richard P. Gangloff
Graduate Assistant:	Michael J. Haynes, (direct) Ph.D. candidate
UVa Department:	MS&E
NASA-LaRC Contact:	W.B. Lisagor and D.L. Dicus
Start Date:	September, 1992
Completion Date:	March, 1997
Employment:	Texas Instruments

Objectives

The first goal of this Ph.D. research is to characterize the initiation and growth fracture toughness of AA2519-type alloys as a function of temperature. A second goal is to establish the microscopic fracture mechanisms at ambient and elevated temperatures by studying the evolution of microvoid nucleation, void growth, and shear instability controlled coalescence. A third goal is to evaluate and improve a critical strain-critical distance micromechanical model of microvoid-based fracture.

Background and Problem Statement

A significant effort is currently aimed at developing advanced aluminum alloys for elevated temperature aerospace applications, particularly for airframes such as the high speed civil transport[1,2]. Since existing precipitation hardened aluminum alloys (e.g., 2024, 7075/7475 and 2090/8090) may not be sufficient to meet microstructural stability combined with strength/toughness requirements, new compositions of wrought ingot metallurgy, spray deposited, and rapidly solidified powder metallurgy (RS/PM) alloys are under development. As promising compositions are determined, it is necessary to characterize the critical effects of loading rate and temperature on fracture toughness and creep-fatigue damage tolerance, and to

establish metallurgical fracture mechanisms and predictive micromechanical models for such properties.

Technical Approach

Research is currently focused on two alloy sheets from the advanced ingot metallurgy class: 1) aluminum alloy (AA) 2519+Mg+Ag-T87: Al-5.75Cu-0.52Mg-0.30Mn-0.49Ag-0.16Zr-0.09V-0.06Fe-0.05Si by wt% and 2) C416-T8: Al-5.4Cu-0.5Mg-0.5Ag-0.3Mn-0.12Zr-0.07Fe-0.05Si by wt%.

The general approach was outlined in past renewal proposals[3-6]. In summary, our approach focuses on:

(1) Characterizing the microstructure of as-received alloys through optical, scanning electron, and transmission electron microscopy.

(2) Implementing J-Integral fracture mechanics methods and direct current potential drop (DCPD) crack length measurements on compact tension (C(T)) specimens to determine equivalent (LEFM) fracture initiation toughness (K_{JICi}) and propagation resistance (K_J-Δa) at ambient and elevated temperatures.

(3) Establishing microstructural fracture paths and mechanisms through quantitative SEM fractography, fracture surface reconstructions, deformed tensile-bar profiles, crack-tip profiles, and transmission electron microscopy.

(4) Performing uniaxial compression tests to determine yield strength, strain hardening exponent and strain rate sensitivity for use in modeling.

(5) Employing smooth and notched tensile tests to estimate intrinsic fracture strains as a function of stress state triaxiality.

(6) Evaluating the predictive capabilities of micromechanical models in explaining the temperature dependence of ductile fracture initiation toughness, K_{JICi}.

Progress During the Reporting Period

The results for this period are divided into two sections. Section I discusses research on C416-T8 that was an element of the manuscript, "Elevated Temperature Fracture Toughness of

Al-Cu-Mg-Ag Alloys: Characterization and Modeling" (submitted to Metallurgical Transactions A and currently in review)[7]. Section II explains why fracture strain rises with temperature for AA2519+Mg+Ag, based on the temperature dependence of void sheet formation.

Section I: Fracture Toughness Behavior of C416-T8

Temperature and displacement-rate dependent fracture toughness of AA2519+Mg+Ag and the governing microvoid fracture mechanisms were the subject of previous NASA-LaRC sponsored research, as summarized in an archival publication[7], past proposals[3-6], and past progress reports[8-12]. This section discusses parallel work on C416 sheet. New conclusions are listed below and discussed.

1. *Replicate K_J-Δa measurements for C(T) specimens of C416 exhibit significant scatter, related to out-of-plane crack growth.*

Figure 1 displays three replicate K_J-Δa curves for 2.3 mm thick C(T) specimens of C416, which were fractured at 25°C and a load line displacement rate of 0.26 μm/sec. Two of the R-curves agree, but the third exhibits significantly higher crack growth resistance. Research at the NASA Langley Research Center correlated this enhanced crack growth resistance to cracks that deviate from the Mode I fracture plane (out-of-plane)[13]. The C(T) specimen corresponding to the highest R-curve in Figure 1 exhibited out-of-plane crack growth, while the other two specimens did not, consistent with the findings of NASA. We do not know the cause of out-of-plane crack growth.

2. *Compared to AA2519+Mg+Ag, C416 with a reduced Cu content and a lower volume fraction of undissolved θ particles exhibits significantly higher initiation (K_{JICi}) and growth (K_J^{2mm}) toughnesses between 75 and 150°C.*

The superior initiation and growth toughnesses of C416 over AA2519+Mg+Ag are established in Figures 2(a) and 2(b), which plot K_{JICi} and K_J^{2mm} versus temperature, respectively. While K_{JICi} and K_J^{2mm} are comparable for the two alloys at 25°C, they are clearly higher for C416 between 75 and 150°C. The low value of K_{JICi} for C416 at 175°C is not understood. Higher values of toughness for C416 are consistent with the reduction in size of θ constituents, which was observed by optical metallography[7]. However, a reduced constituent spacing for C416

results in comparable toughnesses at ambient temperatures. This reduced spacing is less important at elevated temperatures due to stress relaxation at the smaller constituents.

3. *Fracture of C416 evolves by primary void nucleation at small constituents, followed by moderate void growth, secondary void nucleation at dispersoids, and void sheeting. Primary void nucleation at large constituents, analogous to that seen in AA2519+Mg+Ag, was rare.*

Microvoid coalescence is the dominant fracture mechanism in AA2519+Mg+Ag and C416 at both ambient and elevated temperatures, as illustrated in Figures 3(a) and 3(b) respectively. A trimodal distribution of dimple sizes characterizes each surface. The population of largest dimples (5 to 30 μm in diameter) on the AA2519+Mg+Ag surface (Fig. 3(a)) is associated with primary void initiation and growth from the large undissolved θ particles, with some contribution from manganese and iron bearing constituents. Intermediate sized dimples are associated with void nucleation and growth from the population of small constituent particles. The primary dimples in C416 are of intermediate size (Fig. 3(b)), consistent with their smaller constituents.

The smallest dimples in both alloys coalesce to form void sheets (indicated by "vs" in Figs. 3(a) and 3(b)) and are associated with the nucleation and growth of voids from submicron dispersoid particles. Another observed feature is intergranular or grain boundary ductile fracture (marked by "i" in Fig. 3(b)).

The relative amounts of these four features vary for the two alloys. Quantitative fracture surface information was derived for C416 and AA2519+Mg+Ag fractured at 25°C, from montages composed of thirty 1000X fractographs (not shown). The percentage of grid points associated with dimples nucleated from large constituents, dimples nucleated from small constituents, and dimples nucleated as void sheets are 38.2%, 18.6%, and 41.4% respectively. The remaining 1.8% is from intergranular fracture. For C416, the percentage of grid points for large constituent dimples is very small (2.5%). Primary void nucleation and growth in this alloy is controlled by smaller constituents, which account for 57.4% of the grid points. The remaining grid points are divided between void sheets (24.8%) and intergranular fracture (15.3%). Clearly,

the absence of the largest constituents in AA2519+Mg+Ag removes a detrimental feature and alters the fracture process.

The extent of primary void growth (the ratio of the dimple radius (R_D) to the particle radius (R_0) was measured for both alloys and is higher for C416. For AA2519+Mg+Ag, R_D equals 9.2±0.7 μm, R_0 equals 2.85±0.08 μm, and R_D/R_0 equals 3.2±0.2 (error ranges are based on the t-distribution and a 95% confidence level). For C416, R_D equals 4.8±0.4 μm, which is substantially smaller than primary void sizes in AA2519+Mg+Ag. However, R_D/R_0 is higher for C416, since R_0 equals 0.99±0.02 μm.

Section II: Temperature Dependent Void-Sheet Formation

The temperature dependence of void-sheet formation, and its effect on the temperature dependence of fracture strain for AA2519+Mg+Ag, is the subject of a manuscript currently in preparation for Metallurgical Transactions A. The conclusions from this manuscript are listed below, and new findings are discussed.

1. At 25°C, nearly all dispersoids nucleate secondary voids in a band of strain localization between primary voids (denoted intravoid strain localization or ISL). The number densities of dispersoids and void-sheet dimple centers are nearly equal, and the distributions of nearest-neighbor spacings are similar for both.
2. At elevated temperatures (150 to 175°C), the participation of dispersoids in secondary void nucleation within an ISL band is greatly reduced. The number density of dimple centers is six to eight times lower than the density of dispersoids, and the nearest-neighbor spacing is three to four times higher.
3. Void nucleation at dispersoids occurs by particle fracture and particle/matrix decohesion. Dispersoids just below notched-tensile bar fracture surfaces, but outside regions of strain localization, nucleated voids infrequently suggesting that ISL is a prerequisite for profuse voiding at dispersoids.
4. For AA2519+Mg+Ag deformed at 25°C, the flow stress and strain-hardening exponent are insensitive to strain rate between 6.7×10^{-5} and 1×10^{-1} s^{-1}. As temperature increases to 175°C, or as the strain rate at 150°C decreases from 1×10^{-1} to 6.7×10^{-5} s^{-1}, the flow stress

and strain-hardening exponent decrease monotonically. A temperature compensated strain rate parameter ($Z_{eff} = \dot{\varepsilon}/D_{eff}$ dominated by dislocation pipe diffusion below 175°C, describes data at various temperatures and strain rates.

5. The strain-rate sensitivity of flow stress increases linearly with increasing temperature, from near zero at 25°C to 0.022 at 175°C.
6. For dispersoid diameters between 0.1 and 0.4 μm in AA2519+Mg+Ag, the HK stress relaxation model predicts a transition from dislocation accumulation at dispersoids to dislocation bypassing by climb as Z_{eff} decreases from 4.0×10^{16} to 6.5×10^{14} m^{-2}, which is consistent with a sharp decline in strain hardening as Z_{eff} decreases below 1×10^{17} m^{-2}.
7. The globally applied strain necessary for particle/matrix decohesion is predicted to increase sharply as temperature increases or strain rate decreases at elevated temperature, due to a reduction in flow stress and strain hardening. The predicted increase corresponds reasonably with the transition from dislocation accumulation to dislocation bypassing.
8. As temperature increases, modeling suggests that ISL and void sheeting are retarded and fracture strain increases for AA2519+Mg+Ag, despite a decrease in material hardening within an ISL band, because the strain to nucleate secondary voids increases sharply.

Increased fracture strain and retarded void sheeting with increased temperature were established in a publication[7] and previous NASA-LaRC progress reports[8-12]. The HK stress relaxation model was also discussed previously [10]. The remaining conclusions are amplified in a section of void nucleation at dispersoids, a section on temperature and strain-rate dependent deformation, and a section on modeling of temperature dependent void nucleation. The first section summarizes new microstructural and fractographic findings, the second section reports temperature and strain-rate dependent stress-strain behavior, and the third section employs a continuum particle/matrix decohesion model to predict the temperature dependence of void nucleation. Together, these three sections explain why fracture strain rises with temperature, by characterizing the temperature and strain-rate dependence of plastic deformation and void nucleation at dispersoids.

Void Nucleation at Dispersoids: Dispersoid participation in void nucleation within an ISL band decreases with increasing temperature for AA2519+Mg+Ag, as shown by Figures 4(a)-4(c). As temperature increases from 25 to 150 and 175°C the nearest-neighbor spacing of dimples on void sheets (Δ_{VS}) increases and the number of dimples per unit area (N_A^{VS}) decreases. These quantities are based on measurements from several fractographs. By assuming the thickness of the void-sheet is roughly equivalent to the thickness of a TEM foil, Δ_{VS} and N_A^{VS} are comparable to equivalent values for dispersoids (Δ_{foil} and N_A^{foil}) taken from several TEM micrographs. Nearly all dispersoids nucleate voids within a void sheet at 25°C. The number densities of dispersoids (N_A^{foil} =0.82 μm^{-2}) and void-sheet dimples (N_A^{VS} =0.81 μm^{-2}) are nearly equal, and a Δ_{VS} of 0.68 μm is only slightly higher than a Δ_{foil} of 0.53 μm. At elevated temperatures (150 and 175°C), reduced void nucleation at dispersoids is reflected by values of N_A^{VS} (0.14 and 0.1 μm^{-2}) and Δ_{VS} (1.74 and 2.08 μm).

Dispersoids in AA2519+Mg+Ag nucleate voids by particle fracture (Figure 5(a)) and particle/matrix decohesion (Figure 5(b)). From notched-tensile bars fractured at 25 or 150°C, we observed the vast majority of voids well within 20 μm of the fracture surface. Void nucleation at dispersoids is infrequent, with only 8.2% and 1.8% of dispersoids nucleating voids at 25 and 150°C, respectively. Dispersoid participation is much higher on void-sheet fracture surfaces, which implies that ISL is a prerequisite for profuse voiding at dispersoids.

Temperature and Strain-Rate Dependent Deformation: Stress(σ_{fl})-strain(ε) behavior of AA2519+Mg+Ag was measured as a function of temperature and strain rate with uniaxial compression experiments. Compression samples were tested at temperatures ranging from 25 to 175°C and at actuator displacement rates corresponding to average strain rates between 6.7×10^{-5} and 1.0×10^{-1} s^{-1}. A temperature-compensated strain-rate parameter (Z_{eff}) was employed to consolidate results from different temperatures and strain-rates into one independent coefficient parameter[14]. The parameter Z_{eff} is defined as the strain rate normalized by an effective diffusion coefficient (D_{eff}) composed of bulk and dislocation pipe diffusion components. D_{eff} is given by[14]:

$$D_{eff} = \left[1.7x10^{-4}\exp\left(\frac{-Q_{L1}}{RT}\right) + 6x10^{-7}\exp\left(\frac{Q_{L2}}{RT}\right)\right] + 2.8x10^{-6}\exp\left(\frac{Q_P}{RT}\right)\left[80\left(\frac{\sigma_{fl}}{E}\right)^2\right] m^2 s^{-1} \quad [1]$$

where Q_{L1} (142 kJ/mol) and Q_{L2} (115 kJ/mol) are activation energies for lattice self-diffusion at high and intermediate temperatures, respectively, and Q_P (82 kJ/mol) is the activation energy for dislocation-pipe diffusion. Temperature (T) is in units of Kelvin and R is the universal gas constant. The flow-stress (σ_{fl}) dependent term in brackets is an estimate of the fraction of atoms participating in dislocation pipe-diffusion. Below 200°C, the dislocation pipe-diffusion term dominates D_{eff}. Table 1 lists calculated Z_{eff} for 16 compression tests in order of decreasing magnitude.

Compression σ-ε data were analyzed with the Ramberg-Osgood (R-O) constitutive equation, which includes as fitting parameters a reference stress (σ_0), a constant (κ), and the inverse of the Ludwik strain hardening exponent (1/n). Total strain is given by:[15]

$$\varepsilon = \frac{\sigma_{fl}}{E} + \frac{\kappa\,\sigma_0}{E}\left(\frac{\sigma_{fl}}{\sigma_0}\right)^{\frac{1}{n}} \quad [2]$$

where σ_{fl} is the flow stress, and the first and second terms represent elastic (ε^e) and plastic strains (ε^p), respectively. Over a range of plastic strain ($0.008 < \varepsilon^p < 0.05$), 1/n was determined as the linear regression slope of ε^p versus σ_{fl} plotted logarithmically. The linear regression intercept is a function of κ, σ_0, E, and 1/n, and a physically realistic σ_0 was calculated from it by setting κ equal to 1.

The stress-strain behavior is independent of strain rate between $6.7x10^{-5}$ and $1.0x10^{-1}$ s^{-1}, as reflected by nearly equal values of σ_0 and 1/n (Table 1). As temperature increases, or as strain rate at 150°C decreases from $1.0x10^{-1}$ s^{-1} to $6.7x10^{-5}$ s^{-1}, σ_0 and n decrease monotonically and reflect a decreasing resistance to plastic flow (Table 1). The R-O constitutive parameters σ_0 and 1/n are relevant to modeling of void nucleation of dispersoids.

Modeling of Temperature-Dependent Dispersoid/Matrix Decohesion: Argon and coworkers employed the criterion that void nucleation by decohesion occurs when the interfacial stress (σ_I) exceeds the interfacial strength (σ_I^*)[16]:

$$\sigma_I = \sigma_m + \sigma_{fl} \geq \sigma_I^* \qquad [3]$$

where σ_m is the mean or hydrostatic stress acting on the dispersoid/matrix interface and σ_{fl} is the magnitude of stress induced at the north and south poles of the particle/matrix interface due to (deviatoric) plastic flow around a rigid inclusion. The plastic component of the Ramberg-Osgood relationship (Eq. 2) defines the dependence of σ_{fl} on $\bar{\varepsilon}^p$, and can be combined with Eq. 3 to determine the void nucleation strain ($\bar{\varepsilon}_n^p$) as a function of R-O parameters, σ_m/σ_{fl}, and σ_I^*:

$$\bar{\varepsilon}_n^p \geq \frac{\sigma_0 \kappa}{E}\left(\frac{\sigma_I^*}{(1+\sigma_m/\sigma_{fl})\sigma_0}\right)^{\frac{1}{n}} \qquad [4]$$

where σ_m/σ_{fl} is known as the stress-state triaxiality. Void nucleation is implicitly driven by plastic strain.

It is necessary to estimate σ_I^* for dispersoid/matrix interfaces in AA2519+Mg+Ag because $\bar{\varepsilon}_n^p$ depends strongly on this parameter. To obtain a lower bound estimate of σ_I^*, a circumferentially notched tensile bar (σ_m/σ_{fl}=1.13) of AA2519+Mg+Ag was deformed at 25°C to a plastic strain of 0.08 (based on diametral contraction and Bridgman's analysis[17]), interrupted, and unloaded. An FEM study suggests that $\bar{\varepsilon}^p$ at the center of the notch root is half of the Bridgman strain, or 0.04[18]. The notched bar was sectioned to the midplane, polished, and ion milled to remove polishing artifacts. For several fields of view, void nucleation was not observed for magnifications as high as 10,000X. Based on the given σ_m/σ_{fl} and a lower bound plastic nucleation strain ($\bar{\varepsilon}_n^p$(25C)) of 0.04, a lower bound σ_I^* of 1159 MPA was calculated from Eq. 4 with E equal to 72.4 GPa, κ equal to 1, σ_0 equal to 497 MPa, and 1/n equal to 17.5.

As temperature increases, σ_I^* is assumed to decrease in proportion to E, which is justified by observations that E correlates with interfacial energy[19]. Assuming that E for AA2519+Mg+Ag displays the same temperature dependence as E for pure aluminum[20], lower bound σ_I^* values at 25, 50 ,75, 100, 125, 150, and 175°C equal 1160, 1130, 1100, 1080, 1060, 1040, and 1020 MPA, respectively.

Employing Eq. 4, estimates of temperature-dependent σ_I^* and E, and R-O flow properties from Table I, $\bar{\varepsilon}_n^p$ is estimated as a function of Z_{eff} for σ_m/σ_{fl} equal to 1.13 (a reasonable estimate of the stress-state triaxiality in an ISL band[21]). Figure 6 plots a relative nucleation strain ($\bar{\varepsilon}_n^p$ normalized by $\bar{\varepsilon}_n^p$(25C)) which remains constant at 1 between Z_{eff} values of $2x10^{21}$ m^{-2} and $1x10^{16}$ m^{-2}, increases rapidly as Z_{eff} decreases below $1x10^{16}$ m^{-2}, and rapidly approaches a very high ratio at $1x10^{13}$ m^{-2}. At 175°C and a strain rate of $7x10^{-5}$ s^{-1} (Z_{eff}=$2.8x10^{13}$ m^{-2}), $\bar{\varepsilon}_n^p$ /$\bar{\varepsilon}_n^p$ (25C) equals 536.7 and is not plotted. A relative nucleation strain was chosen to highlight the temperature-dependence of void nucleation, since the absolute nucleation strain is clouded by substantial uncertainty in σ_I^*. Figure 6 indicates that void nucleation at dispersoids becomes exceedingly difficult as temperature increases above a critical value, depending on the strain rate.

For the AA2519+Mg+Ag specimens that produced the fracture surfaces studied, a rough estimate of the strain rate in notched-tensile bar experiments or in fracture mechanics experiments (30 μm ahead of a crack-tip) is $6.7x10^{-5}$ s^{-1} [7]. For this strain rate, high strains are required to reach σ_I^* and nucleate voids at 150°C or above, due to reduced flow stress and strain hardening. However, if strain rate increases by a factor of 10 or more due to ISL, flow stress and strain hardening increase significantly and σ_I^* is reached at lower strains.

It is crucial to note that the prediction in Figure 6 is only semi-quantitative given the uncertainty in the absolute value and temperature dependence of σ_I^*. If a new reference nucleation strain of three times the original value is chosen ($\bar{\varepsilon}_n^p$(25C)=0.11), σ_I^* is calculated as 1240 MPa at 25°C. Assuming the same temperature dependence of σ_I^*, a similar curve is predicted (Figure 6), but it is shifted to higher Z_{eff} (lower temperature or higher strain rate) by about an order of magnitude. However, within the constraint of reasonable estimates of σ_I^* and its temperature dependence, there is always a sharp increase in the nucleation strain for AA2519+Mg+Ag when σ_0 and n fall below critical levels. Decohesion of dispersoid/matrix

interfaces in AA2519+Mg+Ag becomes exceedingly difficult above some critical temperature. Decohesion is still possible, however, if strain-rate increases. We propose that reduced void nucleation at dispersoids at elevated temperature retards void-sheet coalescence, enhances primary void growth, and results in a higher fracture strain.

Tasks for the Next Reporting Period

Michael Haynes' Ph.D. work will be completed in the Spring of 1997. The majority of the research effort during this period will involve writing the Ph.D. dissertation and archival publications.

References

1. W.B. Lisagor, in Thermal Structures and Materials for High-Speed Flight, E.A. Thornton, Ed., Volume 140, *Progress in Astronautics and Aeronautics*, A.R. Seebass, Editor-in-Chief, AIAA, Washington, DC, pp. 161-179, (1992).

2. R.P. Gangloff, E.A. Starke, Jr., J.M. Howe and F.E. Wawner,Jr., "Aluminum Based Materials for High Speed Aircraft", University of Virginia, Proposal No. MS-NASA/LaRC-5691-93, November (1992).

3. R.P. Gangloff, "NASA-UVa Light Aerospace Alloy and Structures Technology Program", Proposal No. MSE-NASA/LaRC-6074-94, November (1993).

4. R.P. Gangloff, "NASA-UVa Light Aerospace Alloy and Structures Technology Program", Proposal No. MSE-NASA/LaRC-6478-95, November (1994).

5. R.P. Gangloff, "NASA-UVa Light Aerospace Alloy and Structures Technology Program", Proposal No. MSE-NASA/LaRC-6855-96, November (1995).

6. R.P. Gangloff, "NASA-UVa Light Aerospace Alloy and Structures Technology Program", Proposal No. MSE-NASA/LaRC-7272-97, October (1996).

7. M.J. Haynes and R.P. Gangloff, "Elevated Temperature Fracture Toughness of Al-Cu-Mg-Ag Alloys: Characterization and Modeling", Metallurgical and Materials Transactions A, in review, (1997).

8. R.P. Gangloff, "NASA-UVa Light Aerospace Alloy and Structures Technology Program", University of Virginia Report No. UVA/528266/MSE94/114, March (1994).

9. R.P. Gangloff, "NASA-UVa Light Aerospace Alloy and Structures Technology Program", University of Virginia Report No. UVA/528266/MSE94/116, July (1994).

10. R.P. Gangloff, "NASA-UVa Light Aerospace Alloy and Structures Technology Program", University of Virginia Report No. UVA/528266/MS94/117, March (1995).

11. R.P. Gangloff, "NASA-UVa Light Aerospace Alloy and Structures Technology Program", University of Virginia Report No. UVA/528266/MS95/118, July (1995).

12. R.P. Gangloff and E.A. Starke, Jr., "NASA-UVa Light Aerospace Alloy and Structures Technology Program", University of Virginia Report No. UVA/528266/MSE96/119, January (1996).

13. D.L. Dicus, Personal Communication, NASA Langley Research Center, Hampton, VA, 1996.

14. H. Luthy, A.K. Miller, and O.D. Sherby, "The Stress and Temperature Dependence of Steady-State Flow at Intermediate Temperatures for Pure Polycrystalline Aluminum," Acta Metallurgica, vol. 28, pp. 169-178, (1980).

15. Y. Leng, W.C. Porr, and R.P. Gangloff, "Tensile Deformation of 2618 and Al-Fe-Si-V Aluminum Alloys at Elevated Temperatures," Scripta Metallurgica, vol. 24, pp. 2163-2168, (1990).

16. A.S. Argon, J. Im, and R. Safoglu, "Cavity Formation from Inclusions in Ductile Fracture," Metallurgical Transactions A, vol. 6A, pp. 825-837, (1975).

17. P.W. Bridgman, Studies in Large Plastic Flow and Fracture, McGraw-Hill Book Co., New York, NY, pp. 9-37, (1952).

18. J.W. Hancock and D.K. Brown, "On the Role of Strain and Stress State in Ductile Fracture," Journal of the Mechanics and Physics of Solids, vol. 31, pp. 1-24, (1983).

19. L.E. Murr, Interfacial Phenomena in Metals and Alloys, Addison Wesley, Reading, MA, p. 127, (1975).

20. L.F. Mondolfo, Aluminum Alloys Structure and Properties, Butterworth and Co., Woburn, MA, p. 82, (1976).

21. J.W. Hancock and A.C. Mackenzie, "On the Mechanisms of Ductile Failure in High-Strength Steels Subjected to Multi-Axial Stress-States," Journal of the Mechanics and Physics of Solids, vol. 24, pp. 147-169, (1976).

Table 1 - Flow and Hardening Properties over a Range of Temperatures and Strain-Rates; κ=1

Temperature (°C)	$\dot{\varepsilon}$ (s^{-1})	$\dot{\varepsilon}/D_{eff}$ (m^{-2})	σ_{ys} (MPa)	$\sigma_{fl}^{3\%}$ (MPa)	σ_0 (MPa)	1/n	γ
25	$1.03x10^{-1}$	$2.1x10^{21}$	470	527	496	17.9	373.1
25	$1.06x10^{-2}$	$2.1x10^{20}$	470	532	498	17.1	375.4
25	$1.06x10^{-3}$	$2.1x10^{19}$	474	534	500	17.4	381.8
25	$1.05x10^{-4}$	$2.1x10^{18}$	477	529	495	17.4	369.6
25	$6.67x10^{-5}$	$1.3x10^{18}$	457	529	494	17.7	389.6
50	$7.04x10^{-5}$	$1.1x10^{17}$	433	511	474	16.4	400.0
150	$1.02x10^{-1}$	$1.1x10^{17}$	432	491	469	25.1	280.1
75	$7.03x10^{-5}$	$1.2x10^{16}$	453	504	471	20.4	286.4
150	$1.09x10^{-2}$	$1.2x10^{16}$	400	474	448	21.3	314.5
150	$1.15x10^{-2}$	$1.3x10^{16}$	440	476	459	29.5	237.0
100	$6.62x10^{-5}$	$1.8x10^{15}$	437	485	463	23.6	259.8
150	$1.08x10^{-3}$	$1.3x10^{15}$	421	461	447	41.1	155.0
125	$6.44x10^{-5}$	$3.5x10^{14}$	425	456	436	23.4	190.3
150	$1.05x10^{-4}$	$1.3x10^{14}$	422	455	445	62.0	109.4
150	$6.71x10^{-5}$	$8.5x10^{13}$	421	444	434	48.8	115.8
175	$7.06x10^{-5}$	$2.8x10^{13}$	374	405	396	41.2	83.0

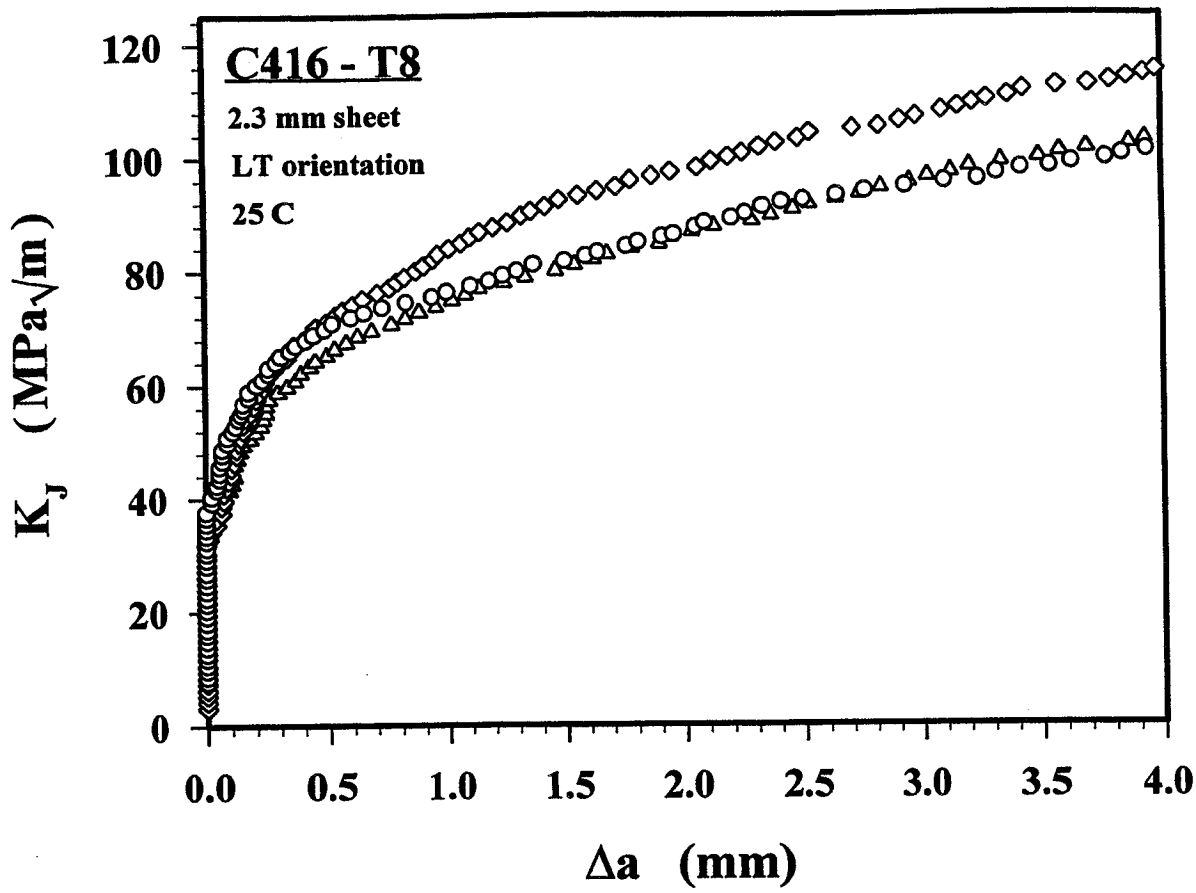

Figure 1 - Replicate resistance curves for C(T) specimens of 2.3 mm thick C416-T8 fractured at 25°C. Load-line displacement rate = 0.26 μm/sec.

a)

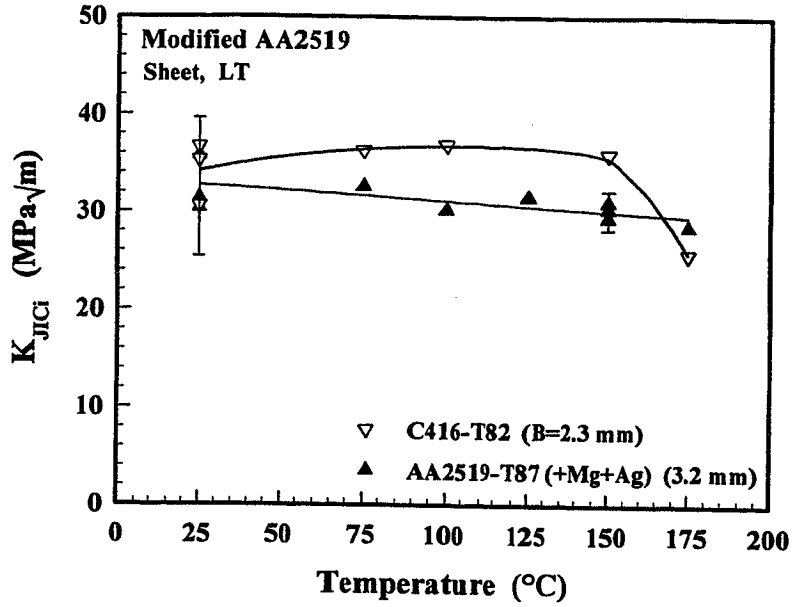

b)

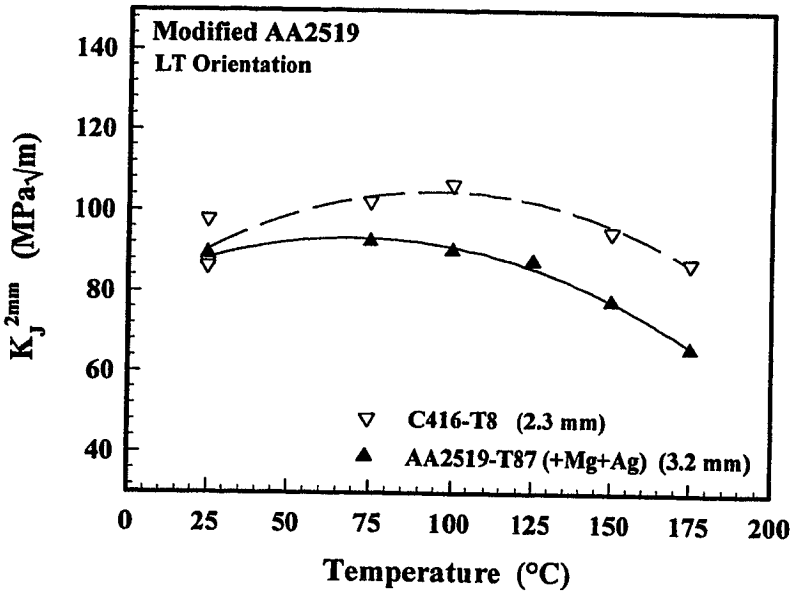

Figure 2 - Temperature-dependencies of a) initiation (K_{JICi}) and b) growth (K_J^{2mm}) toughnesses for AA2519+Mg+Ag-T87 and C416-T8. Load-line displacement rate = 0.26 μm/sec.

a)

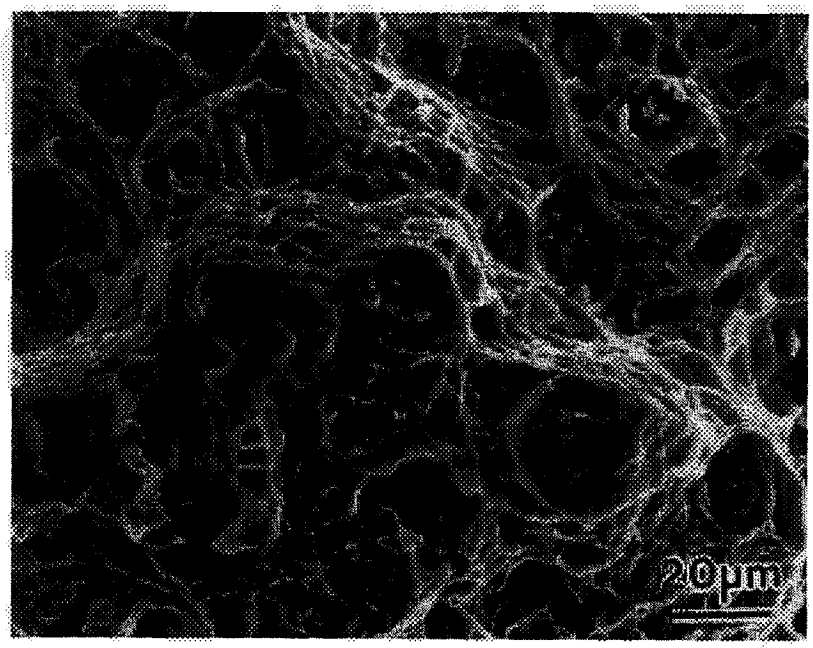

b)

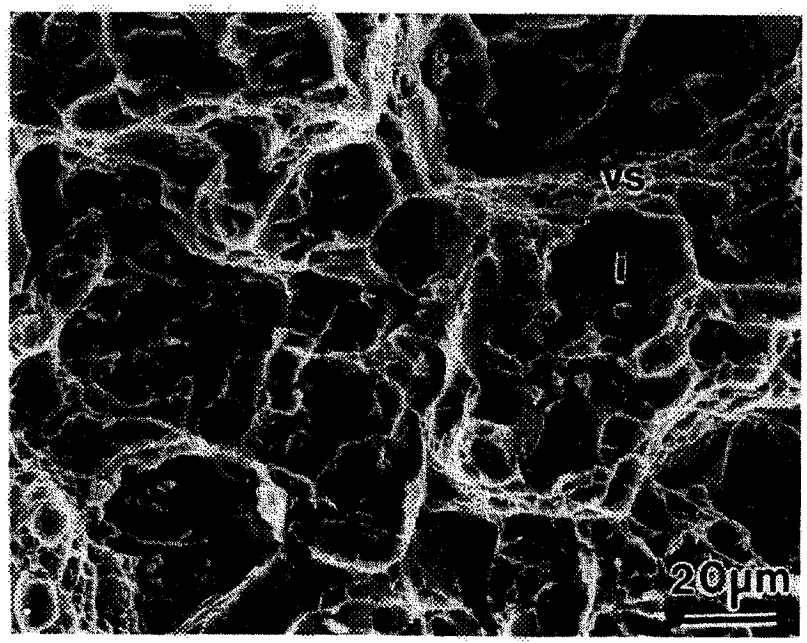

Figure 3 - SEM fractographs demonstrating microvoid fracture in a) AA2519+Mg+Ag-T87 and b) C416-T8.

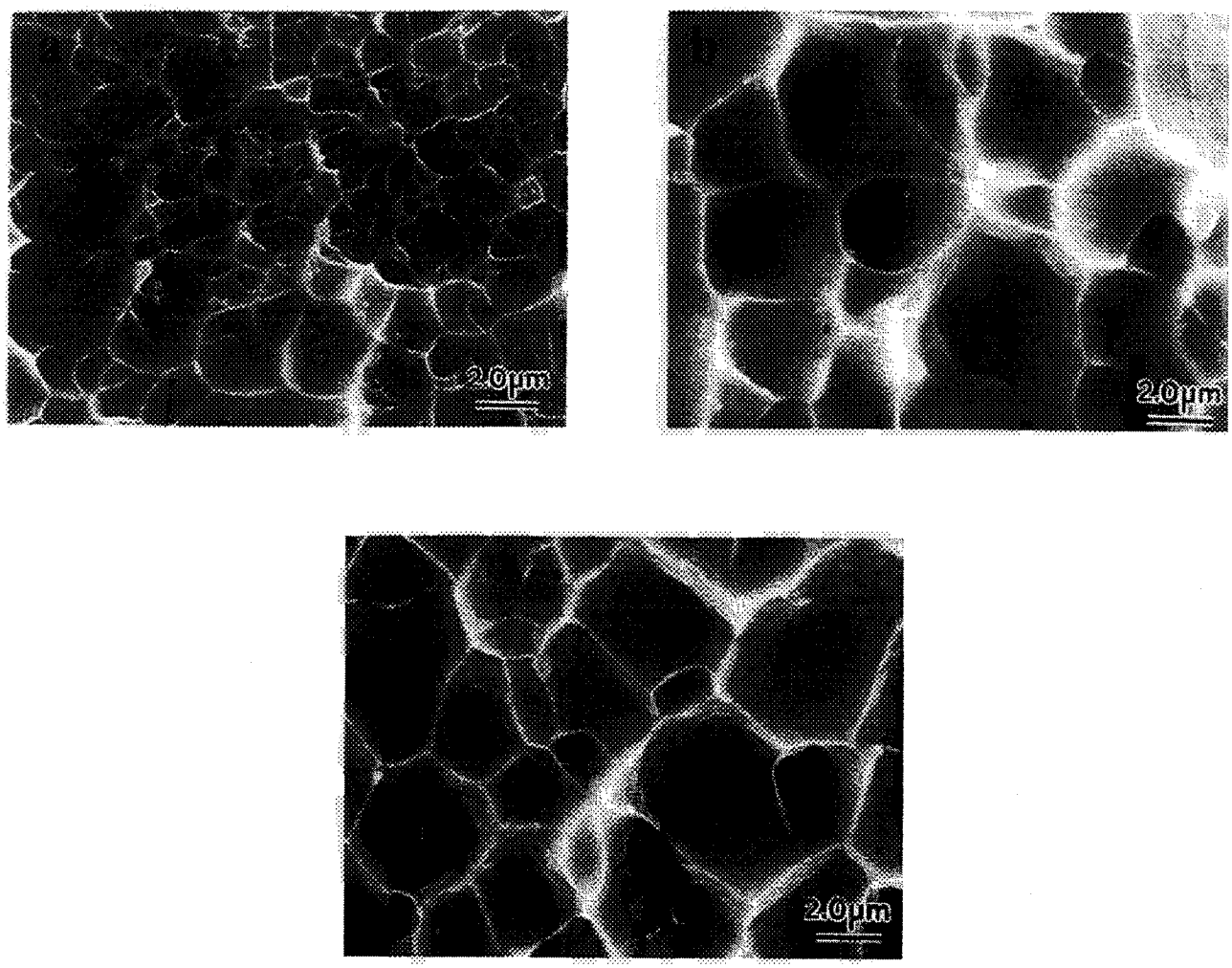

Figure 4 - SEM fractographs from C(T) specimens illustrating the morphology of dimples on void sheet surfaces at (a) 25°C, (b) 150°C, and (c) 175°C. (a), (b), and (c), are tilted 75°, 47°, and 45°, respectively away from the fracture plane about an axis parallel to the crack front, and crack growth is from right to left.

a)

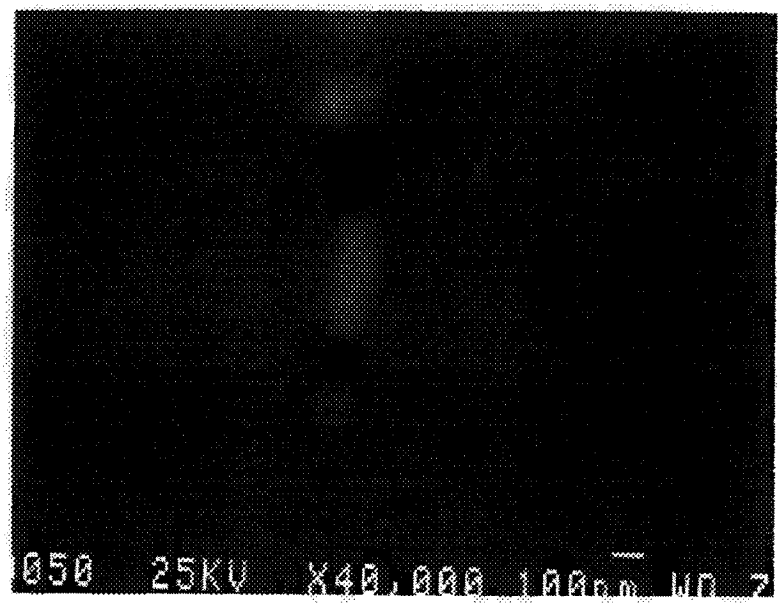

b)

Figure 5 - Nucleation of microvoids at dispersoids at 25°C by: a) dispersoid fracture and b) interface decohesion. The loading direction is vertical.

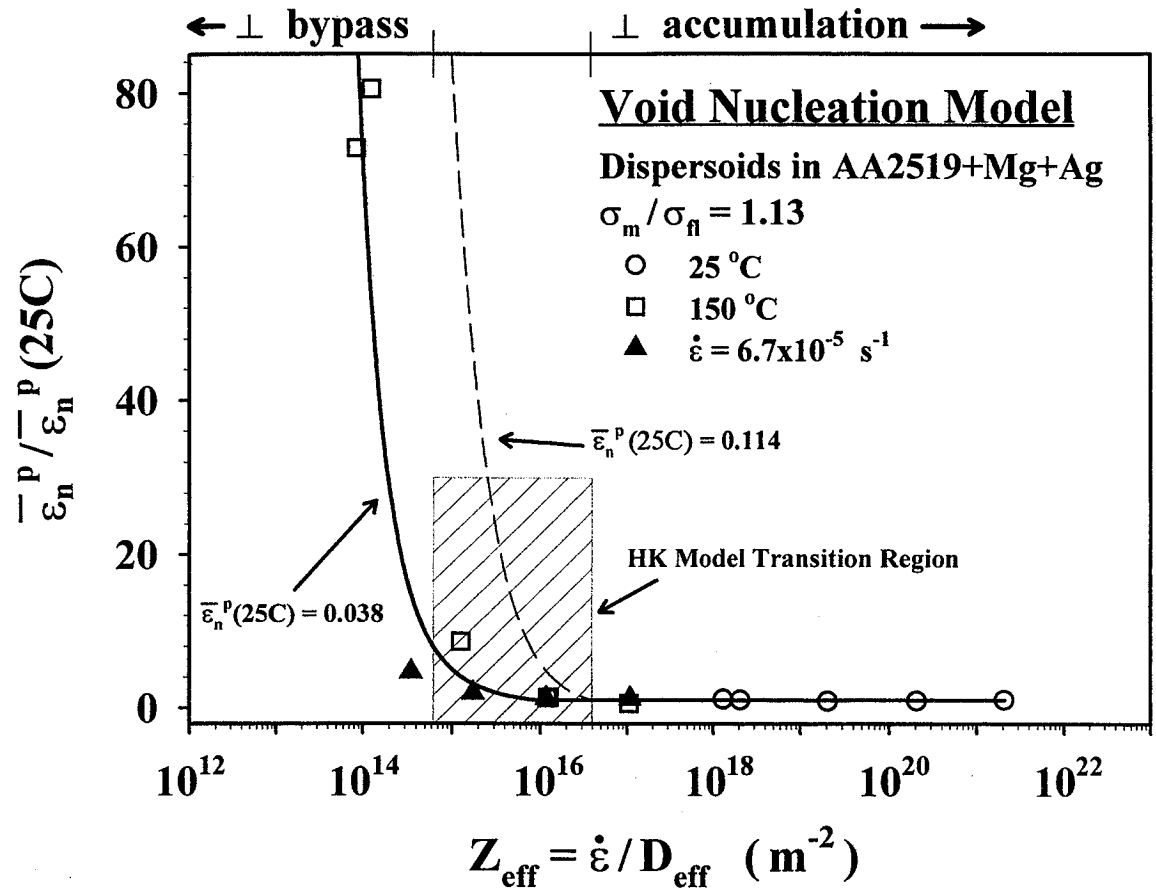

Figure 6 - Predicted temperature and strain-rate dependence of the effective plastic strain to nucleate voids at dispersoids, based on compressive flow properties and particle/matrix decohesion at a critical interfacial stress. Nucleation strains are normalized by a reference nucleation strain, $\bar{\varepsilon}_n^p$ (25C), at which an ambient temperature interfacial strength is calculated. The model shows results for two values of $\bar{\varepsilon}_n^p$ (25C).

Project #2: LOCALIZED CORROSION AND STRESS CORROSION CRACK INITIATION IN ADVANCED Al-Li-Cu ALLOYS

Faculty Investigators:	G.E. Stoner and J.R. Scully
Graduate Student (Ph.D.):	Brian J. Connolly
NASA-LaRc Contact:	M.S. Domack (Metallic Materials)
Start Date:	May 1996
Completion Date (approximate):	May 1999

Problem Statement

Previous projects sponsored by this grant have concentrated on the intrinsic factors which lead to environmental cracking of Al-Li-Cu alloys (e.g. 2090 and 2095) due to either dissolution assisted stress corrosion, hydrogen embrittlement, or some combination of the two [1-11]. Microstructural/temper, chemical-electrochemical, as well as hydrogen absorption and trapping at various energy states have been explored for 2090 and in some instances 2095 along with characterization of the local crack chemistry and fractography. Efforts have also been conducted to understand possible beneficial effects of minor alloying additions (e.g., Zn) [3,9]. This diversity of approach was successful in providing information and techniques appropriate for examination of environment-assisted fracture mechanisms. However, previous projects did not enable clear separation of initiation from propagation. Nor did they enable the complete analysis of SCC in an Al-Li-Cu alloy system from the standpoint of local corrosion and its possible transition to intergranular corrosion and stress corrosion; with focus on the critical localized corrosion "condition" that causes SCC initiation. This project is our first attempt to investigate this transition in a manner which enables more complete understanding of localized corrosion, the transition to stress corrosion, short crack growth behavior, and, in a separate project [Scully/Pawlick, 1997], long crack behavior. The two projects will provide microstructural and electrochemical information concerning: the critical factors that cause initiation of localized corrosion, the critical factors that govern the transition to environment-assisted cracking, and, possibly, define crack growth rate-stress intensity relationships for short cracks. The investigation will focus on some of the latest variants of Al-Li-Cu-X alloys (AA 2096 and C155 or C255), with AA 2090 as a

control/comparison material. The project will also provide the foundation upon which future life-prediction protocols involving the transition from localized corrosion to SCC may be built.

Overall Project Objectives

The objective of this research project is to understand the mechanisms for localized corrosion and the critical factors governing the transition to initiation of environment-assisted cracking of selected advanced Al-Li-Cu alloys. The susceptibility of alloys AA2096 and C155 to stress corrosion crack initiation will be defined in terms of selected metallurgical (i.e., composition, aging condition and subsequent strengthening precipitate development, constituent particles, and specimen orientation), electrochemical (i.e., applied potential, localized corrosion site identity, size(depth) and propagation rate), chemical (i.e., macrocell and microcell compositions), and mechanical (i.e., dynamic strain rate, stress/strain state, localized corrosion flaw size and geometry) variables. Particular emphasis will be given to the role of Ag.

Technical Approach

Materials

The following alloys will be investigated: *C155* (approx. 3.1% Cu, 1.8% Li, 0.35% Mg, 0.16% Zr, 0.6% Mn, 0.35% Zn max wt. pct.) and *2096* (approx. 3.0% Cu, 1.9% Li, 0.8% Mg, 0.18% Zr, 0.6% Ag, 0.25% Zn max. wt. pct.). These alloys have approximately the same Cu/Li ratio, but 2096 contains Ag. However, it is recognized that Mn will getter some Cu in C155 to form coarse constituents; this will alter the effective Cu/Li ratio. C155 has not been obtained from Alcoa. AA 2096 extrusions in the T3 and T8 tempers have been obtained from M. Domack . All under aged tempers in this study are heated to 160 C.

Experimental Approach

In a preliminary effort, the localized corrosion behavior of the AA 2096 and C155 alloys will be characterized in the T3, various UA and PA conditions. The following test procedures will be used to achieve conventional characterization of the localized corrosion properties in deaerated 0.6 M NaCl solution:

- Determination of pitting potentials by the potentiodynamic method, electrochemical scratch/repassivation method, and/or a physical scratch/repassivation method. A straining electrode polarization experiment will be conducted to determine critical potentials in the presence of dynamic plastic deformation which produces film rupture.
- Determination of open circuit potentials in aerated and deaerated 0.6 M NaCl and in a chromate inhibited NaCl solution to ascertain tempers expected to pit at OCP when immersed in 0.6 M NaCl. Determine approximate pit growth rates by serial removal/image analysis, or other means.
- Determine the effects of pit size/depth on repassivation potential for AA2090 and AA2096 by utilizing the cyclic potentiodynamic test method followed by optical analysis of pit sizes and distributions. From this analysis pit size will be related to charge passed.

One initial goal of this effort will be to ascertain whether or not SCC susceptible alloy/temper/environments can be clearly linked with standard localized corrosion characteristics. The follow-on effort to the above basic tests will involve characterizing pit current noise associated with potential holds at aerated open circuit potentials using advanced electrochemical methods [12]. This second goal will be to make a connection between pit growth/repassivation/depth characteristics and the SCC susceptibility of certain alloys/tempers/environments. The goal of this effort will be to ascertain whether SCC susceptible alloy/temper/environments can be clearly linked with certain more detailed localized corrosion characteristics.

Following characterization of the conditions for localized corrosion in standard laboratory SCC environments, the conditions for localized corrosion behavior will be established in more realistic precursor "macrocell" local chemistry environments and refined local environments using advanced electrochemical diagnostics (fast current transient detection and electrochemical noise) [12]. This latter effort will be more suitable to life-prediction where environments are less aggressive than standard laboratory environments.

The next phase will involve application of mechanical variables such as dynamic strain rate, stress/strain state, and/or cyclic strain to define windows of susceptibility to crack initiation using blunt notch specimens. Selected exposure/temper/mechanical conditions to be investigated will be guided by the SCC screening underway. This task will initially utilize *ex-situ* crack initiation

detection by metallographic sectioning, SEM techniques, and the breaking load method, but will also include in the latter stages of *1997 in-situ real time* detection using a long focal length microscope. This microscope was cost shared in the 1996 budget by U.Va.-SEAS. This microscope, coupled with electrochemical current detection, will enable us to characterize the critical corrosion site "condition" and microstructural identity that initiates SCC.

In subsequent years, attempts will be made to determine threshold stress intensities and possibly growth rates from short cracks optically sized. This will allow us to ascertain any evidence of differences between the behaviors of short versus long cracks, i.e. a "chemical crack length" effect.

Does Ag affect the localized corrosion behavior to influence SCC initiation?

A key focus of this project will be to identify the role of silver in SCC resistance (if observed). The Ag containing alloy will be compared to the non-Ag alloy. The aim will be to understand whether Ag alters electrochemical activity and, possibly, SCC resistance relative to AA 2090. Therefore, in addition to performing the traditional localized corrosion tests described above, metastable pit growth rates and the criteria for transition to stable pitting will be defined using the procedures developed in the NASA LA^{2}ST project conducted by Sheldon Pride [12]. Outputs will include:

- Electrochemical criteria for pit stabilization for Ag vs. non-Ag containing alloys; based on the I_{pit}/r_{pit} ratio. If this ratio remains the same for both alloys, then the conclusion can be made that the same critical pit solution (simulated by concentrated $AlCl_3$ is required to stabilize pits in Ag vs. non-Ag alloys. If this ratio differs with Ag additions, then the following experiment is proposed.
- The anodic dissolution rate inside of pits can be defined by conducting polarization experiments in concentrated $AlCl_3$ (simulating the environment inside a pit). Anodic dissolution rates in solutions ranging from 0.01 to 6M $AlCl_3$ (sat) are proposed to determine whether Ag alters the critical concentration required for pit stabilization by altering the E - log(i) dissolution behavior of the alloy. Recall that the critical pit concentration causes a transition from passivity to active dissolution.

Recent Findings

Recent work has shown that AA2096 is susceptible to SCC in the UA4 and UA8 tempers when exposed to a 0.6 M NaCl alternate immersion environment (see Figure 1). Moreover, Figure 1 illustrates that the 8 day NaCl/CO_2 pre-exposure did not produce cracking in the susceptible UA4 and UA8 tempers. The question is raised as to why SCC occurred in the AI test but not the pre-exposure test; does localized corrosion differ, or do differences lie elsewhere? Figure 2 displays breaking load data for AA2090 UA-B pre-exposed 8 days in 0.6 M NaCl + 2 days 100% RH CO_2 under constant strain (G49), and alternate immersion 0.6 M NaCl (60 days planned if no failure) under constant strain (G49). Here again we see a distinct difference in the results. The pre-exposure tensile specimens display a high breaking load value while the specimens exposed to the AI environment all failed, between 2 and 6 days. Therefore an effort was made to determine whether or not differences in localized corrosion behavior plays a governing role in this behavior. Cyclic potentiodynamic scans with varying vertex current densities were performed on AA 2096 (T3, UA4, UA8, and UA12) and AA 2090 (UA-B) in order to determine the effect of pit size on repassivation potential. Test coupons (1 mm^2) were subjected to vertex current densities from 5 $\mu A/cm^2$ to 1mA/cm^2. The subsequent repassivation potentials were recorded and maximum pit size was quantified using post-test optical image analysis. Figure 3 indicates that the repassivation potential decreases with increasing maximum pit size for all materials and tempers. It should be noted that AA2096 T3 displays slightly more positive repassivation potentials as a function of pit size, while the relationship between repassivation potential and pit size for AA2096 UA4, UA8, and UA12 is indistinguishable, lying within the same scatter band. Data for AA2090B lies between AA2096 T3 and the 2096 under aged tempers, although there is no statistical verification of this.

It is important to understand the electrochemical relationship between total charge (integrated applied anodic current density with respect to time) and pit geometry. When this is known, a critical pit condition can, in theory, be "dialed in" and SCC initiation in smooth or blunt notched specimens should be observed in susceptible tempers if initiation is controlled by pit size. Figure 2 also displays the breaking load data for several tensile specimens where a given maximum pit radius is distributed galvanostatically upon the notch. Maximum pit sizes of 108.4 μm and 306 μm were used in two conditions:

1) the maximum pit size was distributed galvanostatically on to the notch of the tensile specimen, after the electrochemical experiment the tensile specimen was immediately ultrasonically cleaned in DI water and methanol, followed by performing the breaking load method in a desiccated environment. This experiment determined the mechanical affect of pit size alone on the breaking load of the material assuming minimal alteration of intrinsic fracture toughness.

2) the maximum pit size was distributed galvanostatically on to the notch of a tensile specimen under constant strain (G49), exposed for 2 days in 100% RH CO_2, followed by the breaking load method in a desiccated environment. This experiment replicates the 8 day exposure test except that the pit size is applied more quickly.

From these observations it can be postulated that the specimens pre-exposed to NaCl for 8 days + 2 days CO_2 failed at a lower breaking load than the control tensile specimen due solely to the pit size (no SCC). However, the 2090 UA material experienced SCC both when exposed to CO_2 during AI and after pits were distributed galvanostatically when exposed to CO_2. Please note that the specimen exposed to CO_2 for 2 days with 108.4 mm pits failed during removal from the G49 test rig. This result must be duplicated before further comment can be made. (It should be noted that pits as large as 306 μm were never seen on the tensile specimens after exposure testing: AI and NaCl/CO_2 pre-exposure.) Therefore, the results suggest that pit size and depth is a factor but does not exclusively control SCC crack initiation in susceptible Al-Li-Cu tempers. Further work must be done to confirm this conclusion but it is supported by the observation that alternate immersion SCC failures (in 2 to 6 days for AA2090 UA) appears to have smaller pits than after the 8 day pre-exposure. It should also be noted that a 306 μm pit (galvanostatically applied) did not trigger the most severe cracking.

Research Objectives For 1996-1997

The second year should then begin to yield information regarding pit/notch configuration or other localized corrosion condition (growth rate) causing transition to environmental crack growth, the understanding of which will be the main objective of this project.

Future Work

Second Year

- Further determination of critical potentials (i.e., repassivation, and breakdown/ pitting) using a straining electrode polarization experiment will be performed in order to discern the effect of dynamic plastic strain which produces localized film rupture. Recent evidence revealed a distinct difference in corrosion morphology (strained vs unstrained condition) when a test coupon is galvanostatically subjected to 35.79 amp*sec (306 μm maximum pit radius).

- As stated above AA2096 UA4 and UA8 are susceptible to SCC attack in AI environments. It should be noted that the UA4 temper cracks in 0.6 M NaCl alternate immersion between 10 and 16 days (Scully/Pawlick 1997). This exposure time is comparable to the pre-exposure testing in $NaCl/CO_2$. No SCC failure was seen in the pre-exposure environment and the breaking load data measured after exposure did not vary statistically with the control case (see Figure 1). It will be an important goal for the next year to determine whether differences in localized corrosion involved in the AI environment compared to the pre-exposure in NaCl control SCC initiation or whether differences lie elsewhere. This goal will be accomplished in part through a 'dissection' of the AI test. Serial time immersions will be conducted followed by a detailed optical analysis of the sectioned notched tensile bar specimen. This analysis will provide insight in identifying the critical corrosion site needed for SCC initiation. TDS will identify whether differences in hydrogen absorption control SCC (Scully/Pawlick).

- Conditions for localized corrosion behavior will be characterized in precursor macrocell local chemistry environments and refined local environments using advanced electrochemical diagnostics (i.e., monitoring of current transient).

- Mechanical variables such as dynamic strain rate, stress state, and/or cyclic strain will be superimposed with environment in order to define a 'window' of susceptibility to stress corrosion crack initiation using blunt notch specimens. These experiments will be guided by preliminary screening of SCC properties conducted in conjunction with (Scully/Pawlick Project). As such, preliminary crack initiation studies will be conducted either in the $NaCl/CO_2$ pre-exposure environment or analogous chromate inhibited NaCl environment on AA 2090-UA ST specimens to correlate SCC initiation with localized corrosion "conditions". Metallographic sectioning and SEM analysis will be employed to detect crack initiation ex-situ. In-situ detection of crack

initiation will be accomplished using a long focal length microscope and electrochemical current monitoring.

Third Year

- Threshold stress intensities and growth rates from short cracks will be determined to ascertain any evidence of differences between the behaviors of short versus long cracks (i.e., a chemical crack length effect).

- In addition to performing the traditional localized corrosion tests described above, given the more positive critical potentials of AA 2096 and its SCC resistance, metastable pit growth rates and an electrochemical criterion for pit stabilization based on the I_{pit}/r_{pit} ratio will be defined for the Ag containing alloy (2096) and the non-Ag containing alloy (C155). If the I_{pit}/r_{pit} ratio differs with Ag additions, polarization experiments in concentrated $AlCl_3$ will be performed to define the anodic dissolution rates in a simulated pit environment. Anodic polarizations in solutions ranging from 0.1 M to 6 M $AlCl_3$ are proposed to determine whether Ag alters the critical concentration required for pit stabilization by altering the dissolution kinetics of the alloy.

Payoff/Coordination

The proposed work will provide correlation's between localized corrosion and SCC initiation that will lead to improved mechanistic understanding of the factors controlling the transition to SCC. K_{th} for short cracks along with critical corrosion site flaw sizes will be obtained.

The two projects are designed to be complimentary, but not redundant. For perhaps the first time a comprehensive understanding of the *transition* from localized corrosion to SCC initiation and propagation may be achieved.

Investigation of the same two alloys will strengthen understanding of the roles of metallurgy, processing and composition on SCC: (initiation versus propagation debate). Results from each study will provide direct input to the other. Examples include:

- Characterization of local macrocell chemistry developed in an alternate immersion double beam bolt loaded configuration will provide guidance on environments for blunt notch SCC initiation experiments.

- Determination of windows of SCC initiation susceptibility will guide follow-on conventional SCC initiation and growth test conditions.
- The electrochemical activity of T, Ω, or other phase with and without partitioning of Ag may be compared and contrasted to their function as hydrogen trapping states. Clear guidance on alloy design may emerge.

In summary, a coherent comprehensive picture of localized corrosion behavior and the transition to SCC initiation and growth will be developed.

References

1. R.G. Buchheit, Jr., J.P. Moran, F.D. Wall, and G.E. Stoner, "Rapid Anodic Dissolution Based SCC of 2090 (Al-Li-Cu) by Isolated Pit Solutions," Parkins Symposium on Fundamental Aspects of Stress Corrosion Cracking, S.M. Bruemmer, E.I. Meletis, R.H. Jones, W.W. Gerberich, F.P. Ford and R.W. Staehle, eds., TMS-AIME, Warrendale, PA, p. 141 (1992).

2. J.P. Moran R.G. Buchheit, Jr., and G.E. Stoner, "Mechanisms of SCC of Alloy 2090 (Al-Li-Cu) - A Comparison of Interpretations from Static and Slow Strain Rate Techniques," Parkins Symposium on Fundamental Aspects of Stress Corrosion Cracking, S.M. Bruemmer, E.I. Meletis, R.H. Jones, W.W. Gerberich, F.P. Ford and R.W. Staehle, eds., TMS-AIME, Warrendale, PA, p. 159 (1992).

3. R.J. Kilmer, T.J. Witters and G.E. Stoner, "Effect of Zn Additions on the Precipitation Events and Implications to Stress Corrosion Cracking Behavior in Al-Li-Cu-Mg-Zn Alloys," Proceedings of the Sixth International Al-Li Conference, M. Peters and P.J. Winkler, eds., DGM Informationsgesellschaft, Verlag. pp. 755-760 (1992).

4. R.G. Buchheit, Jr., F.D. Wall, G.E. Stoner and J.P. Moran, "Stress Corrosion Cracking of Al-Li-Cu-Zr Alloy 2090 in Aqueous Cl^- and Mixed Cl^-/CO_2^{-3} Environments," CORROSION/91, Paper No. 99, NACE, Houston, TX (1991).

5. R.J. Kilmer and G.E. Stoner, "Effect of Zn Additions on Precipitation During Aging of Alloy 8090," Scripta Metallurgica et Materialia, Vol. 25, pp. 243-248 (1991).

6. R.G. Buchheit, Jr., J.P. Moran and G.E. Stoner, "The Electrochemical Behavior of the T_1 (Al_2CuLi) Intermetallic Compound and Its Role in Localized Corrosion of Al-3Cu-2Li Alloys," Corrosion, Vol. 50, pp. 120-130 (1994).

7. R.G. Buchheit, Jr., J.P. Moran and G.E. Stoner, "Localized Corrosion Behavior of Alloy 2090-The Role of Microstructural Heterogeneity," Corrosion, Vol. 46, pp. 610-617 (1990).

8. R.G. Buchheit, Jr., F.D. Wall, G.E. Stoner and J.P. Moran, "Anodic Dissolution-Based Mechanism for the Rapid Cracking, Preexposure Phenomenon Demonstrated by Aluminum-Lithium-Copper Alloys," Corrosion, Vol. 51, pp. 417-428 (1995).

9. R.J. Kilmer and G.E. Stoner, "The Effect of Trace Additions of Zn on the Precipitation Behavior of Alloy 8090 During Artificial Aging," Proceedings, Light Weight Alloys for Aerospace Applications II, E.W. Lee, ed., TMS-AIME, Warrendale, PA, pp. 3-15, 1991.

10. S.W. Smith and J.R. Scully, "Hydrogen Trapping and Its Correlation to the Hydrogen Embrittlement Susceptibility of Al-Li-Cu-Zr Alloys," in TMS Hydrogen Effects on Materials Behavior, N.R. Moody and A.W. Thompson, eds, TMS-AIME, Warrendale, PA, in press (1995).

11. J.R. Scully, T.O. Knight, R.G. Buchheit, and D.E. Peebles, "Electrochemical Characteristics of the Al_2Cu, Al_3Ta and Al_3Zr Intermetallic Phases and Their Relevancy to the Localized Corrosion of Al Alloys," Corrosion Science, Vol. 35, pp. 185-195 (1993).

12. S.T. Pride, J.R. Scully, J.L. Hudson, "Metastable Pitting of Al and Criteria for the Transition to Stable pit Growth," J. Electrochem. Soc., 141(11), p. 3028 (1994).

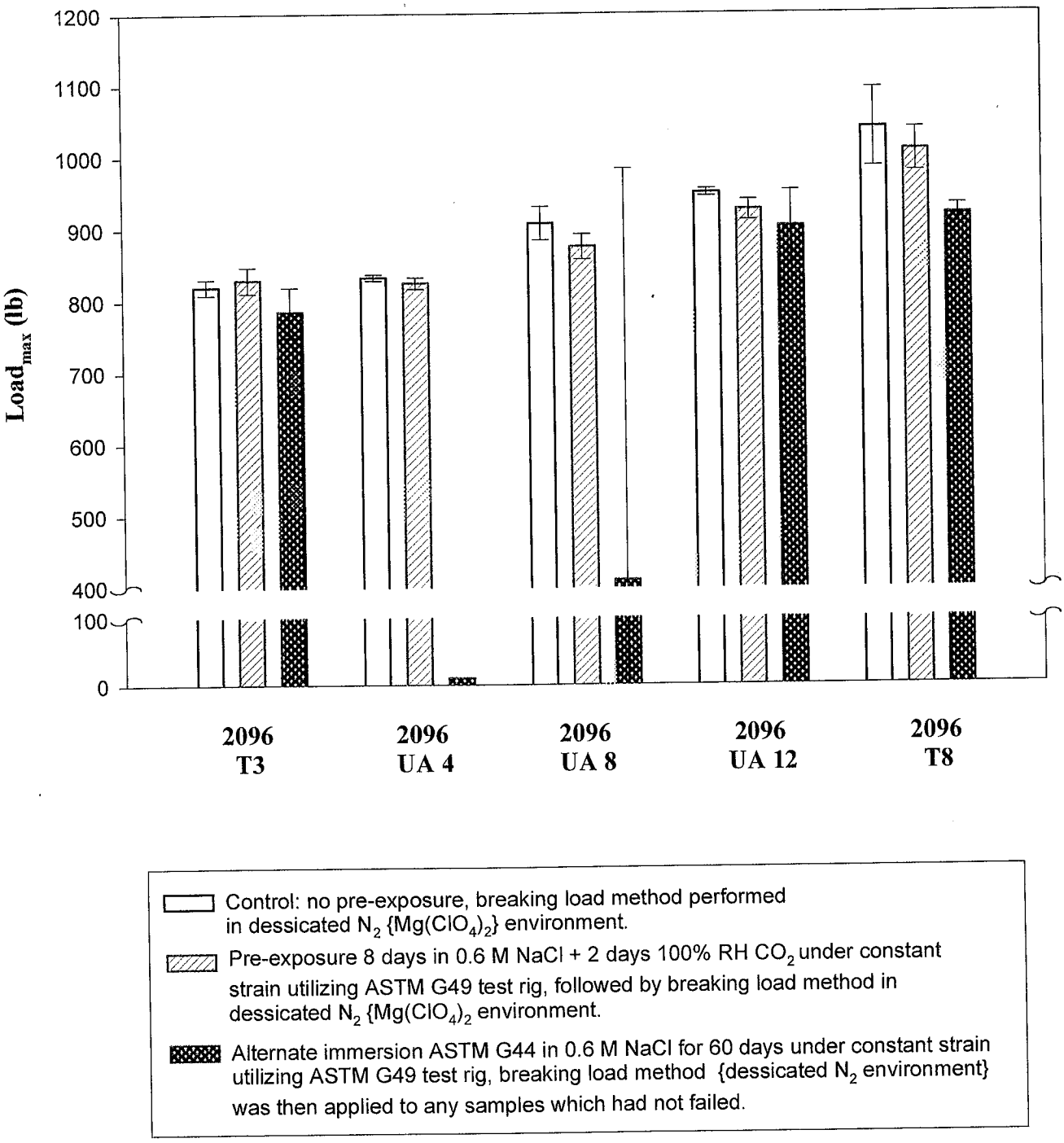

Figure 1: Environmental SCC susceptability testing performed on AA2096.

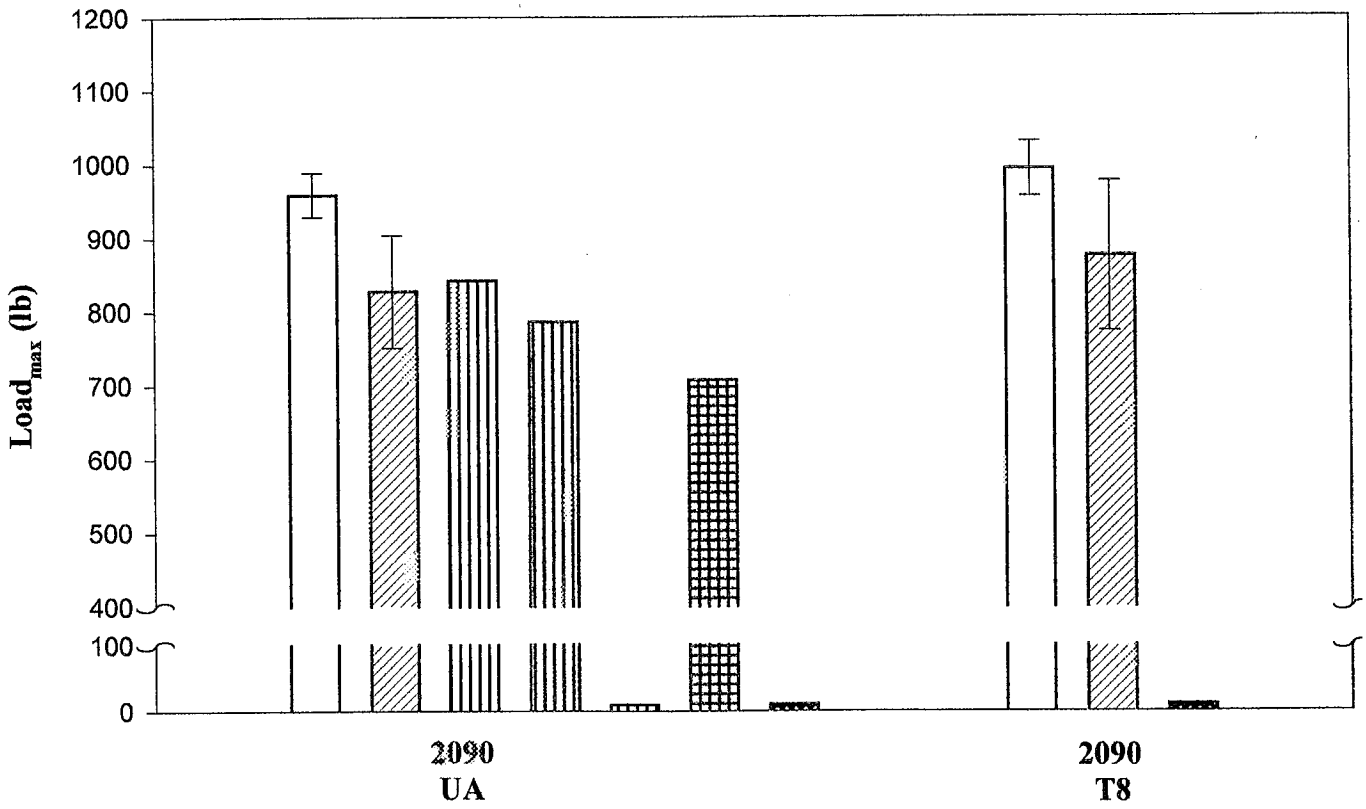

Control: no pre-exposure, breaking load method performed in dessicated N_2 {$Mg(ClO_4)_2$} environment.

Pre-exposure 8 days in 0.6 M NaCl + 2 days 100% RH CO_2 under constant strain utilizing ASTM G49 test rig, followed by breaking load method in dessicated N_2 ($Mg(ClO_4)_2$ environment.

108.4 μm maximum pit radius distributed galvanostatically upon the notch of a tensile specimen, cleaned instantaeously after electrochemical experiment, breaking load method performed in dessicated N_2 {$Mg(ClO_4)_2$} environment.

306 μm maximum pit radius distributed galvanostatically upon the notch of a tensile specimen, cleaned instantaneously after electrochemical experiment, breaking load performed in dessicated N_2 {$Mg(ClO_4)_2$} environment.

108.4 μm maximum pit radius distributed galvanostatically upon the notch of a tensile specimen, exposed to 100% RH CO_2 environment for 2 days under constant strain utilizing ASTM G49 test rig, breaking load method performed in dessicated N_2 {$Mg(ClO_4)_2$} environment.

306 μm maximum pit radius distributed galvanostatically upon the notch of a tensile specimen, exposed to 100% RH CO_2 environment for 2 days under constant strain utilizing ASTM G49 test rig, breaking load method performed in dessicated N_2 {$Mg(ClO_4)_2$} environment.

Alternate immersion ASTM G44 in 0.6 M NaCl for 60 days under constant strain utilizing ASTM G49 test rig, breaking load method {dessicated N_2 environment} was then applied to any test samples which had not failed.

Figure 2: Environmental and electrochemical SCC susceptability testing on AA2090.

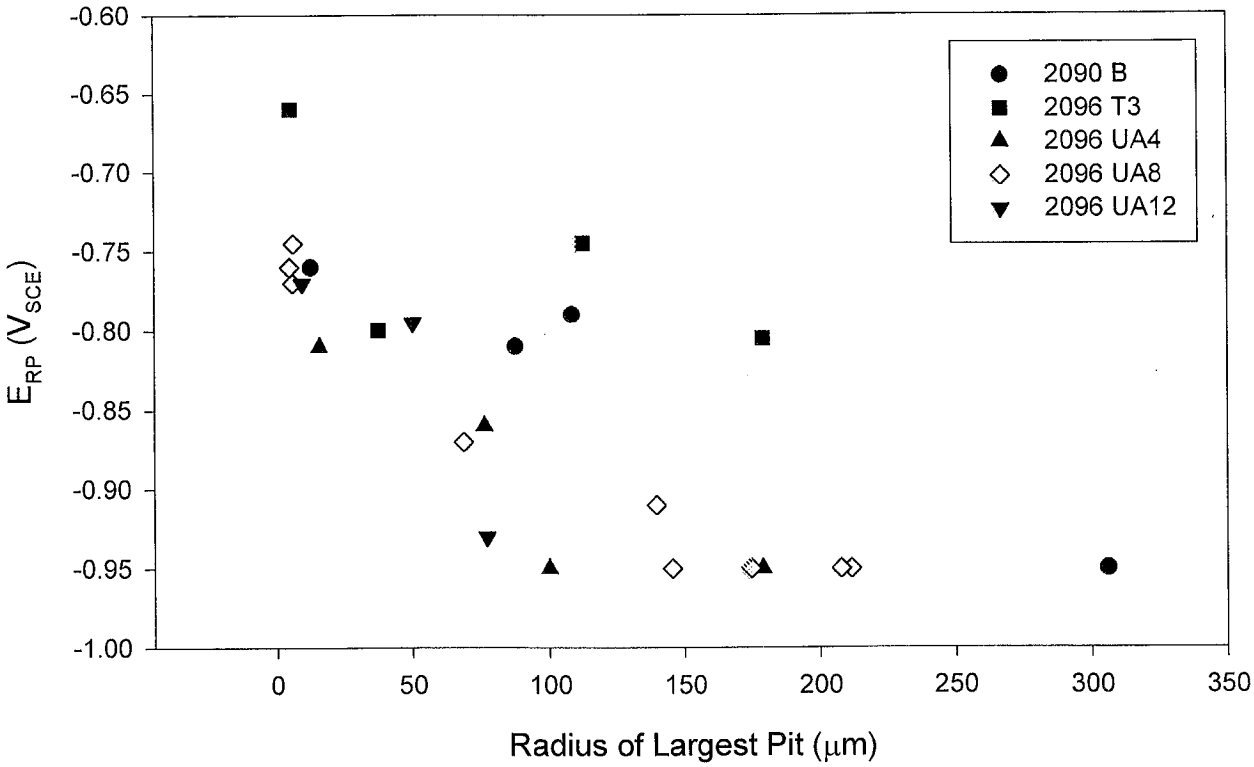

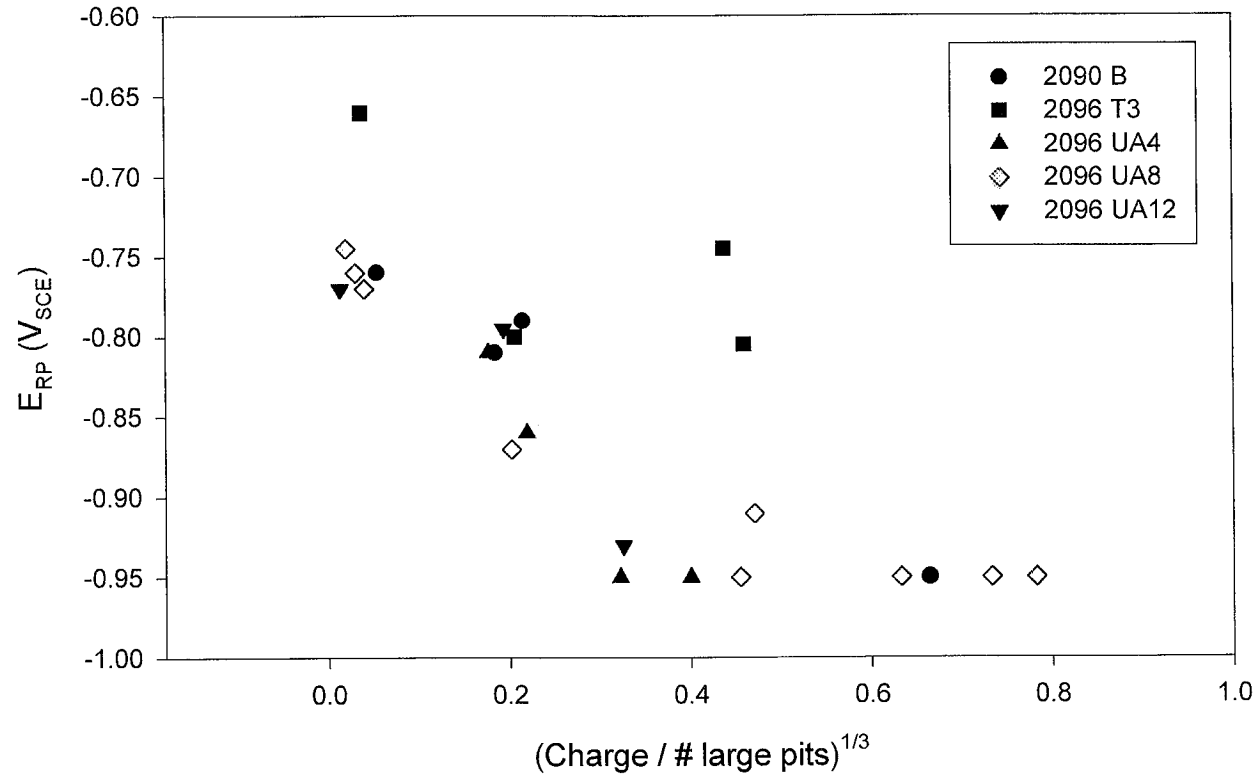

Figure 3: Comparison of the relationships between the repassivation potential (ERP), charge passed, and pit size for AA2090B, AA2096 T3, UA4, UA8, and UA12.

Project # 3: METALLURGICAL FACTORS CONTROLLING STRESS CORROSION CRACKING IN AA2096 AND C155

Faculty Investigator:	J.R. Scully
Graduate Student:	Leigh Ann Pawlick, Ph.D. Candidate
UVa Department:	MS&E
NASA-LaRC contact:	M. Domack, W.B. Lisagor (Metallic Materials)
Start Date:	May 1997
Completion Date:	December 1999

Objectives

This study seeks to characterize two selected alloys (AA 2096 with Ag; and C155 or C255 without Ag) in order to clarify the various roles of alloyed Ag and δ' particles on localized corrosion and SCC under controlled electrochemical conditions. The overall goal is to characterize stress corrosion cracking behavior including K_{ISCC} and stage II crack growth velocities as a function of aging condition using fracture mechanics-based specimens in inhibited chloride solutions (analogous to the Speidel curve). The effects of hydrogen assisted environmental cracking (HEAC), if any, will be analyzed with Thermal Desorption Spectroscopy (TDS). Moreover, we seek to examine on a fundamental level the differences between the aqueous SCC susceptibility of these two alloys or selected other Al-Li-Cu-X alloys without Ag, (should important differences be confirmed), and to understand the exact influence of Ag on SCC behavior. An inhibited chloride-containing solution (preferably non-chromate) will be selected to minimize corrosion product build upon the fracture surface which would obscure the determination of the fracture path by SEM fractography.

There is limited information on newly developed Al-Li-Cu-X alloys in regard to basic mechanical behavior, SCC resistance, and microstructure. Therefore, the immediate goals addressed over the past period of performance has been to determine the windows and conditions under which AA2096 is susceptible to SCC in comparison to similar tempers of AA 2090.

Background

The metallurgical factors governing the stress corrosion cracking behavior of emerging advanced Al-Cu-Li-Ag and Al-Cu-Li-X alloys have not been well defined. The majority of the data in the literature focuses on AA 2090 [1-5]. Mechanism and controlling microstructural features in the SCC of AA 2090 remain controversial in that several different microstructural features and mechanism have been cited as governing the SCC resistance of 2090 and 2195 [1-7]. Shearable δ', boundary T_1 anodic dissolution, precipitate hydrogen trapping and/or hydriding have all been suggested [1-11]. A strong role for Cu depletion at high angle grain boundaries was hypothesized for 2195 [6] and 2090 [7]. Li content and Cu/Li ratio are important variables in SCC initiation and growth. Formation of δ' can be suppressed at high Cu/Li ratios and low Li contents, or by Ag additions, especially with higher aging temperatures [13,14]. Alternatively, δ' formation may be promoted even in the presence of Ag by low temperature long-term aging [14]. Suppression of shearable δ' can alter the deformation mode, reducing the chance for coplanar slip through strong T_1 plate precipitates [15]. Coplanar slip can affect the likelihood of film rupture, has been shown to enhance hydrogen uptake and influences its repartitioning[11] as well as affects air fracture toughness [14]. None of these metallurgical factors have been examined for emerging advanced Al-Cu-Li-Ag and Al-Cu-Li-X alloys (e.g. 2096). Moreover, fracture mechanics-based stress corrosion cracking data such as K_{ISCC} and stage II crack growth velocities as well as quantified localized corrosion data under well-controlled electrochemical conditions in aqueous solutions are lacking for emerging alloys such as AA2096 and 2097 (or C155 and C255). Especially of interest is a better understanding of the role of silver on slip/film rupture/dissolution and/or the slip/film rupture/hydrogen-absorption/local embrittlement scenarios of stress corrosion cracking. In the case where SCC is dominated by anodic dissolution of microstructural precipitates, one may envision a scenario by which Ag promotes the formation of a high density of fine T_1 plates[13,14] which serve to resist formation of an active grain boundary dissolution path. Silver could also be enriched at α/T_1 and/or α/Ω interfaces[16,17], possibly altering their electrochemical activity and propensity for slip localization. Critical questions may also be posed concerning the role of Ag in the context of hydrogen environment assisted cracking (HEAC), either separate from or in conjunction with anodic dissolution processes. Recall that the previous NASA LA^{2}ST HEAC study has identified T_1 plates as a strong hydrogen trap site and that HEAC growth as well as hydrogen embrittlement

decoupled from aqueous dissolution occurred on high angle boundaries containing T_1, T_2 or T_b plates.[10,11] The presence of Ag located at α/T_1 or α/Ω interfaces might alter the hydrogen trap binding energy of these interfaces. It is further possible that Ag's role in promoting a high density of fine T_1 particles may disrupt the connectivity of the stress corrosion crack path regardless of the mechanistic details of SCC. Therefore, a careful examination of the effects of Ag on SCC behavior in a Al-Li-Cu alloy requires further investigation.

Technical Approach

Materials

The alloys AA 2096 (with Ag) and C155 or C255 (without Ag) were specifically chosen for this study in order to clarify the roles of Ag and δ' particles on their SCC resistance. AA2096 (2.6 Cu, 1.6 Li, 0.8 Mg, 0.18 Zr, 0.6 Ag, 0.25 Zn, wt. %) is produced by Reynolds. C155 (similar in composition to AA 2097: 2.8 Cu, 1.5 Li, 0.35 Mg, 0.16 Zr, 0.6Mn, 0.35Zn, wt. %) is produced by ALCOA. These two alloys have nearly identical Li contents and Li/Cu ratios (0.61 vs. 0.57, respectively). C155 does not contain Ag but instead contains Mn. It is recognized that Mn-containing constituents may getter some Cu in Al-Li-Cu alloys containing Mn, changing the effective Li/Cu ratio governing formation of δ', T_1 and θ" strengthening precipitates [18]. Although the Li/Cu ratio of both alloys is greater than 0.25, it may be possible to suppress δ' formation by using a slightly higher aging temperature than usual. Hence, these two alloys offer the unique opportunity to compare Ag vs non-Ag containing Al-Li-Cu-Mg materials with very similar compositions. Moreover, it may be possible to control δ' formation and, consequently, deformation mode. AA 2090 will be used as a control material.

SCC testing

The AA2096 material arrived in February of 1996 in extruded panel form, nominally 5 mm thick, in the T3 and T8 conditions. C155 has yet to be obtained from ALCOA or NASA sources. Therefore, studies during the previous year have focused on the AA2096. These included aging practice development (in conjunction with NASA LaRC), microstructural investigation by optical microscopy, and determination of mechanical properties. Since these alloys are relatively new, the most recent work has focused on determination of basic windows of SCC susceptibility in environments in which other Al-Li based alloys are known to suffer SCC. For example, a pre-exposure embrittlement phenomenon is seen in AA8090, AA7075, and AA2090.[1] Recall that stressed specimens immersed in 3.5 wt. % NaCl are susceptible to pitting corrosion but do not undergo SCC cracking. Removal into a CO_2-containing atmosphere causes rapid stress corrosion

cracking[21]. Removal into a N_2 atmosphere suppresses cracking[21]. Controversy exists as to whether the controlling mechanism is dissolution of the T_1 phase or a mixture of dissolution and hydrogen uptake [1]. In addition to these pre-exposure tests, other environments known to cause SCC (or HEAC) include stressed specimen - alternate immersion testing in NaCl (ASTM G44), and exposure to high relative humidity, water vapor saturated air (WVSA). The latter test can be conducted under room or slightly elevated temperature conditions. This test can be decoupled from aqueous dissolution by avoiding a condensed aqueous phase. For our purposes, all of theses studies were conducted on flat tensile bar specimens with a 2 mm radius "notch".[19,20] The breaking load method (on cleaned specimens in dry N_2) was utilized as a preliminary method to detect SCC crack growth after all environmental exposures (stressed at >100% of yield). This experimental approach enables determination of the windows of SCC susceptibility using a common specimen configuration that enables optical detection of SCC initiation with a long focal length microscope in a sister project on SCC *initiation* ("Mechanisms of Localized Corrosion and Stress Corrosion Crack Initiation in Advanced Al-Li-Cu Alloys" - Brian Connolly, Glenn Stoner, John R. Scully).

Research Progress during the Reporting Period

Aging response

The work over the past year focused upon the AA2096 material. NASA LaRC determined a suitable aging practice and properties for the T8 temper [18]. Various UA tempers were prepared based on aging-hardness determination studies conducted at UVa after aging the as-received T3 material for various times from 4 to 12 h at 160°C. The microstructure of various tempers has been characterized by optical microscopy,[19,20] with the typical pancake unrecrystallized grains elongated in the extrusion direction.

Preliminary assessment of SCC behavior

Figure 1 illustrates the results from breaking load method after exposure of AA 2090 and 2096 to various SCC test environments. Specimens were (I) immersed at open circuit in 0.6 M NaCl for 8 days followed by 2 day exposures in a CO_2 sparged atmosphere at 100% relative humidity, and (II) after conventional alternate immersion cycling for 60 days. The breaking load test was then utilized. Alternate immersion failures (during testing) and reciprocal times to failure (overall rate) are shown in Figures 2 and 3, respectively. AA 2096 (T-orientated) in the T3, 4, 6, 8, 10 and 12 h underaged conditions as well in the T8 condition were compared to a very SCC susceptible underaged (10h) and peak aged 2090 plate (34 mm thick plate of Moran[4,5]. S-

orientation). Additionally, exposure to WVSA at 100% relative humidity for 8 days followed by slow strain rate tensile testing in the same environment has been utilized for a few tempers (e.g. AA 2096 in the T3, UA-12 and T8 conditions). The results indicate that AA 2096 does not exhibit SCC crack initiation and growth in any of the tempers that is detectable by the breaking load method after both 100% relative humidity exposure, and the 8 day/2 day $NaCl/CO_2$ pre-exposure. In comparison, UA and PA 2090 indicated crack initiation and growth in the NaC/CO_2 preexposure test as seen in the literature[21], as well as during alternate immersion testing (Figures 2 and 3). Under the $NaCl/CO_2$ pre-exposure testing conditions, the underaged AA2090 exhibited SCC crack growth almost completely through the tensile specimen thickness. Moreover, all specimens in both the peak aged and underaged AA 2090 tempers separated (failed) during alternate immersion testing. In comparison, AA 2096 either failed in alternate immersion (Figures 2 and 3), or the presence of SCC cracks was indicated by the breaking load method after alternate immersion exposure (Figure 1) in the underaged 4, 6 and 8 h tempers. The large error bars associated with breaking loads after alternate immersion for the 8 h underaged condition are indicative of either complete failure during AI testing or low breaking loads. SEM examination confirmed SCC crack growth in the underaged 4 h specimen. In contrast, the T3, 10 and 12 hour underaged and T8 conditions of 2096 did not exhibit cracks that could be detected by the breaking load method after exposure to any SCC environment.

In summary, the results indicate that AA 2096 resists SC cracking or cracks slowly in the T3 and T8 tempers while the AA 2090 plate does not. AA 2090 clearly indicates susceptibility in both underaged and peak aged tempers (Figures 1-3). Careful re-examination of older 2090 experiments either supports this conclusion, or is inconclusive in that the breaking load method and/or metallographic crack detection were not comprehensively used to verify the presence or absence of cracking in the T3 or T8 tempers of non-failed alternate immersion specimens. Moreover, fracture toughness testing of hydrogen pre-charged AA 2090 sheet and fine grain recrystallized material indicated HE susceptibility in the T3, UA and PA tempers [10,11]. The result of the present study also indicate that the 8 day/2 day $NaCl/CO_2$ pre-exposure of stressed blunt notched specimens did not produce the necessary localized corrosion "condition" necessary to cause SCC (Figure 1) in even the most susceptible AA 2096 tempers (e.g. the 4 and 6 h underaged condition) in the alternate immersion test. In contrast, the 8 day/2 day $NaCl/CO_2$ pre-exposure produced SCC in AA 2090 (Figure 1). Moreover, times to failure in AI were much shorter (Figure 3) for AA 2090. These results suggest that AA 2090 either exhibits faster SCC crack initiation and growth than AA 2096 or that the critical localized corrosion "condition" for SCC initiation is more readily achieved in this alloy. Caution is warranted, however, since AA 2090 exhibits a much lower fracture toughness in air (e.g. <20 MPa-$\sqrt{m}$ in the T8 temper) compared to AA 2096 (e.g. 30 MPa-$\sqrt{m}$ in the T8 temper). Thus, AA 2090 will be more sensitive to the presence of cracks

when tested by the breaking load method. Tests are underway to confirm that pitting or other forms of localized corrosion damage do not produce significant load decreases in the breaking load method that could be mistaken for SCC. Moreover, all specimens are being examined by scanning electron fractography and metallographic sectioning to confirm the presence or absence of SC cracks. In addition, all trends will be confirmed by follow-up fracture mechanics-based SCC testing in precracked specimens with fatigue pre-cracks. These experiments will be guided by SCC screening results.

Comparison of AA 2090 to AA 2096: Metallurgical Factors

Apparent differences in AA 2090 and AA 2096 SCC susceptibility have been indicated, (although caution is warranted regarding possible differences in sensitivity of the breaking load to cracks as stated above). Understanding the origins of the differences in SCC susceptibility between these two alloys is of interest given the need to optimize the SCC resistance of Al-Li-Cu alloys. The results suggest that AA 2096 is most susceptible in severely underaged tempers while the AA 2090 is susceptible to SCC in both underaged and peak aged tempers and cracks more quickly. A review of Li/Cu ratios and precipitation behavior of both alloys indicates that δ', GP zones ⇙ θ', and T_1 and/or Ω phases (AA 2096) all contribute to strengthening of the peak aged tempers of both 2090 and 2096 aged isothermally at 160°C [13,14]. Of course, the volume fraction, size, morphology and, possibly, coherency of each strengthening phase differ for these alloys at each stage of the aging process. Ag is known to promote the precipitation of fine T_1 or Ω precipitates at the expense of δ' for Li concentrations from 1.1-1.4 % [13-14]. δ' is known to coarsen with aging in 2090 but remains coherent and shearable in peak aged tempers. In contrast, δ' is reported to be absent in peak aged 2095 [14]. Boundary T_1, T_2 and T_B particle formation in peak aged tempers is known to adversely affect fracture toughness of 2090 [10,11]. Does reduced cracking susceptibility in AA 2096 compared to 2090 in the T8 condition relate to an intrinsic metallurgical difference? Possible metallurgical factors include reduced slip planarity and homogenization of deformation due to fewer shearable δ' precipitates compared to strong, less shearable T_1 in peak aged 2096 [15]. Also, differences in boundary T_1 particle size, morphology, distribution, and/or Ag segregation may, subsequently, alter hydrogen trapping or electrochemical activity in 2096. Unfortunately, the comparisons are not as direct as desired. The short transverse loading of the AA2090 plate (the typically most SCC susceptible orientation) cannot be performed in the AA2096 thin sheet extrusion product form, which was loaded in a T orientation. The grain shape and textures of the two alloys may also be sufficiently different, such that the results are a manifestation of varying grain shapes and orientations relative to the stress state. It was also noted above that the fracture toughness of the two alloys differ, changing the sensitivity to the breaking load method.

Alternatively, the differences in localized corrosion susceptibility may exert a critical influence since the SCC tests conducted thus far include SCC initiation and growth stages. [see Connolly, Stoner, Scully - "Localized Corrosion and SCC Initiation in Advanced Al-Li-Cu Alloys."]. These questions will be addressed during the upcoming year.

Research Plan for 1997

In 1997 research will be divided into three closely related thrusts and will be coordinated with the LOCALIZED CORROSION AND STRESS CORROSION CRACK INITIATION IN ADVANCED AL-Li-Cu ALLOYS project (#4).

Defining the windows of SCC susceptibility for AA 2096

Additional breaking load method SCC testing will proceed to define the metallurgical, environmental, and orientation factors governing the SCC susceptibility/resistance of AA 2096. Blunt notched specimens of AA2096 in the underaged tempers in a ASTM G-44 alternate immersion test will continue for 60 days. AI testing of some underaged 2096 tempers has only proceeded for 30 days at this time. The ASTM G-44 is a relatively aggressive SCC test compared to the 8 day NaCl/2 day CO_2 preexposure test. These studies will address the issue of whether the repeated cyclic NaCl full immersion/CO_2 atmospheric exposure might provide the critical localized corrosion site depth/chemistry change, or hydrogen accumulation rate that triggers SCC of AA 2096. Alternatively, localized corrosion site depth may be achieved more rapidly by potentiostatic polarization prior to CO_2 exposure (See project #4).

Several diagnostics can be envisioned using the SCC screening methods utilized so far. Susceptible underaged tempers of AA 2096 may be examined in the L orientation to test the notion that SC cracking occurs on high angle boundaries compared to subgrain boundaries. Underaged AA 2096 may be tested after aging under conditions that suppress or minimize shearable δ'. AA 2096 and 2090 will also be tested using the blunt-notch breaking load method after longer exposure in humid air in the most susceptible tempers. Recall that exposure to high relative humidity environments facilitates hydrogen absorption and diffusional ingress, and enables decoupling of dissolution-controlled SCC from the effects of hydrogen uptake and

embrittlement. AA 2090 plate in the S orientation or T oriented sheet will continue as a control material in several environments.

The outcomes of the preliminary SCC testing will guide future SCC testing. Moreover, the outcome of these tests will guide SCC initiation tests to be addressed by Connolly in LOCALIZED CORROSION AND STRESS CORROSION CRACK INITIATION IN ADVANCED AL-Li-Cu ALLOYS (Project #4)

The role of hydrogen in SCC

The ability of Ag to modify hydrogen uptake, diffusion and trapping will be investigated using thermal desorption spectroscopy (TDS) in this project. The extent of TDS testing pursued will be guided by the outcome of SCC testing of AA 2090-UA and AA 2096 in moist air which will decouple and examine the role of hydrogen. Recall that hydrogen trapping at high angle grain boundaries was implicated along with grain shape as governing factors in the hydrogen embrittlement of AA 2090[10,11]. TDS testing may also shed light on the role of hydrogen ingress in NaCl/CO_2 pre-exposure testing. Recall that NaCl pre-exposure followed by atmospheric exposure in N_2 suppresses SCC. Does this environment also suppress hydrogen uptake, already known to be severe in after alternate immersion exposure?

SCC propagation from pre-existing fatigue precracks

Preliminary technique development will begin in 1997 with the aim of developing a fatigue pre-cracked specimen design for AA 2096. Since the extrusion can not be testing using an ST or SL double cantilever beam specimen, efforts will focus on either a compact tension specimen or single edge notched sample. The single edge notch specimen will likely consist of a T oriented tensile bar with a TL or TS fatigue pre-crack grown from a EDM notch or diamond saw cut.[22, 23] Preliminary testing will consist of fatigue precracking specimens and exposing them to selected environments guided by the SCC results discussed above using the breaking load method. Crack length and approximate growth rates will be accomplished by replication, photomicroscopy, or post-test destructive analysis. At a later stage, SCC growth test specimens (in the third year of this program) will be instrumented for real time direct current potential drop monitoring of crack

growth.[24] This will not be accomplished in this up-coming year. AA 2090 material may be used to aid in technique development.

References

1. R.G. Buchheit, F.D. Wall, G.E. Stoner, and J.P. Moran, Corrosion, vol. 51, no. 6, pp. 417 428, 1995.

2. R.G. Buchheit, "Mechanisms of Localized Aqueous Corrosion in Aluminum-Lithium Copper Alloys", Ph.D. Thesis Dissertation, University of Virginia, January 1991.

3. R.G. Buchheit, J.P. Moran, F.D. Wall, G.E. Stoner, "Rapid Anodic Dissolution Based SCC of an Al-Li-Cu Alloy by Isolated Pit Solutions," Parkins Symposium on Fundamental Aspects of Stress Corrosion Cracking, edited by S.M. Bruemmer, E.I. Meletis, R.H. Jones, W.W. Geberich, F.P. Ford, and R.W. Staehle, pp. 141-158, 1992.

4. J.P. Moran, "Mechanisms of Localized Corrosion and Stress Corrosion Cracking of an Al-Li-Cu Alloy 2090", Ph.D. Thesis Dissertation, University of Virginia, January 1990.

5. J.P. Moran,R.G. Buchheit, G.E. Stoner, "Mechanisms of SCC of Alloy 2090 (Al-Li-Cu) - A Comparison of Interpretations from Static and Slow Strain Rate Techniques," Parkins Symposium on Fundamental Aspects of Stress Corrosion Cracking, edited by S.M. Bruemmer, E.I. Meletis, R.H. Jones, W.W. Geberich, F.P. Ford, and R.W. Staehle, pp. 159-170, 1992.

6. F.D. Wall, Jr., "Mechanisms of environmentally Assisted Cracking in Al-Li-Cu Alloys 2090 and 2095", Ph.D. Thesis Dissertation, University of Virginia, January 1996.

7. C. Kumai, J. Kusinski, G. Thomas, T.M. Devine, "Influence of Aging at 200°C on the Corrosion Resistance of Al-Li and Al-Li-Cu Alloys," Corrosion J., 45, pp. 294-302, 1989.

8. A.K. Vesudevan, J. Liu, R.E. Ricker "Mechanisms of SCC growth resistance of Al-Li-Cu Alloys: Role of Grain Boundary Precipitates," In Env. Degradation of Eng. Materials III, eds. M.R. Louthan, Jr., R.P. McNitt, R.D. Sisson, Jr., pp. 321-327, 1987.

9. R. Balasubramaniam, D.J. Duquette, K. Rajan, "On SCC in Al-Li Alloys," Acta. Metall. Mater. 39, pp. 2597-2605, 1991.

10. S.W. Smith, "Hydrogen Interactions and Their Correlation to the Hydrogen Embrittlement Susceptibility of Al-Li-Cu-Zr Alloys," Ph.D. Thesis Dissertation, University of Virginia, May 1995.

11. S.W. Smith, J.R. Scully, "Hydrogen Trapping and Its Correlation to the Hydrogen Embrittlement Susceptibility of Al-Li-Cu-Zr Alloys", TMS Conference on Hydrogen in Metals, Jackson, Wyoming, 1994.

12. J.M. Silcock, J. Inst. of Metals, 88, pp. 357-364, 1959-60.

13. J.R. Pickens, K.S. Kumar, S.A. Brown, and F.W. Gayle, "Evaluation of the Microstructure of Al-Cu-Li-Ag-Mg Weldalite Alloys", NASA Contractor report 4386, 1991.

14. C.P. Blankenship, Jr., and E.A. Starke, Jr., Acta Metall., 42, pp. 845-855, 1994.

15. C.P. Blankenship, Jr., E. Hornbogen, E.A. Starke, Jr., "Predicting Slip Behavior in Alloys Containing Shearable and Strong Particles," Materials Science and Engineering, A169, pp. 33-41, 1993.

16. K. Hono, et al., Acta Metall., 41, pp. 829-838, 1993.

17. J.M. Howe, Private communication, U.Va., September, 1994

18. Personal Communication with Dr. Edgar Starke, University of Virginia, 1996.

19. NASA LaRC report, June 29, 1996.

20. NASA LaRC report, January, 1996.

21. J.G. Craig, R.C. Newman, M.R. Jarrett, and N.J.H. Holroyd, "Critical Chemistry of Stress-Corrosion Cracking in Al-Li-Cu-Mg Alloys," J. de Physique, 48, pp. C3-825-C3/833, 1987.

22. J.C. Newman Jr., and I.S. Raju, Engineering Fracture Mechanistic, 15, pp. 185-192, 1981.

23. J.C. Newman Jr., In Small Crack Test Methods, ASTM 1149, J. Larsen, J.E. Allison, Eds., ASTM, Philadelphia, pp. 6-33, 1992.

24. R.P. Gangloff, et al., In Small Crack Test Methods, ASTM 1149, J. Larsen, J.E. Allison, Eds., ASTM, Philadelphia, pp. 116-168, 1992.

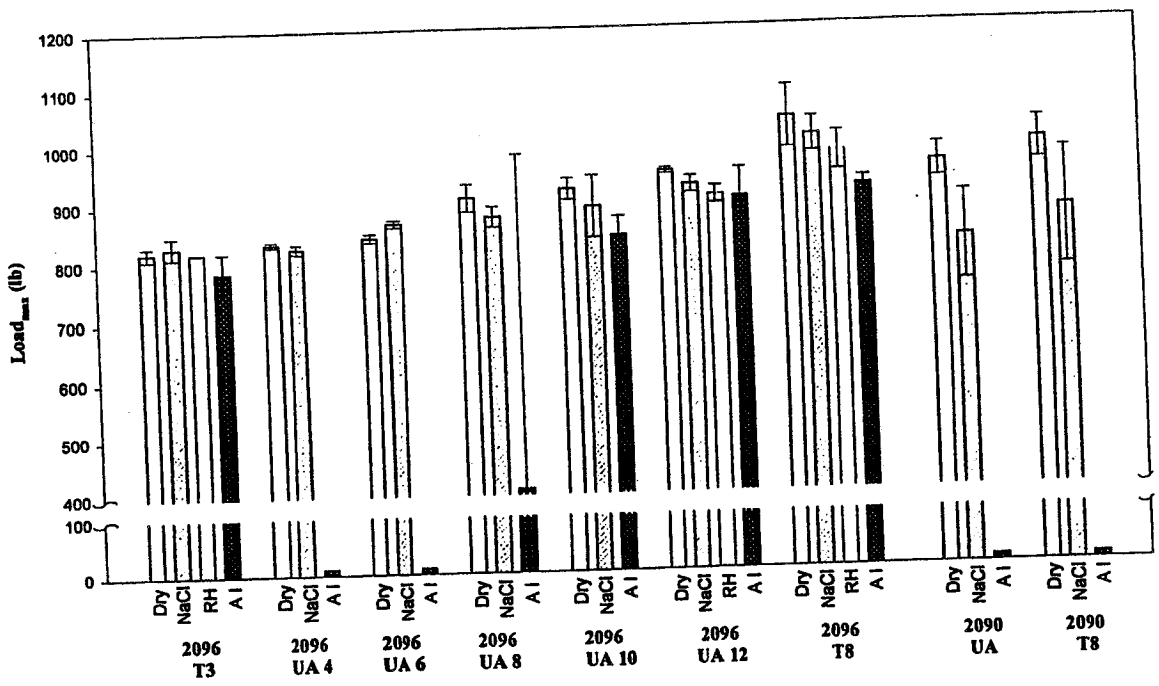

Dry: No pre-exposure, tensile testing in dessicated (Mg-perchlorate) N_2
NaCl: Pre-exposure 8 days in 0.6 M NaCl + 2 days 100% RH CO_2, tensile testing in dessicated (Mg-perchlorate) N_2
RH: Pre-exposure 8 days in 100% RH, tensile testing in 100% RH
A I : Alternate immersion 0.6 M NaCl (60 days)

Figure 1. Results of breaking load testing on blunt notched tensile specimens machined from AA2096 extrusions (T-orientation) and AA 2090 plate (S-orientation) subjected to various environments compared to the dry air baseline breaking loads. Note that complete failure in alternate immersion testing is indicated by breaking loads of zero.

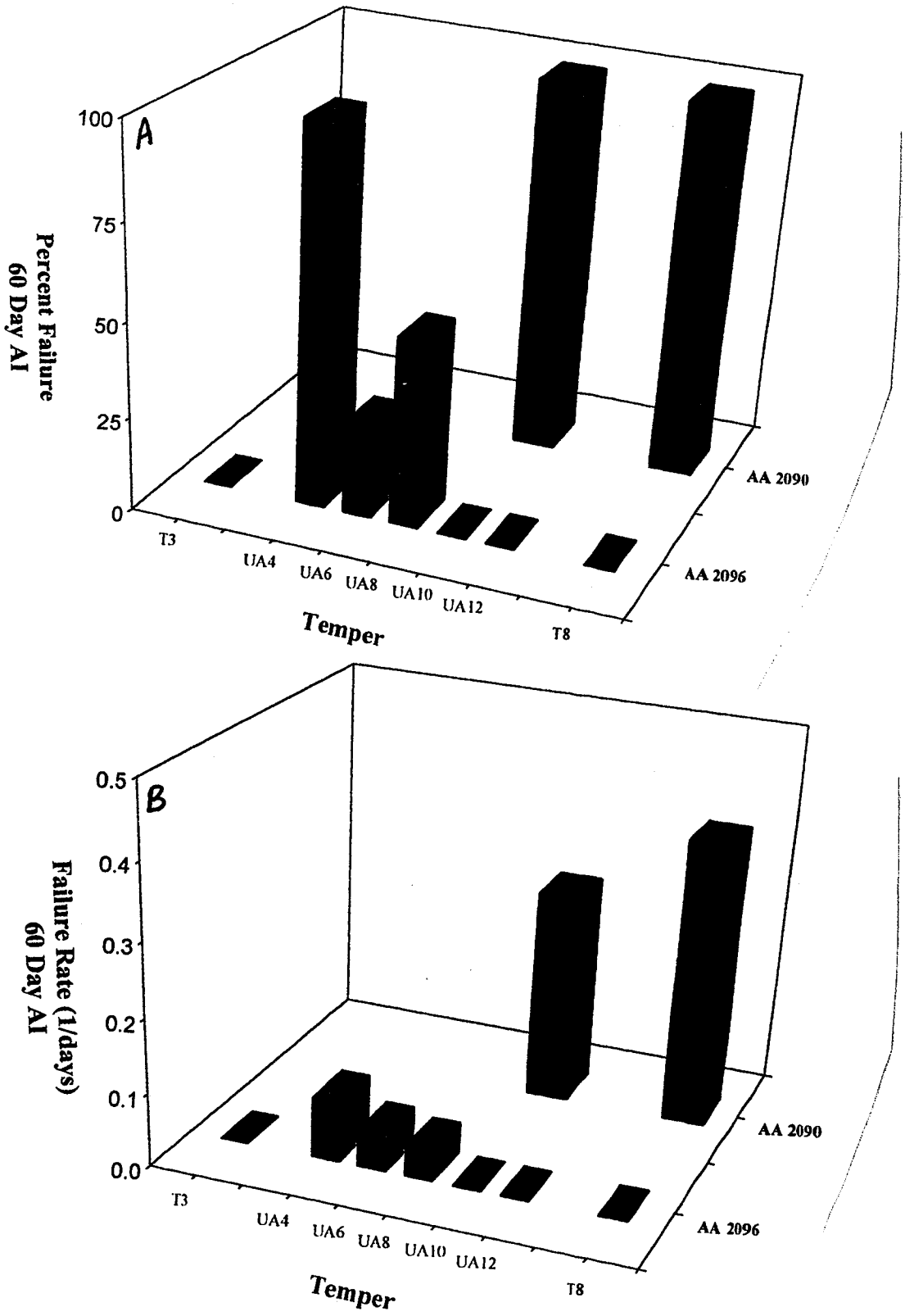

Figure 2. Results of alternate immersion testing on blunt notched tensile specimens machined from AA2096 extrusions (T-orientation) and AA 2090 plate (S-orientation) subjected to the ASTM G-44 test environment. (a) % of failed specimens for the indicated condition, (b) Failure rate as indicated by reciprocal total failure times including initiation and propagation stages of SCC.

Project #4A: MECHANISMS OF DEFORMATION AND FRACTURE IN HIGH STRENGTH TITANIUM ALLOYS: EFFECTS OF TEMPERATURE AND HYDROGEN

Faculty Investigator: R.P. Gangloff
Graduate Assistant: Sean P. Hayes

Reported in (HSR) report

Project #4B: MECHANISMS OF DEFORMATION AND FRACTURE IN HIGH STRENGTH TITANIUM ALLOYS: EFFECTS OF TEMPERATURE AND MICROSTRUCTURE

Faculty Investigator: E.A. Starke, Jr.
Graduate Assistant: Susan M. Kazanjian
Post Doctoral Fellow: Hinrich Hargarter

Reported in (HSR report)

Project #5: DETERMINATION OF THE CORROSIVE SPECIES FOUND WITHIN AIRCRAFT LAP-SPLICE JOINTS

Faculty Investigator:	R.G. Kelly
Graduate Assistant:	Karen S. Lewis (M.S. Candidate, 8/96)
Estimated completion:	5/98

Research Objectives

The first objective of this research is to characterize the chemical composition of solutions from corroded aircraft lap-splice joints. This knowledge will allow for the creation of a more accurate simulant environment for future laboratory studies of corrosion and cracking of aerospace aluminum alloys. Capillary electrophoresis is used to identify and quantitate the ionic species present and electrochemical testing will be used to determine the importance of each of these species in corrosion of AA 2024-T3. Once the simulant composition is determined, it will be used to develop a model that will help determine corrosion rates within lap-splice joints.

Background and Approach

As the fleet of both civilian and military aircraft ages, the need for accurate predictive corrosion models becomes increasingly important. Occluded sites on aircraft represent a particularly important modeling need due to the changes which occur in the local chemistry during corrosion. The region of overlap between the inner and outer skins, known as the lap-splice joint, has been shown to suffer extensive corrosion in some cases. The first step in the development of a predictive model for such joints is an understanding of the solutions that evolve within these joints during service.

Samples, obtained by scraping corrosion products from a riveted joints into sterile Petri dishes with a cut glass rod, were received from Dr. Robert Piascik of NASA-LaRC. These samples were soaked in two milliliters of 18 MΩ-cm water for 24 hours to allow time for the soluble species to redissolve. This solution was then filtered and 0.2 milliliter was placed into a vial for analysis. Capillary electrophoresis was performed using four different electrolytes. Two of these detected anions (chromate and phosphate) and the other two detected cations (UVCat1 and UVCat2). Each electrolyte allowed for detection of some species that did not appear in the others such as aluminum in UVCat2 and organic acids in phosphate. The use of two electrolytes

for each type of ion also allowed for comparison of the concentrations when an ion can be detected in both. For example, chloride can be detected by both chromate and phosphate. Interspersed among the samples were standards and high purity water. The standards allowed for quantitation of the species seen in the electropherograms. Knowing the concentrations of each of the ions present in the solutions allowed for electroneutrality calculations to be performed. From these, the pH of the solution can be estimated. This solution can then be made up in bulk to saturation using the appropriate salts. Because the volume of the original solution inside the lap-splice joint is not known, a solution would be first made in low concentrations using the experimentally determined concentration ratios. The amounts of all of the species would then be increased, while keeping the concentration ratios constant. When the first precipitate appears, the solution is deemed saturated because adding any more of any of the salts would change the concentration ratios. Due to the low solubility of several of the species, the lap-splice joint is thought to be saturated with respect to the least soluble species. Electrochemical tests that include an open circuit and a potentiodynamic scan are then performed on a sample of AA 2024-T3 in this proposed solution. This approach will give an estimate of the corrosion rate within the joint during service.

Progress During the Reporting Period

Two sample sets have been received in the past four months. Both of them were obtained from riveted joints on commercial DC-9 aircraft. The first set was obtained in November 1996 and the second in January 1997. The first set, containing eight samples, has been analyzed by capillary electrophoresis in each of the four electrolytes. One goal of this sample set was to determine the best technique for obtaining the samples. It contained four samples from the scraping method described above and four obtained by placing water on the corroded surface, waiting a several minutes, and then collecting that water with a filter paper. These filter papers were later soaked in water and analysis samples were collected in the same manner as the scraping samples. The other goals of these analyses were to look at the samples qualitatively and to do approximate quantitative work. All of the peaks in the electropherograms have been identified using spiking, a process by which a small amount of the suspected ion is added to the sample. If the peak size increases, then the ion is positively identified. There was some variation

among each of the eight samples, but several ions were present in every sample. These ions are sodium, aluminum, magnesium, potassium, calcium, chloride, nitrite, and sulfate. A majority of the samples also contained nitrate, phosphate, and carbonate. Due to the lack of a priori knowledge of the presence and variation in the quantity of each of these species in the solution, insufficient standards were analyzed initially. Best practice dictates that the standards be run in the same sample set as the unknowns, but in the present case several were run later. This course of events meant that the quantitation is only approximate for this set. The following two charts concentration ratios of each of the ionic species found in the first sample set using sodium and chloride as bases.

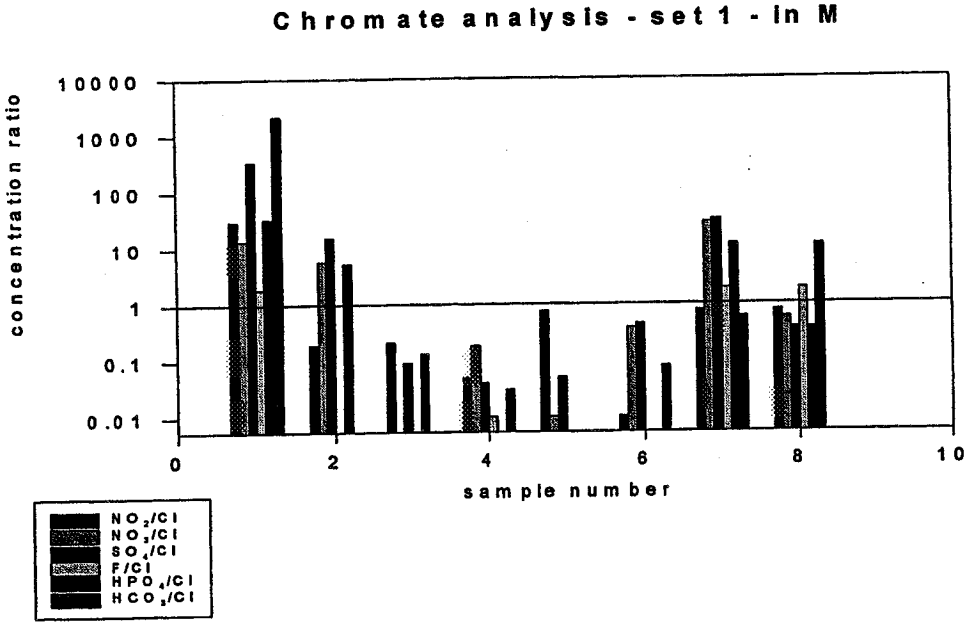

The above chart is an anion analysis performed in chromate electrolyte. The concentration ratios were calculated using the molar concentrations of each of the species. Any ratios above the line at one indicates that more of that species was present than of chloride. Nitrate, sulfate, and phosphate were the ions most often present in greater concentration than chloride. The following chart shows results from a cation analysis performed in UVCat2. Concentrations above the line at one indicate more of that species than of sodium. Potassium is almost always in greater concentration than sodium.

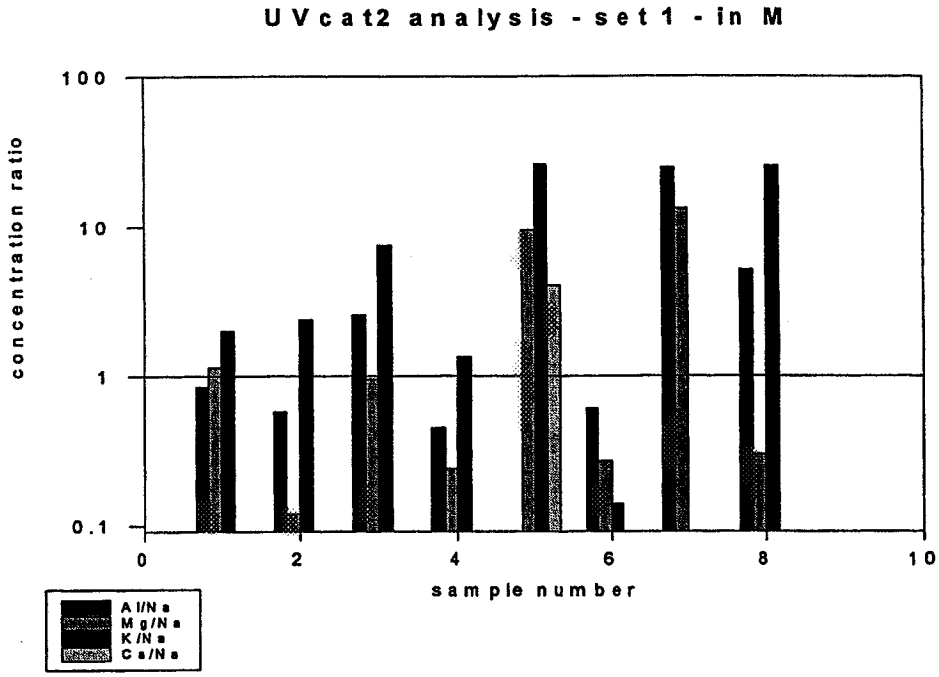

Electroneutrality calculations for this set show that the majority of the sample solutions have a pH of 10 to 11. This result was the expected value due to some preliminary research on this topic performed by Maria Inman.[1] However, three of the eight samples have a calculated pH value of 2 to 3. Aluminum is amphoteric (corrodes at both low and high pH values). Both acid[2] and alkaline[3] pH values have been measured at localized corrosion sites. All three of the samples calculated to have low pH were obtained by scraping. The effect of the sampling method on the results obtained remains to be understood.

Analysis has begun on the second sample set containing 16 samples all obtained by scraping. One cation (UVCat2) and one anion (chromate) electrolyte have provided preliminary results. These samples contain the same ions seen in the first set plus one or two additional anions that are yet to be identified. This result is favorable for forming a future model because it demonstrates that a majority of species will be present in all samples. Current work is being done to quantitate these samples and identify the unknowns. The chromate samples are being spiked and all of the samples are being diluted to values within the calibration and hence the quantitation range. Simultaneously, these samples are also being analyzed using the other two electrolytes.

Conclusions

The first sample set has shown that there are many ions present in the solutions that enter into aircraft lap-splice joints. These results question the applicability of corrosion models performed in acidified 3.5% sodium chloride solution. Several ions including potassium, nitrate, sulfate, and phosphate often occur in greater concentration than sodium and chloride. The observed consistency between samples is also important because it will allow for a more certain future model.

It has also been noticed that the ratio of magnesium to aluminum in our samples is much higher than the known ratio of (1:51.3) in a AA 2024-T3 metal. In contrast, the average ratio for the experimental set is (1:1.7) with a range from (1:0.7) to (1:4.8). The aluminum concentration is low, as expected, because of the formation of insoluble aluminum hydroxide. The high magnesium concentration may mean that all of the magnesium that has corroded from the alloy is being detected. If this can be proven, it may lead to a means to estimate alloy dissolution rates. Faraday's second law states that the number of gram atoms lost to corrosion equals the total current (I) times the time (t) divided by the valence change (n) and Faraday's constant (F). The experimental magnesium concentration could be converted into the number of gram atoms lost and the time could be estimated. This information would allow for the calculation of the average current which is proportional to the dissolution rate.

Tasks for Next Reporting Period

The primary goal is to have a first "best guess" for the solution composition prepared by June 1997. This solution will then be recreated for electrochemical and corrosion fatigue testing on AA 2024-T3. The immediate goals of this project focus on finishing the analysis of the second sample set. This work includes performing capillary electrophoresis on each of the samples in the two remaining electrolytes and quantitating all of this data. Due to the knowledge gained from the first set, better standard selection and dilution procedures will lead to more accurate quantitative information. As all of these samples were collected by scraping, the electroneutrality calculations on this better quantified data will be important.

It is also possible for more sample sets to be received in the next six months. A program for collection of these samples by the personnel that work with the corroding aircraft is being

developed. Under this program, willing sites will receive kits that contain all of the necessary materials for sample collection including collection containers (currently Petri dishes), a scraper, gloves, and a wash bottle containing 18 MΩ-cm water. The primary difficulty in sample collection is the need for no contamination of the sample. Capillary electrophoresis is capable of detecting ions to the part per billion range and is therefore very sensitive to any contaminants.

Other work will include testing the theory of magnesium dissolution. This will require dissolving a known amount of alloy with a known composition in concentrated sodium hydroxide solution. This solution will then be evaporated to dryness, rehydrated, and analyzed with capillary electrophoresis for magnesium. There are several possible results that may be obtained from performing this test. One result may be that not all of the magnesium will dissolve during the rehydration procedure. This result could be due to the kinetics of dissolution or magnesium may form an insoluble salt similar to aluminum hydroxide. Another possible result is that the magnesium may be difficult to detect due to a high concentration of sodium. Magnesium and sodium have similar migration times and large dilutions are often necessary for both of them to be detected. If the magnesium concentration is not high enough, its absorbance peak might be lost in the dilutions. If this second possibility becomes problematic, potassium hydroxide (potassium migrates about one minute earlier than sodium or magnesium) could be substituted or the ratio of magnesium to sodium increased.

References

[1] M. E. Inman, R. G. Kelly, S. A. Willard, R. S. Piascik, "Coordinated Metallographic, Chemical and Electrochemical Analyses of Fuselage Lap Splice Corrosion," Proc. of the ASIP Conference, Atlanta (submitted August, 1996).

[2]F. D. Wall, "Mechanisms of Environmentally Assisted Cracking in Al-Li-Cu Alloys 2090 and 2095," Ph.D. Dissertation, University of Virginia, p. 6 (January, 1996).

[3]Ibid.

Project #6: EVALUATION OF WIDE-PANEL ALUMINUM ALLOY EXTRUSIONS

Faculty Investigator: John A. Wert
Graduate Student: Mark T. Lyttle; Ph. D. Candidate
UVa Department: MS&E
NASA-LaRC Contact: Steve Hales (Metallic Materials)
Start Date: January, 1994
Anticipated Completion Date: May 1997

Research Objectives

The overall objective of this project is to experimentally observe and model the effects of microstructure and texture on yield strength in wide panel aluminum alloy extrusions. The modeling results will enable the prediction of locations and tensile axis orientations corresponding to minimum yield strength where localized yielding could occur in service. A generalized form of these models can be applied to any combination of microstructure and texture found in other aluminum alloys.

Background and Approach

Tubular aluminum extrusions with integral stiffeners offer a possibility of reducing the cost and improving the performance of stiffened panels found in many types of aerospace vehicles. The manufacturing process developed in the former Soviet Union and now under study in a variety of laboratories worldwide involves extrusion of tubular forms with longitudinal L-shaped stiffeners protruding from the outer surface. The extruded tube is slit longitudinally and flattened in a series of rolling and stretching operations. The final product is a wide, flat panel with integral stiffeners on one side. The integrally stiffened panels may provide an economical alternative to conventional riveted or adhesively bonded aircraft and launch vehicle structures.

Although the integrally stiffened panels offer an economical method for fabricating stiffened panels, there are issues related to panel performance in service that remain unresolved. The manufacturing operations described above result in complex metal flow patterns in many portions of the panel, creating microstructure and crystallographic texture characteristics that are far different from those found in conventional rolled aluminum sheet products. This is especially true in the vicinity of the stiffeners where the metal flow pattern during extrusion and flattening

operations varies greatly over short distances (on the order of several millimeters). Since mechanical properties depend on microstructure and texture, the mechanical properties also vary with location in the panels, particularly in the vicinity of the stiffeners. Thus, there may be small regions of the material which have yield strengths considerably different than the skin region between the stiffeners. In addition, substantial out-of-plane loading will occur in the vicinity of the stiffeners, and the variation of yield strength with direction is an important consideration also. These considerations indicate that an understanding of the dependence of mechanical properties as a function of both location and loading direction in the panels is needed for efficient and safe use of wide-panel aluminum alloy extrusions in aerospace vehicles.

Work on the present project is addressing these questions through a combination of experimental measurements and modeling of the influence of microstructure and texture on tensile properties. Four aspects of the material are being characterized experimentally at selected locations: texture, grain morphology, deformation substructure, and precipitate morphology. These characteristics are incorporated into previously developed models that predict yield strength based on individual characteristics. Although the individual models have been developed by previous investigators, some refinement of the separate models has been undertaken with the scope of the present investigation. Further, the models have been blended in such a way that the contributions of various factors to yield strength and yield strength anisotropy can be evaluated as functions of location and stress axis orientation for the selected alloy. The model is being tested and refined by comparison with tensile test results generated by NASA, ALCOA, and by additional tests at UVa.

The model is capable of predicting the extreme values of yield strength, and the associated stress axis orientations, as a function of location in and near the stiffeners. These results can then be used to define limiting load conditions for the panels such that localized yielding is avoided. It is possible that the results could also be used to recommend changes in processing conditions (for example: extrusion temperature, die geometry, or flattening procedure) that would raise the minimum yield strength or change its stress axis orientation, resulting in improved panel performance.

A major goal of this research is to predict yield strength and yield strength anisotropy from microstructural characteristics and texture. Models based on fundamental principles now

exist for understanding the contribution of precipitate particles, solute in solid solution and dislocation substructure to yield strength [1-3]. However, as a result of the complexity of microstructural features found in real engineering materials, synthesis of these various strengthening mechanisms into a unified model that can accurately predict yield strength anisotropy has not been previously described.

The two primary microstructural characteristics that influence yield strength anisotropy are slip plane orientation and precipitate morphology and orientation. Evaluation of the additional factors, such as grain morphology, reveals that they have a secondary influence on yield anisotropy in the alloys under consideration. As a result, microstructure characterization has been focused on the two main factors:

1. Texture measurements enable Taylor/Bishop-Hill yield anisotropy predictions for both in-plane and out-of-plane tensile axis orientations. Using texture results obtained from pole figure data, a set of grains representative of the orientations present in each area of the extrusion is generated. Combining Taylor/Bishop-Hill analyses with the representative set of grains, the active set of slip systems and corresponding Taylor factor in each grain is determined. Averaging over all grains yields the average Taylor factor for the specified uniaxial stress orientation.
2. Microstructural assessment by TEM reveals the precipitate type, size, habit plane, volume fraction, and morphology as a function of location. Since the dislocation substructure is inhomogeneous, the precipitate characteristics may vary as a function of location within the extrusions. The precipitate characteristics at each location are inserted into the appropriate precipitate strengthening model to assess the contribution of precipitate strengthening to yield strength and yield strength anisotropy.

Progress During the Reporting Period

This progress report describes a series of yield strength observations made from the AA2096 and AA2195 integrally stiffened extrusions in which the texture and precipitate volume fractions vary with location. Comparison of the experimental observations with model predictions provides insight into the influence of precipitates on yield anisotropy, and into the

relative contributions of the matrix texture and multiple precipitate types to yield strength anisotropy.

Table 1. Composition of Extrusions (weight %)

	Cu	Li	Mg	Ag	Zr
AA2090 T86	2.8	2.2			0.12
AA2195 T3	4.10	0.98	0.43	0.46	0.12
AA2096 T3	2.78	1.38	0.50	0.30	0.14

Extrusions of three different aluminum alloys were provided by NASA Langley. The net shape extrusions were in the form shown schematically in Figure 1. The composition of the extrusion is listed with their as-received heat treatments in Table 1. Comprehensive experimental and modeling results from the AA2090 extrusion have been discussed in previous progress results and the significant results have been published [4]. During the present reporting period, compression testing of the skin, cap, and web regions in all of the extrusions has been completed. The plastic anisotropy of the AA2195 and AA2096 extrusions has been characterized and compared to the results from the AA2090 extrusion.

Of the six regions evaluated in the AA2195 and AA2096 extrusions, all had textures similar to a typical aluminum alloy rolling texture. In all regions, the predominant texture components were spread along the Euler-space fiber defined by the copper and brass type textures. Variations in texture among the regions investigated was limited to relative intensities of the copper and brass components. No other significant texture components were observed. In the web and cap regions, the pole figures exhibited nearly orthorhombic sample symmetry, but were distinctly rotated about the short transverse direction. This deviation from a standard orthorhombic pole figure is predicted to cause an asymmetric plastic anisotropy (yield strength variation is different for tensile axis orientations in the ranges 0° to 90° and 0° to -90° relative to the extrusion direction).

Figures 2-7 show the experimentally determined variation in yield strength for the skin, cap, and web regions of the AA2195 and AA2096 extrusions. Duplicate tests were performed for each orientation and the values given in the figures represent an average of the 2 tests. All the regions exhibit a yield anisotropy similar to that observed in fcc metals and alloys with a

mixture of copper and brass texture components. Yield strength maxima are observed at 0° and 90°, and a minimum is observed between 45° to 60°.

Measurements were made from -90° to 90° in the AA2195 web region to test the model prediction in a region expected to produce an asymmetric yield strength variation. The average experimental yield strengths for the AA2195 web region are shown with the Taylor factor model predictions superposed in Figure 8. The model correctly predicts the asymmetry in that that every positive orientation is weaker than the corresponding negative orientation. The Taylor factor model predicts the yield strength maxima at 0° and -75°, and the yield strength minima at 60° and -60°.

A comparison of the experimental yield strength values and the Taylor factor model for all regions is shown in Table 2. There is a good agreement between the predicted Taylor factor and the experimental results. Microstructural characterization has not yet been performed, but as indicated by the AA2090 results, the inclusion models can only improve the prediction of Taylor factor alone.

Table 2. Correlation coefficient and standard deviation of the error between the prediction of the Taylor factor model and experimental results for AA2195 and AA2096.

Region	ρ^2 (Taylor factor)	Standard Deviation (Taylor factor)
AA2195 Skin	0.53	13 MPa
AA2195 Cap	0.84	29 MPa
AA2195 Web	0.84	9 MPa
AA2096 Skin	0.26	18 MPa
AA2096 Cap	0.66	9 MPa
AA2096 Web	0.73	11 MPa

In addition to considerable experimental evaluation to determine the yield anisotropy of the AA2195 and AA2096 extrusions, additional progress was made with the plastic and elastic inclusion models. These models evaluate the interactions between the strain increment imposed on the sample and the strain increment experienced by the precipitate particles. The orientation of plate-shaped precipitate particles relative to the sample axes depends on both the habit plane and the grain orientation relative to the sample axes. Previous investigators and earlier

implementations of the plastic and elastic inclusion models in the current study have relied on computational methods to perform the matrix manipulations needed to determine the contributions to strengthening by precipitates in grains of various orientations. For the case of plate shaped precipitates, closed-form analytical expressions for the precipitate strengthening contribution have been derived for the plastic and elastic inclusion models. These expression considerably simplify the determination of precipitate contributions to yield strength anisotropy and, for the first time, provide a simple way to understand the source of differences between the yield anisotropy predictions of elastic and plastic inclusion models.

Finally, contributions have also been made to a related program being conduced by H. Hargarter and E.A. Starke. In this cooperative effort, the effects of selective formation of certain precipitate variants has been explored. This cooperative work resulted in a joint paper presented at the TMS/ASM Materials Week '96 in October 1996.

Conclusions

1. The plastic inclusion model, incorporating grain morphology and precipitate characteristics, accurately predicts the yield anisotropy observed in all the regions tested in the three extrusions. Advantages of quantitatively modeling of yield anisotropy include the ability to evaluate anisotropy contributions from various sources, such as multiple precipitate types and matrix texture vs precipitate effects, and to consider non-orthorhombic sample symmetry.
2. All of the regions in the AA2195 and AA2096 extrusions exhibit plastic anisotropy that is similar to that of a typical deformation texture. In these cases, Taylor factor is an adequate predictor of the true anisotropy, although use of the inclusion models will improve the model accuracy.

Tasks for the Next Reporting Period

Experimental characterization of the yield strength and texture is complete for all regions of all extrusions. Microstructural characterization of the AA2195 and AA2096 will be conducted to assess the validity of the inclusion models. A series of aging treatments and limited compression testing will be done on a single region to observe any effect of aging on the

magnitude of the yield anisotropy. This project will be completed during the next reporting period.

References

1. W. F. Hosford and R. H. Zeisloft, "The Anisotropy of Age-Hardened Al-4 Pct Cu Single Crystals During Plane-Strain Compression," *Metall. Trans.*, **3**, 113 (1972).

2. L. M. Brown and W. M. Stobbs, "The Work Hardening of Copper-Silica I. A Model Based on Internal Stresses, with no Plastic Relaxation," *Phil. Mag.* **23**, 1185 (1971).

3. A. J. Ardell, "Precipitation Hardening," *Metall. Trans. A*, **16A**, 2131 (1985).

4. M. T. Lyttle and J. A. Wert, "The Plastic Anisotropy of an Al-Li-Cu-Zr Alloy Extrusion in Unidirectional Deformation," *Metall. Trans. A*, **27A**, 3503 (1996).

5. P. Bate, W. T. Roberts, and D. V. Wilson, "The Plastic Anisotropy of Two-Phase Aluminum Alloys I. Anisotropy in Unidirectional Deformation," *Acta metall.*, **29**, 1797 (1981).

6. P. Bate, W. T. Roberts, and D. V. Wilson, "The Plastic Anisotropy of Two-Phase Aluminum Alloys II. Anisotropic Behavior in Load-Reversal Tests," *Acta metall.*, **30**, 725 (1982).

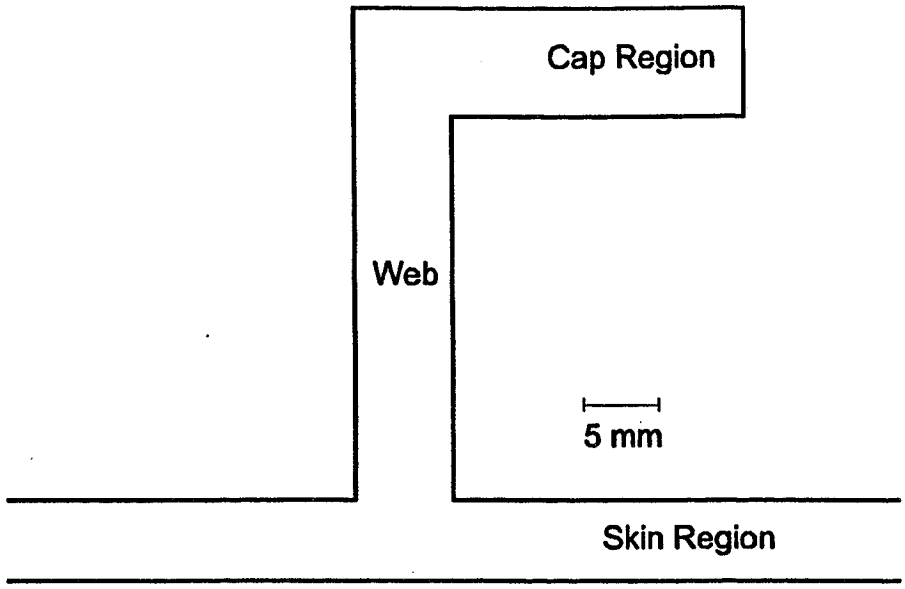

Figure 1. Schematic of aluminum alloy net shape extrusion. The extrusion consists of a flat skin region and J-stiffeners spaced 11.5 cm apart.

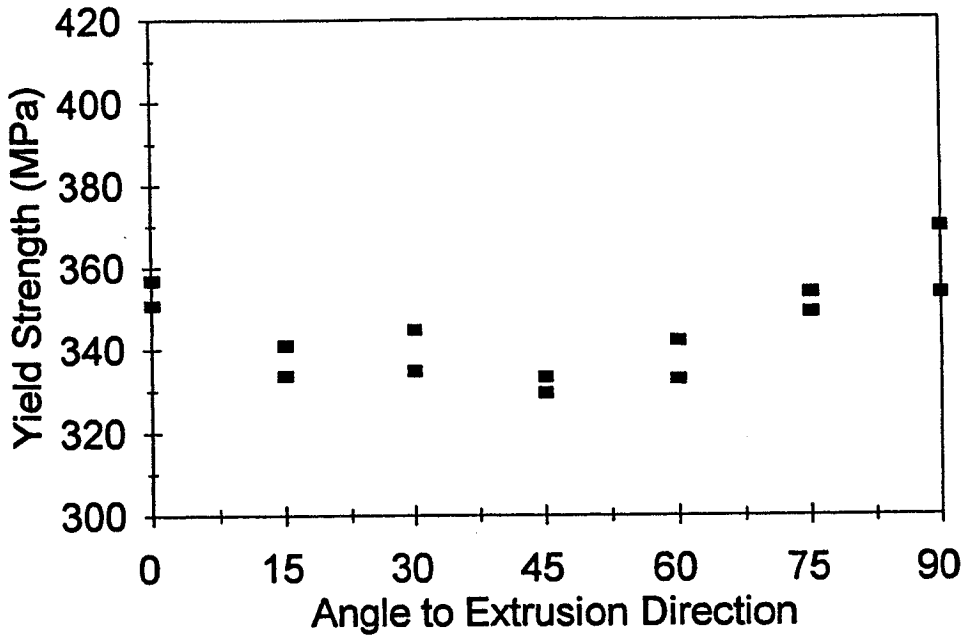

Figure 2. Experimental yield strength measurements for the AA2195 skin region.

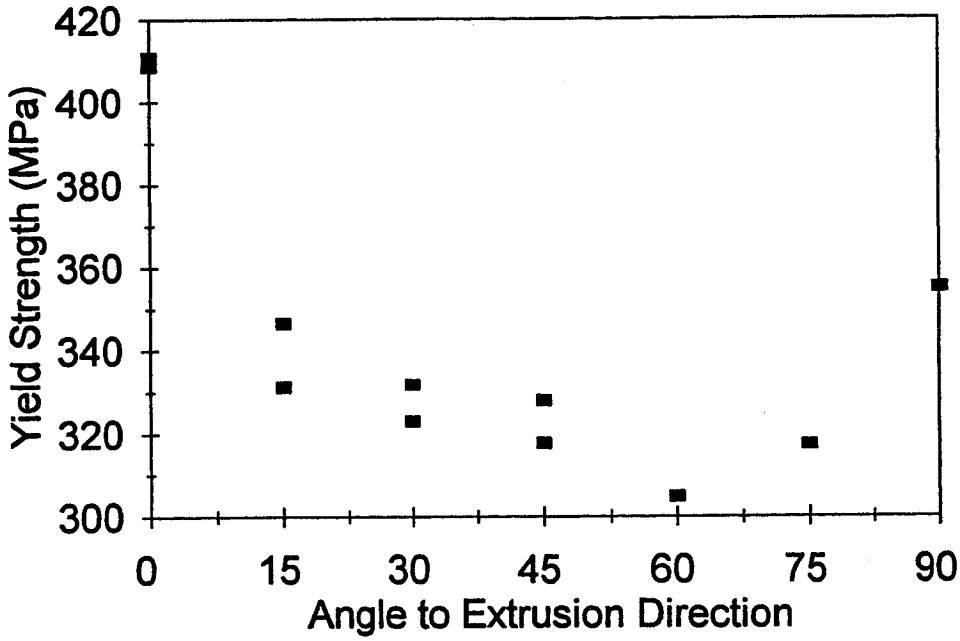

Figure 3. Experimental yield strength measurements for the AA2195 cap region.

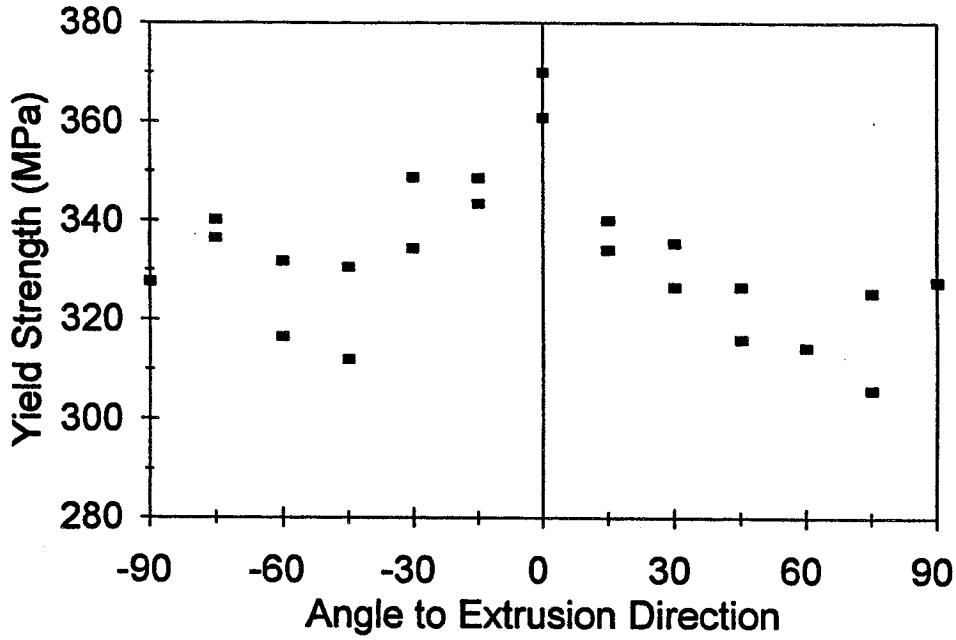

Figure 4. Experimental yield strength measurements for the AA2195 web region.

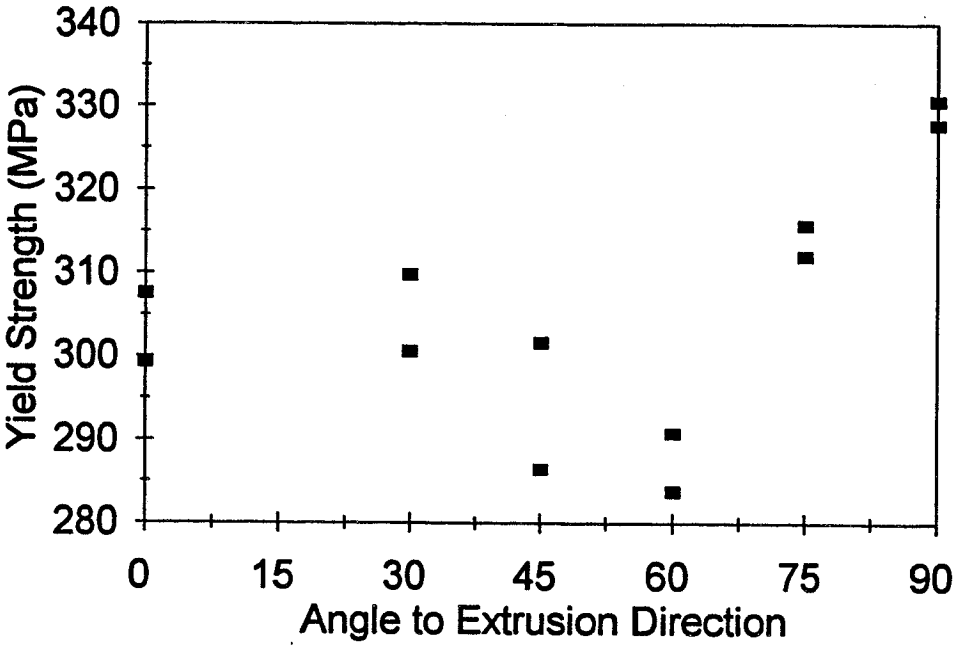

Figure 5. Experimental yield strength measurements for the AA2096 skin region.

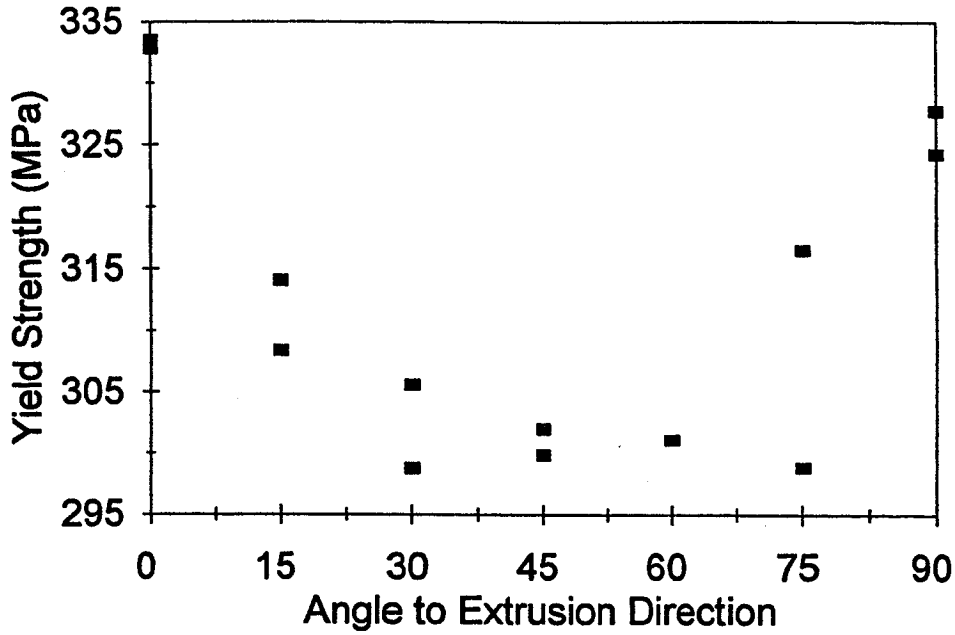

Figure 6. Experimental yield strength measurements for the AA2096 cap region.

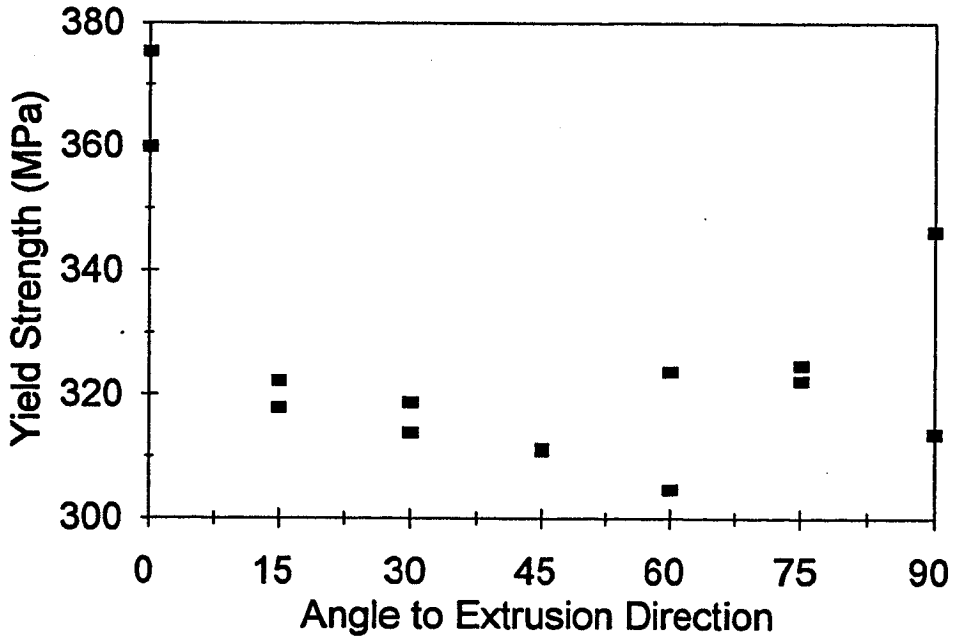

Figure 7. Experimental yield strength measurements for the AA2096 web region.

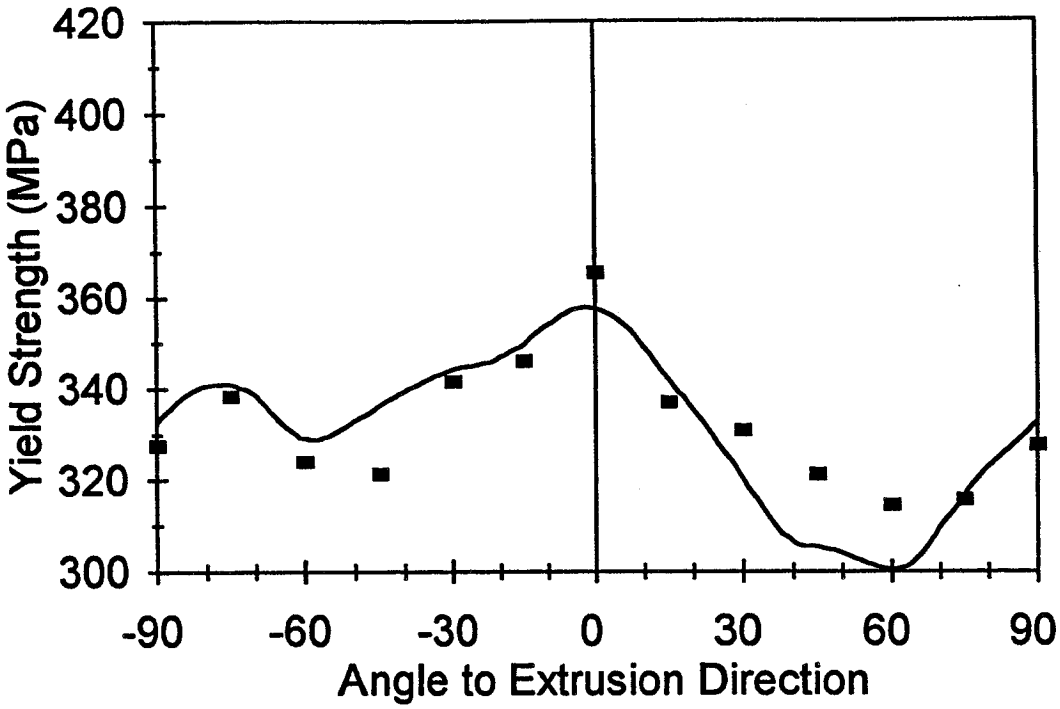

Figure 8. Comparison of the measured values of yield strength with Taylor factor model results for the web region of the AA2195 extrusion.

Project #7: EFFECT OF TEXTURE AND PRECIPITATES ON MECHANICAL PROPERTY ANISOTROPY OF Al-Cu-Mg-X AND Al-Cu ALLOYS

Faculty Investigator: Edgar A. Starke, Jr.
Graduate Assistant: Hinrich Hargarter

Reported in (HSR report).

Project #8: TIME-DEPENDENT ENVIRONMENTAL FATIGUE CRACK PROPAGATION IN 7XXX ALUMINUM ALLOYS

Faculty Investigator: Richard P. Gangloff
Graduate Assistant: Zuhair Gasem

Background

The drive for predicting the life of aging aerospace structures has led to renewed interest in environmentally assisted fatigue crack propagation (EFCP) in 7000 series aluminum alloys. Improved characterization and understanding of the intrinsic and extrinsic factors that govern corrosion fatigue crack growth will allow proper interpretation and extrapolation of experimental data needed for damage-tolerant life prediction.

A considerable number of experimental studies of corrosion fatigue in high strength 7XXX alloys rationalized the accelerated crack growth rates in gaseous and aqueous environments in terms of hydrogen embrittlement [1-3]. Although the exact nature of the underlying interactions is unknown, advances have been made in identifying the controlling hydrogen production and damage processes localized to the crack tip.

In addition to these fatigue-based factors, time-dependent processes include stress corrosion cracking, active path dissolution, and closure-shielding effects. Experimental evidence does not favor active path dissolution as a dominant mechanism for crack growth enhancement in 7XXX alloys [4,5]. However, intense dissolution at the crack tip resulting from the severe occluded chemistry conditions can have two mutually competitive effects on fatigue crack growth rates. Dissolution can accelerate crack growth rates by stimulating cathodic reaction which produces atomic hydrogen, and thus increases hydrogen uptake and embrittlement. On the other hand, accumulation of corrosion product can cause crack wedging leading to fatigue crack growth retardation.

For 7075 aluminum alloy in 3.5% NaCl solution, the formation of a thick corrosion product layer on the fracture surface, and the dependence of crack growth rate on loading time-history, suggests that corrosion product wedging is the responsible mechanism for enhanced crack closure and hence growth retardation [6]. At constant applied ΔK, the extent of retardation was frequency and microstructure dependent. Crack closure was dominant at the

lowest frequency range studied (0.01-0.1 Hz) and was enhanced in the overaged alloy. The reasons for the high closure effect in the T7351 temper, compared to less corrosion product-induced crack closure in a T651 microstructure, are not clear.

Measurements of the extent of environment-induced crack closure did not reveal a clear correlation between the closure-corrected effective stress intensity range ($\Delta K_{eff} = K_{max}-K_{cl}$) and the environment-assisted fatigue crack propagation response. In this initial work, the stress intensity level defining crack closure, K_{cl}, was obtained by two different compliance-based techniques; a standardized method discussed in ASTM standard E647 and the new Adjusted Compliance Ratio method. Neither method provided a reasonable estimate of the shielding effect of corrosion debris in reducing the applied stress intensity range ($\Delta K = K_{max} - K_{min}$) to ΔK_{eff}. The uncertainties associated with each technique must be further investigated.

For 7075-T7351 in 3.5% NaCl, the addition of a chromate-based inhibitor reduced the magnitude of environmental closure in the low frequency range, and eliminated the frequency sequence effect on da/dN. Furthermore, corrosion fatigue crack growth rates were reduced by approximately one order of magnitude over the entire range of frequency studied, compared to cracking in an aqueous chloride solution without chromate. The influence of the chromate addition on crack growth rate and closure levels in peak-aged 7075, which experienced less closure effect as compared to the overaged alloy at the same testing conditions, should be investigated.

Research Objectives

The broad goal of this research is to characterize and understand the loading frequency dependence of fatigue crack growth rate in 7000 series high strength aluminum alloys in corrosive environments. Emphasis is placed on separating intrinsic and extrinsic processes accompanying fatigue crack growth for AA7075 in aqueous NaCl, with and without chromate inhibitor. The objectives of the present report are to:

- Characterize the influence of 7075 alloy microstructure in the S-L orientation on fatigue crack propagation resistance in moist air.
- Determine the closure measurement method that is most appropriate for aqueous environment-induced closure assessment.

- Determine the effect of chromate addition on EFCP rates of 7075-T651 at constant applied ΔK for a wide range of loading frequency.
- Detect microstructure-dependent corrosion behavior which might explain the different EFCP retardation observed in the T651 and T7351 aging conditions of 7075.

Approach

The widely used commercial aluminum alloy 7075, in peak-aged (T651) and over-aged (T7351) conditions, is under investigation. Fatigue crack growth specimens were of the wedge-opening-load (WOL) configuration, 7.62 mm in thickness. The crack plane was in the S-L orientation. All tests were performed at room temperature using a sinusoidal waveform. Crack growth was continuously monitored using the elastic compliance method with a clip gage mounted across the mouth of the machined notch. Tests were conducted in a computer-automated MTS servohydraulic machine using Fracture Technology Associates (FTA) software and performed in general accordance with the ASTM Standard Test Method for Measurement of Fatigue Crack Growth Rates, E647-96.

Fatigue Crack Growth

Three types of controlled stress intensity experiment were employed to measure fatigue crack growth rates: (1) increasing ΔK at constant load ratio ($R = K_{min}/K_{max}$) of 0.1 to produce conventional da/dN *vs* ΔK relationships for laboratory air, (2) constant ΔK of 9 MPa$\sqrt{m}$ at constant R of 0.1 to examine the effects of loading frequency and chromate addition to 3.5% NaCl solution on da/dN, and (3) constant K_{max} tests (at either 6.7 or 10.0 MPa$\sqrt{m}$), each at several constant ΔK levels and the corresponding loading ratios (R = 0, 0.1, 0.3, 0.5, and 0.7) to compare the results of the two closure measurement techniques for fatigue crack growth in moist air. For the first test method, ΔK was increased at a constant K-gradient, defined as C= (dK/da)*1/K.

The WOL specimens were fatigue precracked in the environment of interest at controlled decreasing ΔK, R = 0.1 and f = 20 Hz, such that the final value of ΔK was lower than the value at the outset of each test. Tests conducted under constant K_{max} and constant R conditions utilized one specimen of 7075-T7351, and the sequence of testing was selected to avoid load-interaction induced closure.

A constant crack length increment (0.05 to 0.1 mm) was recorded vs number of load cycles for all tests. The secant method was used to determine fatigue crack growth rates in da/dN-ΔK tests, while linear regression analysis of crack length (a) vs number of cycles (N) data was employed in constant ΔK tests. In all tests post fracture visual crack length measurements were within 3% of the compliance based crack length calculation and thus no corrections in K or da/dN values were necessary.

Closure Measurement Techniques

Assessment of the contribution of environment-induced closure requires a measurement technique that is reproducible, and that correlates crack growth rates consistent with the principles of crack tip shielding mechanisms. For example, if EFCP rate is measured to be constant for given experimental conditions, then the associated value of ΔK_{eff} from the closure measurement technique should be constant. No such technique is presently available.

Existing methods can perhaps be employed if their range of sensitivities and limitations, which depend on testing parameters such as R, K_{max}, and microstructure, can be identified. Here, an attempt is made to compare closure measurements by two methods applied to fatigue crack growth in the SL orientation of 7075 stressed in laboratory air at intermediate ΔK and increasing R values. In this regime plasticity-induced closure is anticipated to play the major role in influencing fatigue crack growth due to minimal surface roughness and oxidation product. Results are compared with a model of plasticity-induced closure due to Newman [7].

Fatigue crack closure was monitored continuously using the global compliance of the specimen measured at the machined notch mouth. Two methods were involved; the ASTM-standardized measurement of opening load at a 2% offset (described in Standard E647-96), and a new method based on an adjusted ratio of specimen compliance (ACR) [8]. The latter method was proposed recently as means of eliminating the arbitrary and physically unreasonable single-point estimate of closure load and to account for the crack-tip strain redistribution taking place below the outset of crack surface contact. While ΔK_{eff} is defined as (K_{max} - K_{cl}) in the ASTM method, no direct determination of opening load is necessary in the ACR method. Instead, U ($=\Delta K_{eff}/\Delta K$) is equated to the ratio of the closure-influenced compliance to the closure-free compliance. The uncracked specimen compliance is subtracted from the measurements such that

the remaining compliances are due solely to the presence of the crack. This method may produce less variability in measurements and is independent of measurement location.

Corrosion Tests

Corrosion immersion tests were performed with coupons of 7075 in 2M $AlCl_3$ solution, selected to mimic the occluded crack tip chemistry [9]. Corrosion samples were taken from the mid-thickness of the plate to simulate the conditions along the S-L oriented corrosion fatigue crack path. Only the surface parallel to the rolling plane was exposed to the testing environment. Chemical resistant mounts were used to cover other surfaces of the sample. Mount material was tested separately in the highly corrosive environment of 2M $AlCl_3$ and no degradation was observed. Corrosion rates were estimated using weight loss calculation. The open circuit potentials of the samples were monitored during a specified interval of time.

Potentiodynamic tests were conducted with 7075 exposed to deaerated 3.5% NaCl and in 3.5% NaCl+0.5M Na_2CrO_4 inhibitor under stagnant flow conditions. Tested surfaces were parallel to the SL-oriented fatigue crack plane. The scan rate was 0.1 mv/sec. Deaeration was accomplished by purging the 3.5% NaCl solution with N_2 for more than 24 hours before the start of the tests, and continuous purging during the tests. Tests in aerated 3.5% NaCl showed evidence of pitting near the open circuit potentials and these polarization scans are not reported here.

Results During the Reporting Period

Crack Growth Behavior

Fatigue crack growth rates *vs* ΔK and ΔK_{eff} are shown in Figure 1 for 7075 (S-L) in both aging conditions, (a) T651 and (b) T7351, stressed in moist air at a fixed R of 0.1. Some amount of crack closure was indicated by each method, at each applied ΔK level and for each microstructure. ΔK_{eff} values from the adjusted compliance ratio method were always higher than the ASTM values at the same da/dN; that is, the ACR method portrayed less crack closure compared to the ASTM method.

Figure 2 compares the fatigue crack growth resistance of peak-aged and overaged microstructures, where da/dN is plotted *vs* ΔK_{eff} with closure accounted for by the ASTM

method. Da/dN *vs* ΔK_{eff} for each alloy appears to be well describable by three power-law segments, as is often the case of environment-enhanced fatigue crack propagation in 2XXX and 7XXX aluminum alloys. The overaged alloy showed slightly better intrinsic fatigue crack growth resistance over the range of ΔK examined. For a 7075 alloy in two aging conditions, Zeghloul and Petit [10] explained this effect of microstructure on FCP resistance in terms of shearable and nonshearable precipitates where the former (peak-aged matrix) promotes hydrogen embrittlement and thus enhanced FCP in moist air. Alpay and Gurbuz [11] reported an increase in FCP resistance in air as a result of overaging, and this tendency was more pronounced in the L-S than in the S-L orientations in a 7000 series alloy.

The effect of aging condition on the hydrogen environmental fatigue crack growth resistance of 7075 is not yet fully understood. As reported in the previous progress report, equal da/dN were observed for the T651 and T7351 conditions of 7075, with S-L oriented WOL specimens stressed in aqueous NaCl at a loading frequency of 0.5 Hz [12]. Static load stress corrosion cracking is not likely to occur to any significant extent in either microstructure at his relatively rapid loading frequency. This comparison is based on da/dN at fixed applied ΔK; the effect of chloride-environmental crack closure was not considered in this earlier work.

Accuracy and Relevance of Crack Closure Measurement by Global Compliance

Closure measurement results from Figure 1 are plotted against the applied ΔK in Figure 3. Both the ACR and ASTM methods suggest that the ratio of ΔK_{eff} to the applied ΔK is nearly constant over a wide range of applied stress intensity that increased with crack extension during the fatigue experiment. The ACR estimates of ΔK_{eff} are consistently equal to a higher fraction of the applied ΔK compared to the closure measurements based on the ASTM method, except at the lowest ΔK levels. (Transient behavior at the start of the test may explain the behavior at the lowest ΔK examined.) Figure 3 shows that the variability in ΔK_{eff} is reduced for the ACR method compared to the ASTM procedure for the same test machine and specimen conditions. The ACR method suggests a somewhat greater closure level in the peak-aged alloy compared to the overaged alloy at low and intermediate ΔK. While variability obscures this comparison for the ASTM measurements of closure, the same trend may be apparent at least at applied ΔK levels below 10 MPa$\sqrt{m}$.

Figure 4 presents closure measurements obtained for overaged 7075 stressed at constant ΔK segments, each at two K_{max} levels. Measured K_{op} is compared to predictions from Newman's model for plasticity-induced closure as a function of R. The model predictions are given for plane stress (α=1) and plane strain (α=3) conditions. The model predicts values of K_{op} (the stress intensity level where the crack is fully open), while the experimental methods measures K_{cl} (the stress intensity level where the crack is partially closed), however, the difference is generally assumed negligible. At relatively high K_{max} of 10.0 or 6.7 MPa$\sqrt{m}$, and the corresponding high crack growth rates in the Paris regime, plasticity-induced closure is the governing closure mechanism and the comparison between the measured and the model prediction is assumed appropriate.

Since the fatigue crack surfaces were always flat, without shear lips, and since the cyclic plastic zone was small compared to the specimen thickness, it is correct to compare measurements to the plane strain model predictions. At low R (< 0.3) and hence high ΔK, the ACR method underestimates closure at both loading levels, while the ASTM method gives results that are comparable with the model predictions. At intermediate R ($0.3 < R < 0.5$), results from the ASTM method begin to deviate from the model prediction while the ACR measurements approach the predictions. At higher R corresponding low ΔK level, the ASTM method overestimates the closure level (predicting an erroneously low effective stress intensity range), while the ACR result is in better agreement with the model. Further investigation is needed to characterize plasticity-induced closure in anisotropic microstructure of the S-L crack orientation, and its relevance to Newman's model which assumes isotropic material properties.

At this point in the research, experimental results have indicated weaknesses with each crack closure measurement method. These results, obtained during this reporting period and coupled with observations reported during the most recent LA^{2}ST Grant review meeting [12], are summarized as follows.

- The ASTM method is challenged by the result that da/dN was observed to be constant for EFCP in 7075-T7351 in NaCl, at constant applied ΔK, while ΔK_{eff} from the 2% offset closure load measurement declined continuously.
- ΔK_{eff} values from the ASTM method exhibit higher variability compared to ΔK_{eff} from the ACR method.

- For higher applied ΔK conditions within the Paris regime, the amount of closure predicted from the ACR method appears to be unrealistically low compared to plasticity-based closure model predictions. The magnitude of ΔK_{eff} from the ASTM method is reasonable in this regime.
- For lower applied ΔK approaching the threshold regime, the situation is reversed. The ACR method appears to provide more accurate estimates of closure, while the ASTM method overestimates K_{cl} and underestimates ΔK_{eff}.

At present, it is not possible to specify which of the global compliance methods is better suited to estimate the contribution of corrosion-product induced crack closure relevant to Paris regime EFCP in aluminum alloys.

Chromate Effect on Environmental Fatigue Crack Growth Rate

The dependence of environmental fatigue crack growth rate on loading frequency is summarized in Figure 5 for the peak-aged and overaged microstructures of 7075 stressed at constant ΔK (9 MPa$\sqrt{m}$) and R (0.1) in 3.5% NaCl with and without chromate-based inhibitor. (The number associated with each data point indicates the position of the specific frequency segment in a single WOL specimen.) Fatigue crack growth rate in laboratory air and at the same ΔK level is included for comparison.

The strong effect of loading frequency on da/dN for each aging condition in the pure chloride solution was discussed in the previous report [12]. Crack arrest at very low frequencies was attributed to corrosion product-induced crack closure that was unexpectedly severe for the overaged microstructure. This crack closure phenomenon resulted in the frequency-sequence effect indicated by the multiple trend lines and arrows for each microstructure in pure NaCl.

For NaCl, and in the mid-frequency regime where crack closure was presumably similar and due only to plasticity for each microstructure, the plateau level of da/dN was 9×10^{-4} mm/cycle for the T651 case and 7×10^{-4} mm/cycle for the T7351 case. These mildly increased rates of EFCP in the peakaged microstructure in pure NaCl, compared to the overaged case, are consistent with the fatigue behavior of 7075 in moist air (Figures 1 and 2, and the dashed line in Figure 5). While this behavior may be traced to a slight enhanced sensitivity of the peakaged alloy to hydrogen environment embrittlement, closure measurements are required to confirm that similar levels of plasticity induced ΔK_{eff} were operative. Perhaps the most important point

regarding microstructure is that, while fatigue crack growth was enhanced by chloride exposure compared to moist air, EFCP rates for the T6 age were not substantially higher than values for the overaged T7 case.

The effect of chromate inhibitor was emphasized during this reporting period; two important effects were observed. First, the chromate addition eliminated the reductions in crack growth rate at very low loading frequencies. The strong frequency-sequence effect, indicated by the arrows on the trend lines for the T7351/pure NaCl case (Figure 5b), was eliminated by the chromate. The amount of corrosion debris was observed to be reduced. *In toto*, these results suggest that corrosion-product induced crack closure was not a dominant factor in EFCP for either microstructure of 7075 in chromate-inhibited chloride solution.

Second, EFCP rates for each aging condition were reduced by nearly an order of magnitude in the mid-frequency regime, as a result of adding the chromate inhibitor. Here, da/dN for chromate/NaCl was reduced to a level less than that for crack growth in moist air, but above the likely value for fatigue in helium (about 3×10^{-5} mm/cycle at ΔK of 9 MPa$\sqrt{m}$ and R of 0.1 [13]). The mid-frequency plateau da/dN for the peak-aged microstructure in chromate solution was 1.2×10^{-4} mm/cycle, while that for the overaged case was 9.5×10^{-5} mm/cycle. Again, the peak-aged microstructure is slightly more susceptible to EFCP compared to the overaged case, but crack closure measurements are required to determine if this is an intrinsic behavior.

This reduction in da/dN as a result of chromate addition is believed to be related to reduced hydrogen production and/or uptake at the crack tip, possibly due to the formation of a stable oxide film. This explanation is consistent with the chromate-concentration dependence of the reduction in da/dN reported in a previous report [12]. It is unlikely that crack closure explains the chromate effect shown in Figure 5. Corrosion product production was greatly reduced in the chromate bearing solution compared to pure NaCl [12]. Plasticity-induced closure, which is the likely mechanism at these conditions, is not expected to change in aqueous solutions.

The frequency dependence of da/dN in the chromate case can be explained, but only in part, in terms of the cyclic rupture of the protective-oxide film and crack tip repassivation kinetics. At high frequencies, where film rupture events occur faster than repassivation, da/dN

is proportional to frequency and approaches the higher crack velocity in the uninhibited solution. Here, crack tip dissolution and hydrogen production amounts are enhanced on a per-unit time basis because the faster crack tip strain rates at higher frequencies increasingly destabilize the otherwise protective passive film.

The mechanism for increased da/dN with decreasing frequency, in the low frequency regime, is not fully understood. Alcoa-funded research at UVa has demonstrated that static-load crack growth rate (da/dt) is on the order of 2×10^{-6} mm/sec for the T651 condition in chromate-inhibited NaCl at the open circuit potential, and less than 1×10^{-7} mm/sec for the T7351 condition of this heat of 7075 and the S-L crack orientation [14]. Such low crack growth rates may contribute to EFCP rates for the T6 case, at loading frequencies below about 0.05 Hz at a ΔK level of 9 MPa$\sqrt{m}$ and R of 0.1 [13]. Linear superposition of this da/dt level could explain the low frequency rise in EFCP da/dN, but there are uncertainties with this calculation. Additionally, the stress corrosion cracking resistance of the T7 microstructure, and the associated very slow da/dt, cannot explain the similar rise in da/dN shown in Figure 5b compared to 5a. Additional work is required to examine the low frequency EFCP behavior of 7075 in the absence of corrosion product-induced closure.

Corrosion results

Experiments were conducted to examine the localized corrosion resistance of each aging condition in an attempt to explain the enhanced corrosion product-induced crack closure observed for the T7 case. Average corrosion rates, calculated from weight loss, are presented in Table I and are based on two sets of samples for each aging condition exposed for 96 and 120 hours. The differences in corrosion rates are not significant. However, the exact condition at the crack tip is not known and the open circuit results in Table I may not reflect the actual corrosion processes at the crack tip. For instance, differences may be associated with the stress-free surface in the immersion sample and the highly stressed crack tip, crack tip potential versus the free corrosion value, and composition of the corrosion coupon surface compared to the intergranular fatigue crack path.

Table I

Corrosion Rates in 2M $AlCl_3$ for 7075 in Two Aging Conditions

Sample	Corrosion Rate (mm/hr)
T651#1	0.021
T651#2	0.026
T7351#1	0.020
T7351#2	0.022

Figures 6 and 7 show polarization scans for each aging condition of 7075 exposed to pure NaCl and chromate inhibited NaCl solutions. These figures illustrate that the T6 and T7 aging conditions have similar polarization behavior when exposed to the simple bulk environments used for the corrosion fatigue experiments. The polarization curves for deaerated 3.5% NaCl display active-passive behavior, with breakdown potentials of -750 mV_{SCE} and -730 mV_{SCE} for the peakaged and overaged conditions, respectively. The polarization curves for deaerated 3.5% NaCl plus chromate also display active-passive behavior, with breakdown potentials of -640 mV_{SCE} and -660 mV_{SCE} for the peakaged and overaged conditions, respectively. Both tempers have similar open circuit potentials of -825 mV_{SCE} in deaerated NaCl. The T6 condition has an identical open circuit potential in the chromate-inhibited chloride solution, but this potential is -790 mV_{SCE} for the T7 condition. The similar open circuit potentials for the inhibited and uninhibited solutions support the coverage mechanism for chromate inhibition rather than this specie acting as an oxidizing inhibitor which shifts the potential to the passive regime.

It appears that neither the immersion tests in simulated crack solution nor the polarization scans in the bulk chloride solutions explain the higher production of corrosion products during low frequency EFCP in the T7351 microstructure.

Conclusions

1. The fatigue crack growth resistance of the overaged microstructure of 7075 alloy in the S-L orientation, stressed in ambient air, shows slight improvement over the peakaged

condition. A similar trend was observed for 3.5% NaCl and 3.5% NaCl+0.5 M Na_2CrO_4 solutions; environmental cracking was not reduced substantially by overaging for fatigue loading at the frequencies examined.

2. The adjusted compliance ratio method for closure measurement produced less scatter in ΔK_{eff} compared to closure results from the ASTM recommended method, and is more suitable for approximating crack closure in experiments involving high R and low ΔK.

3. The ASTM method was associated with wide scatter in ΔK_{eff}, but gave better estimates of model-predicted plasticity-induced closure, compared to the ACR approach, for low R and high ΔK.

4. Chromate addition to NaCl solution has two significant affects on corrosion fatigue crack growth rates in alloy 7075, and is accordingly an important environmental variable.

5. 0.5M Na_2CrO_4 added to 3.5% NaCl reduced da/dN markedly for both aging conditions of 7075 and over a wide range of loading frequency. The beneficial effect was reduced at high frequencies where the presumably protective passive film was destabilized by high crack tip strain rate.

6. The chromate addition reduced crack wake corrosion product accumulation and eliminated the potentially beneficial effect of corrosion-product induced crack closure, particularly in the corrosion-prone T7351 microstructure. EFCP in pure NaCl is arrested at low loading frequencies due to the action of this corrosion product closure mechanism.

7. Simple weight-change immersion and polarization tests did not show a distinction between the corrosion behavior of the T6 and T7 microstructures. It is not possible to explain the pronounced corrosion-product closure effect in the overaged condition.

Tasks for the Next Reporting Period

Future work will emphasize the following:

1. Sources of scatter in the ASTM method for closure measurement will be identified and minimized. This method is more appropriate to employ quantitatively in corrosion fatigue experiments to separate the intrinsic and extrinsic da/dN at low R and moderate ΔK levels. This method will be employed to understand the corrosion fatigue crack response at the low frequency regime, with each microstructure exposed to the chloride solutions.

2. In order to understand the frequency dependence of EFCP da/dN, it is necessary to study the microscopic crack path in air, as well as in the uninhibited, and inhibited chloride environments for various loading conditions. A complete fractographic study will be undertaken.

3. To better understand the effect, if any, of overaging on EFCP kinetics, we will study the influence of crack path orientation on fatigue crack growth resistance in laboratory air at increasing K, and in 3.5% NaCl at constant ΔK with varying loading frequency.

4. The inhibiting effect of chromate is important and must be better understood. We will study the effect of chromate on da/dN in the plateau region, employing constant ΔK (9 MPa$\sqrt{m}$), R (0.1), and frequency (0.5 Hz) to investigate the cause of da/dN reduction for the two conditions of 7075. Improved crack closure measurement should reveal whether the reduction is intrinsic or extrinsic in nature.

5. We will study the effect of chromate concentration (0.1 to 5 M) on corrosion fatigue crack response in one aging condition at constant ΔK (9 MPa$\sqrt{m}$), R (0.1) and f (0.5 Hz) to determine if da/dN would reduce in proportion with increasing chromate concentration.

6. The mechanism of the beneficial effect of chromate will be studied by considering existing models of hydrogen-assisted corrosion fatigue.

References

1. N.J.H. Holroyd, "Environment-Induced Cracking of High-Strength Aluminum Alloys", in Environment-Induced Cracking of Metals, R.P. Gangloff and M.B. Ives, eds., NACE, pp. 311-345, 1990.

2. M.O. Speidel,"Hydrogen Embrittlement and Stress Corrosion Cracking of Aluminum Alloys", in Hydrogen Embrittlement and Stress Corrosion Cracking, R. Gibala and R.F. Hehemann, eds, ASM, pp. 271-295, 1984.

3. R.P. Wei, P.S. Pao, R.G. Hart, T.W. Weir, and G.W. Simmons,"Fracture Mechanics and Surface Chemistry Studies of Fatigue Crack Growth in an Aluminum Alloy", Metallurgical Transactions A, Vol. 11A, pp. 151-158, 1980.

4. N.J.H. Holroyd and D. Hardie, "Factors Controlling Crack Velocity in 7000 Series Aluminum Alloys During Fatigue in an Aggressive Environment", Corrosion Science, Vol. 23, pp. 527-546, 1983.

5. Th. Magnin,"Recent Advances in the Environment Sensitive Fracture Mechanisms of Aluminum Alloys", Materials Science Forum, Vols. 217-222, pp. 83-94, 1996.

6. R.P. Gangloff,"NASA-UVa Light Aerospace Alloy and Structures Technology Program", UVa Report No. UVA/528266/MSE96/119, pp. 127-137, 1996.

7. J.C. Newman, Jr.," A Crack Opening Stress Equation for Fatigue Crack Growth", International Journal of Fracture, Vol. 24, pp. R131-R135, 1984.

8. J.K. Donald, "Closure Measurement Techniques", Presented at the ASTM E08.06.03 Task Group on Crack Closure Measurement and Analysis, 1996.

9. R.G. Kelly, Personal Communication.

10. A. Zeghloul, and J. Petit, Rev. Phy. Appl., Vol. 24, pp. 893-904, 1984.

11. S.P. Alpay and R. Gurbuz, "Effect of Aging on the Fatigue Crack Growth Kinetics of an Al-Zn-Mg-Cu Alloy in Two Directions", Scripta Metallurgica, Vol. 30, pp. 423-427, 1994.

12. R.P. Gangloff, "NASA-UVa Light Aerospace Alloy and Structures Technology Program", UVa Report No. UVA/58266/MSE96/120, p. 91, June, 1996.

13. M.E. Mason and R.P. Gangloff, "Modeling Time-Dependent Corrosion Fatigue Crack Propagation in 7000 Series Aluminum Alloys", in *FAA/NASA International Symposium on Advanced Structural Integrity Methods for Airframe Durability and Damage*

Tolerance, C.E. Harris, ed., NASA Conference Publication 3274, Part 1, NASA-Langley Research Center, Hampton, VA, pp. 441-462, 1994.

14. L.M. Young and R.P. Gangloff, "Electrode Potential and Heat Treatment Effects on Environmental Cracking in High Strength 7XXX Aluminum Alloys", presented at the *TMS-AIME Symposium on Light Weight Alloys for Aerospace Applications*, Orlando, FL, 1997.

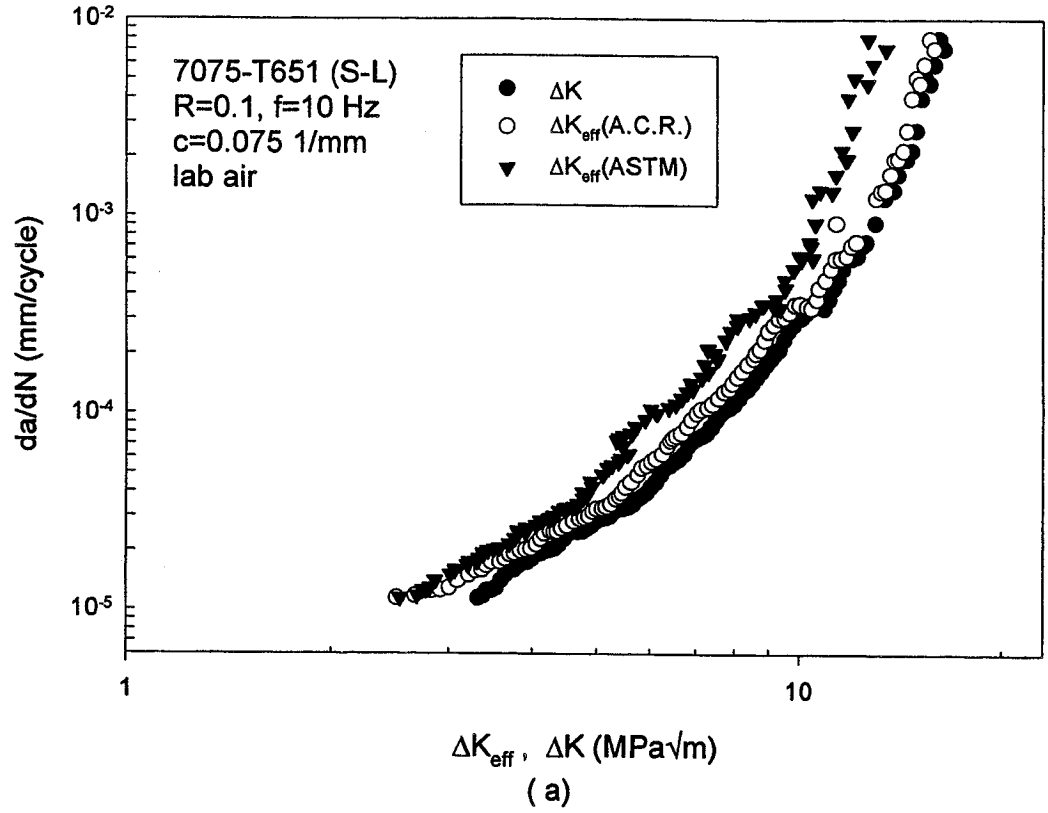

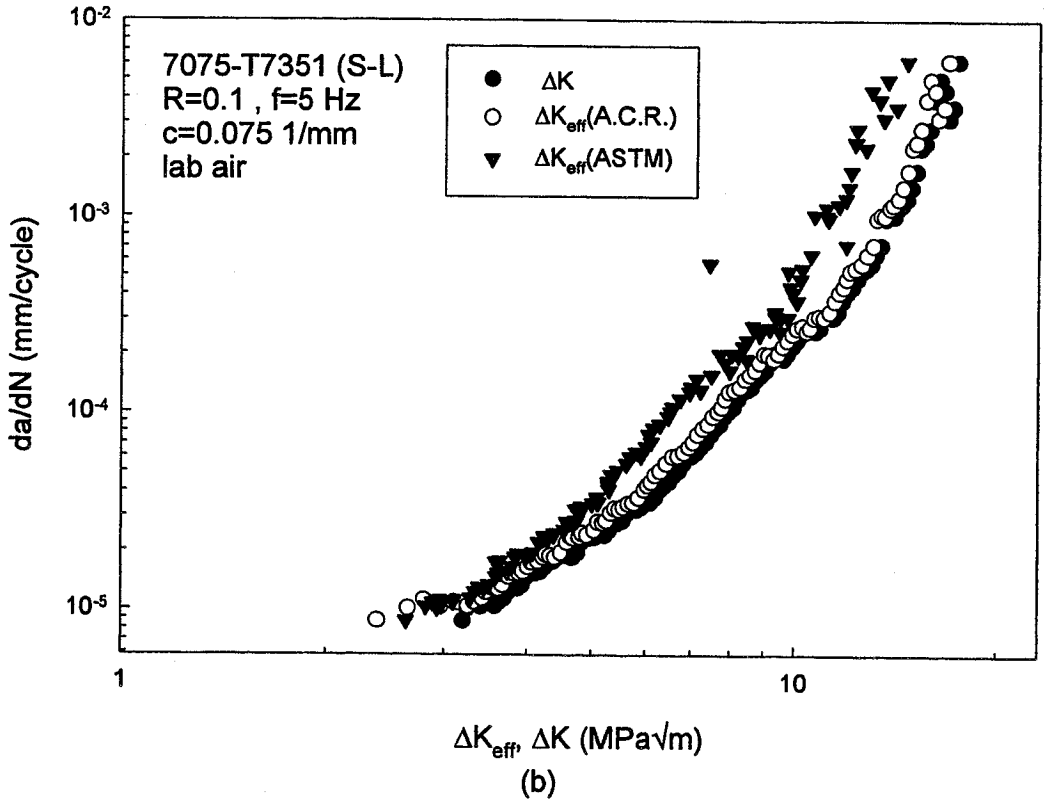

Fig. 1 Fatigue crack growth data vs ΔK and ΔK_{eff} for 7075 in two aging conditions: (a) T651 and (b) T7351, tested in lab air.

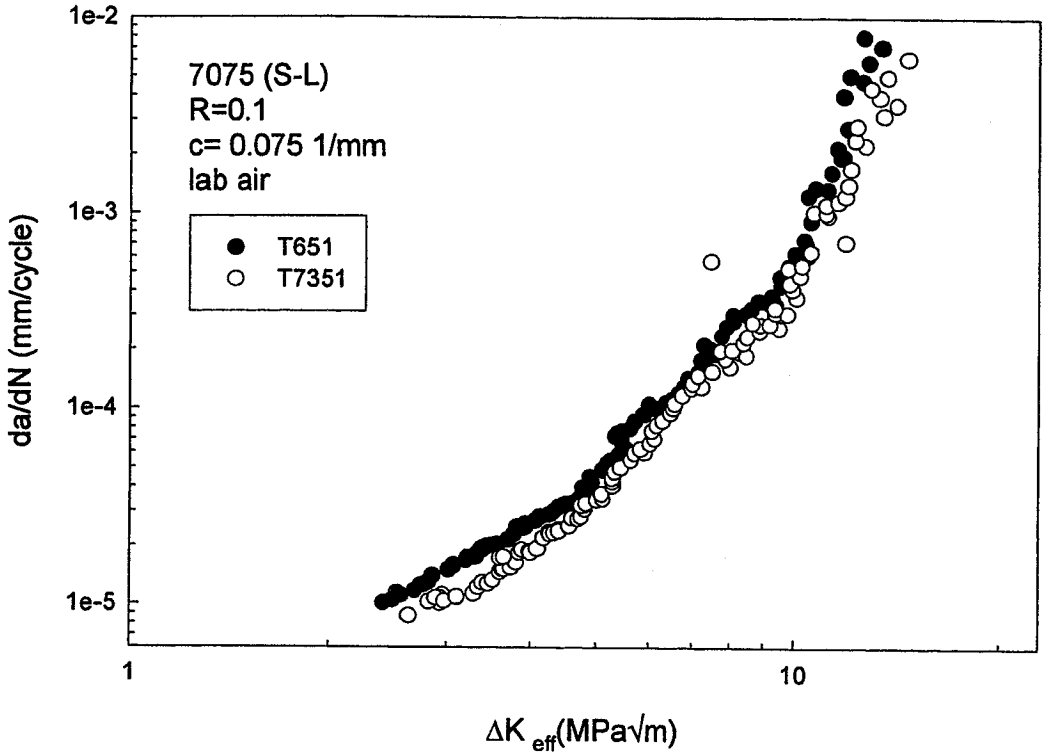

Fig. 2 Comparison of fatigue crack growth data for 7075 in two aging conditions represented in terms of ΔK_{eff} as estimated by the ASTM method.

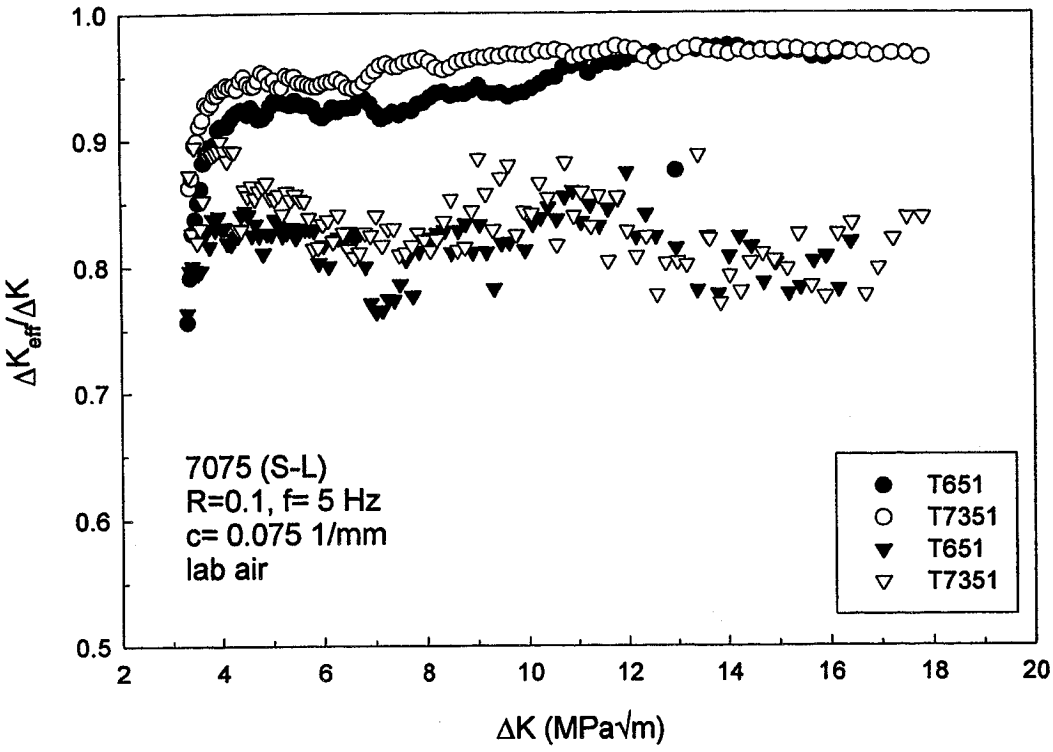

Fig. 3 Comparison of ΔK_{eff} from two closure measurement methods: ACR (circles) and ASTM (triangles), for two aging conditions of 7075 tested in lab air.

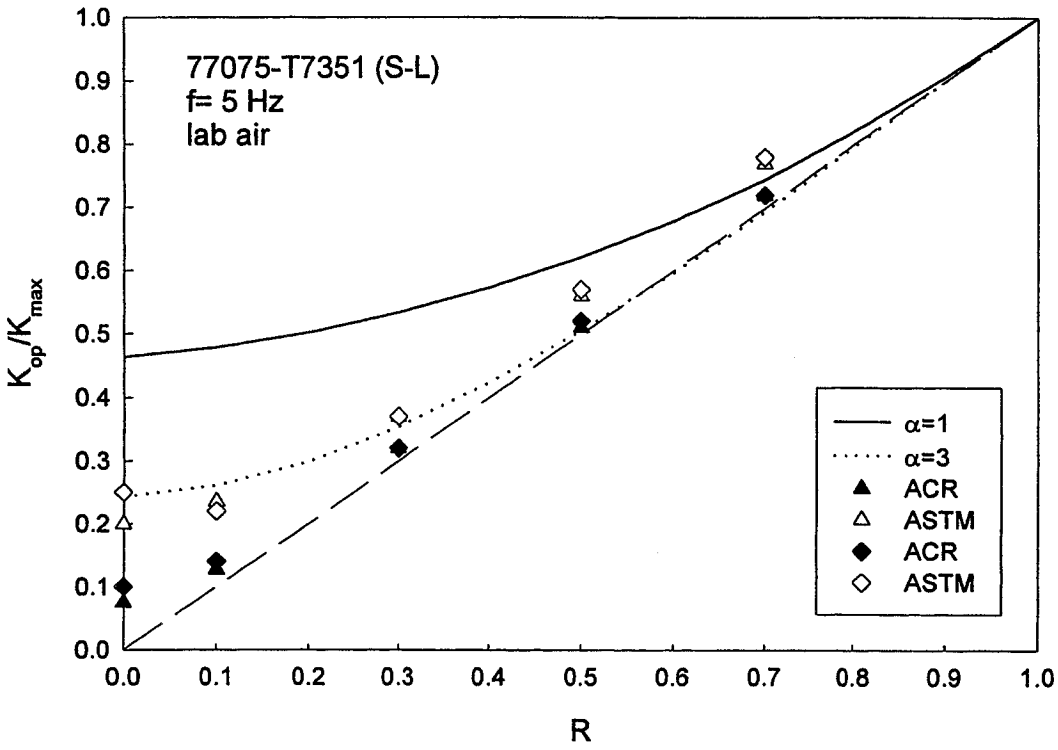

Fig. 4 Measured and Newman's model-predicted plasticity-induced closure for 7075-T7351 at two K_{max} levels: 10.0 MPa$\sqrt{}$ m (triangles) and 6.7 MPa$\sqrt{}$ m (diamonds) .

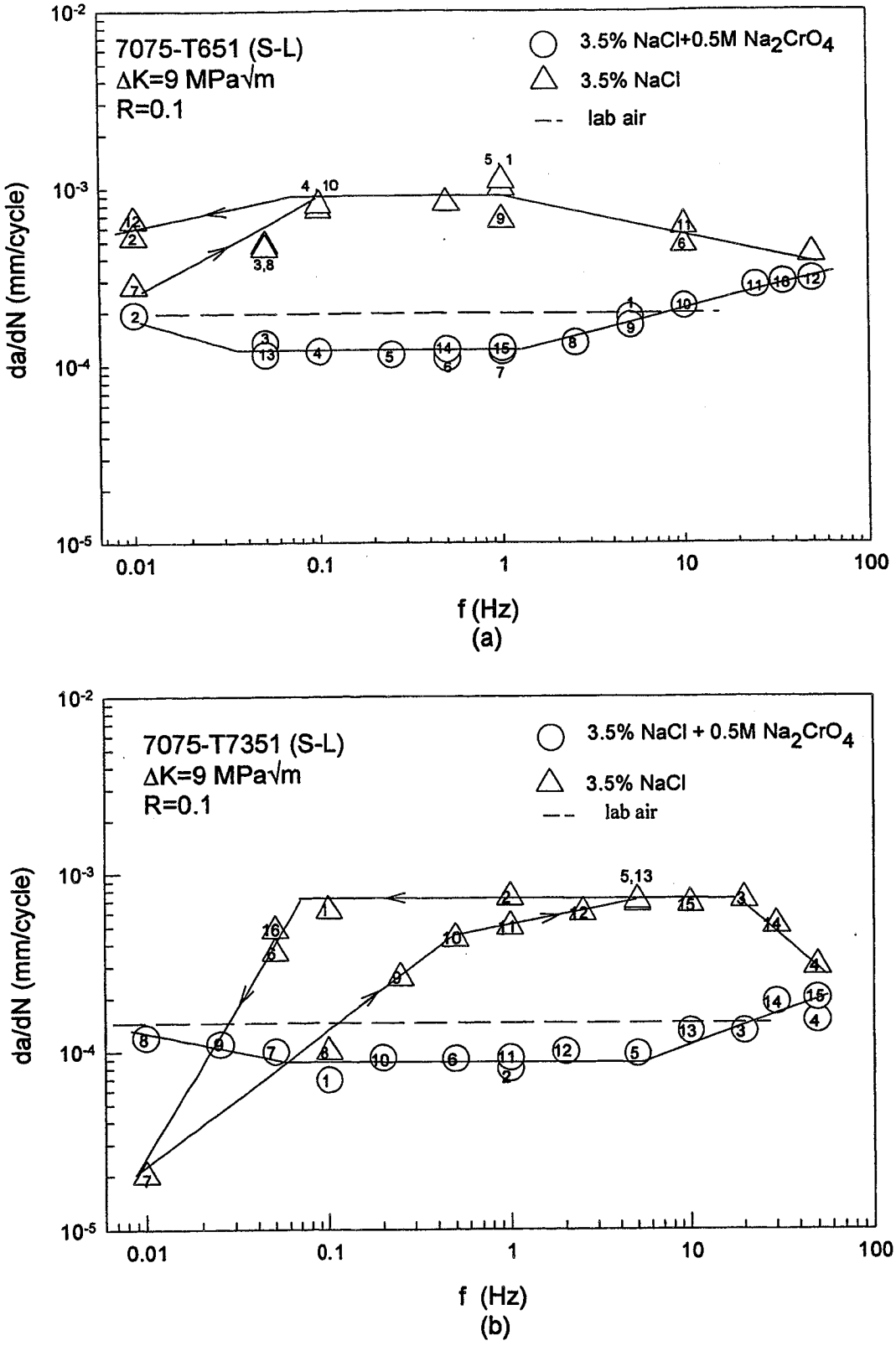

Fig. 5 Da/dN as a function of loading frequency for 7075 : (a) T651 and (b) T7351 at constant $\Delta K = 9$ MPa$\sqrt{m}$ in two environments. Numbers indicate sequence of tests.

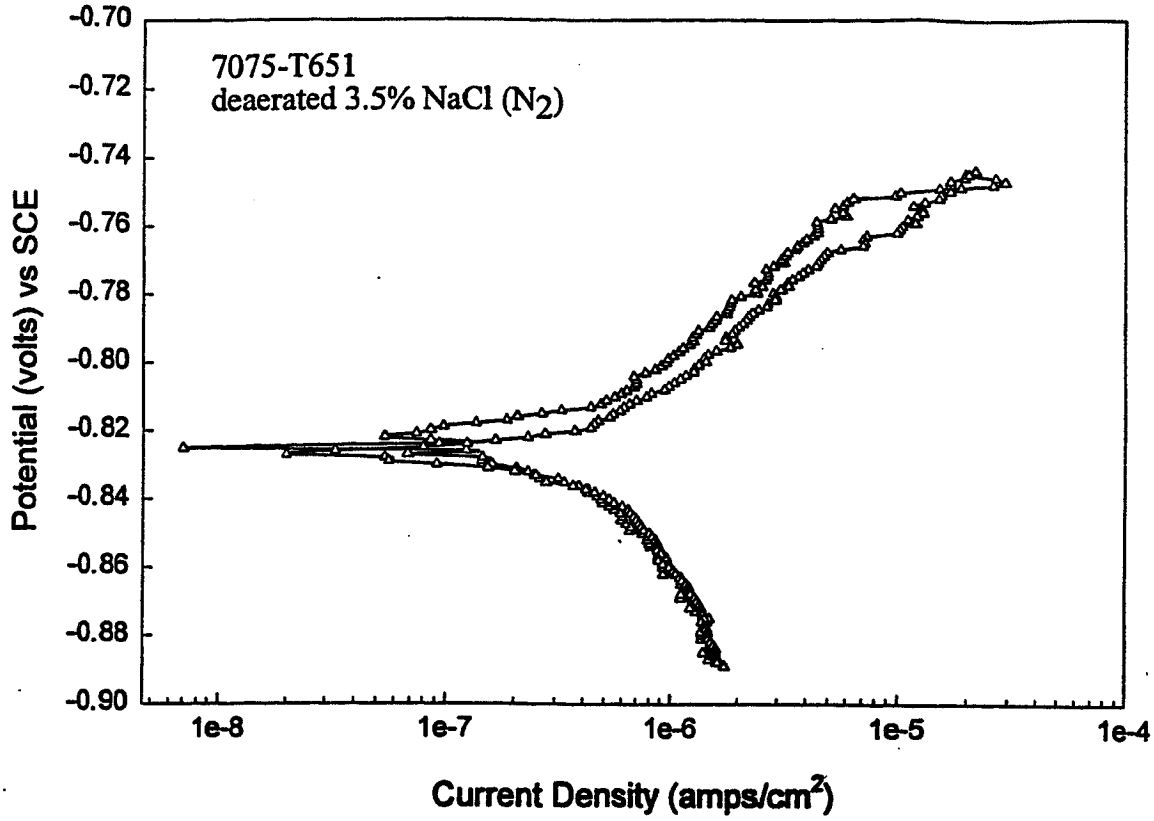

(a)

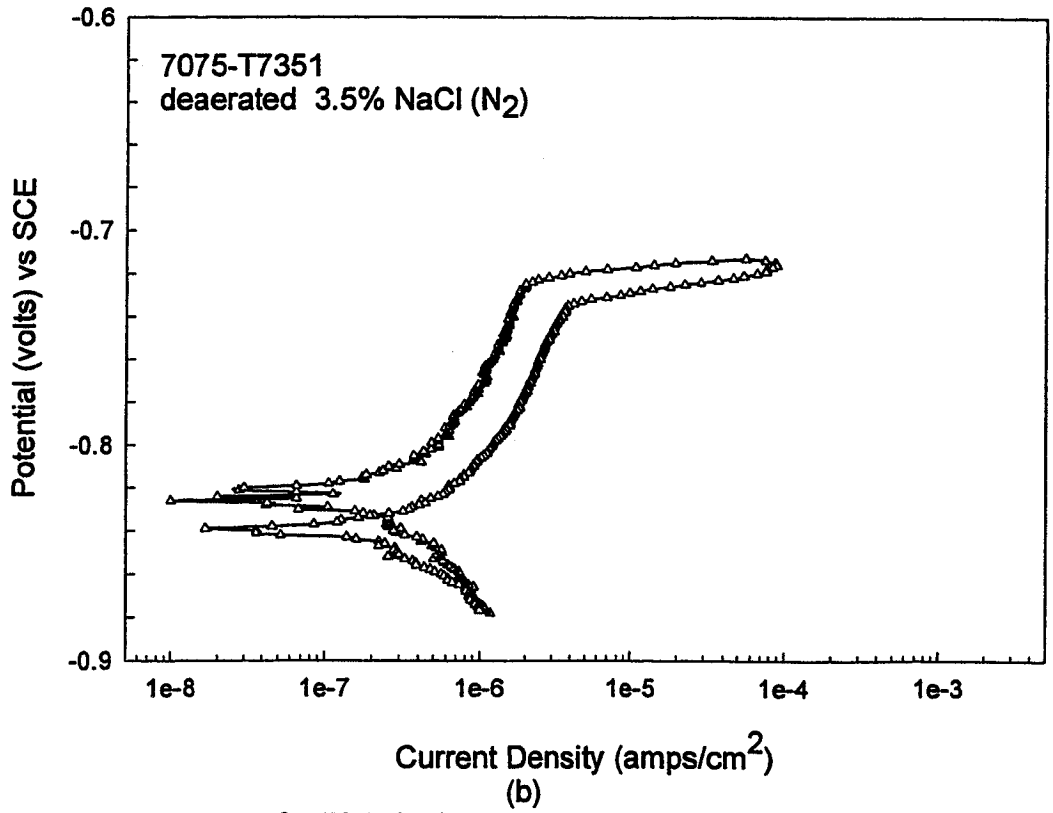

(b)

Fig. 6 Polarization curves for 7075 in deaerated 3.5% NaCl: (a) T651 and (b) T7351. Samples were tested in the L-T plane.

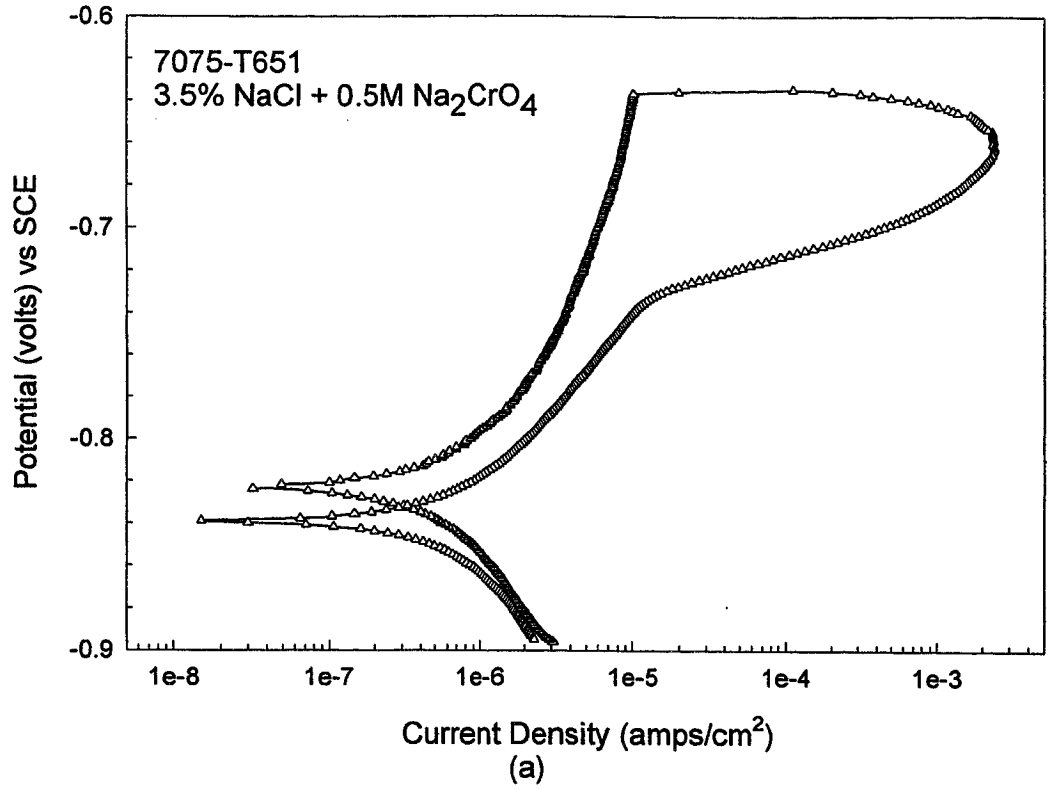

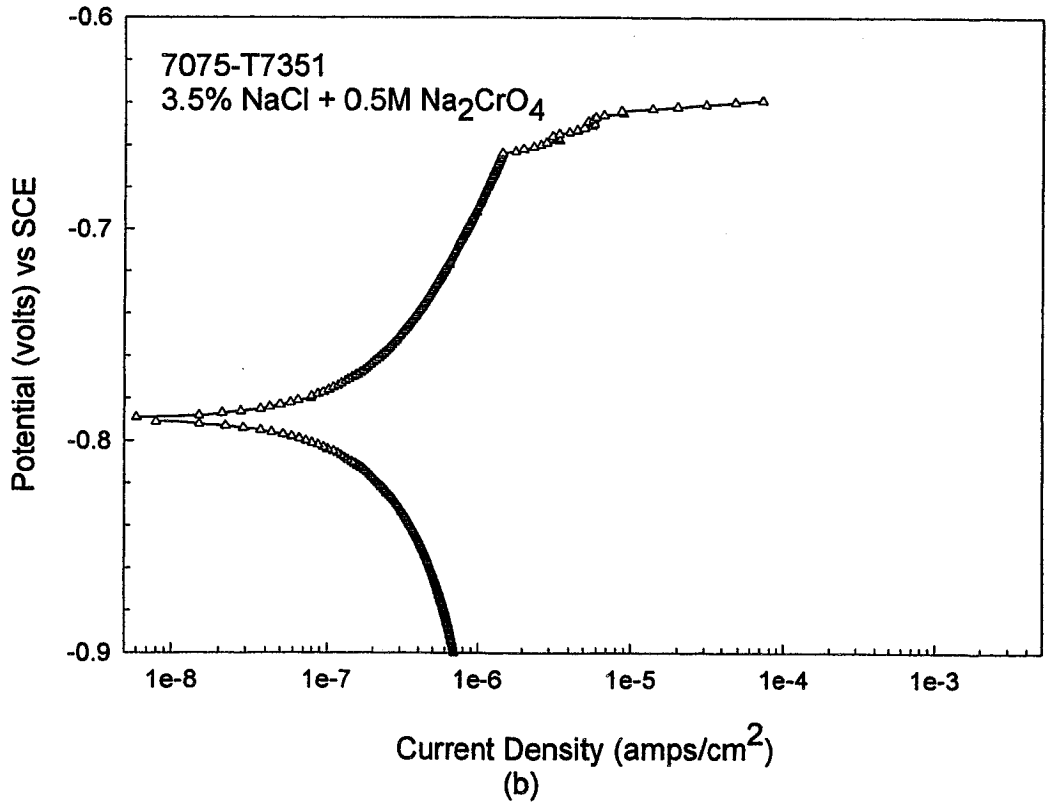

Fig. 7 Polarization curves for 7075 in 3.5% NaCl + 0.5M Na_2CrO_4: (a) T651 and (b) T7351. Sample surfaces were parallel to the crack plane in the rolled plate.

APPENDIX I: GRANT PUBLICATIONS (July 1 to December 31, 1996)

1. M.J. Haynes and R.P. Gangloff, "Elevated Temperature Fracture Toughness of Al-Cu-Mg-Ag Alloys: Characterization and Modeling", Metallurgical Transactions A, in review, (1997).

2. Bin Wu, J.R. Scully, A.S. Mikhailov, J.L. Hudson, "Cooperative Stochastic Behavior in Localized Corrosion: I. Model", submitted to J. Electrochem. Soc., August 1996.

3. T.T. Lunt, S.T. Pride, J.R. Scully, A.S. Mikhailov, J.L. Hudson, "Cooperative Stochastic Behavior in Localized Corrosion: II. Experiments", submitted to J. Electrochem. Soc., August 1996.

4. R.J. Kilmer, S.W. Smith, J.R. Scully, and G.E. Stoner, "Effect of Aging Time on Aqueous Stress Corrosion and Internal Hydrogen Embrittlement in Al-Li-Cu Alloys" submitted to Metall. Trans., September, 1996.

5. G.S. Frankel, J.R. Scully, C.V. Jahnes, "Repassivation of Pits in Aluminum Thin Films," J. Electrochem. Soc., 143(6), pp. 1843-1840, (1996).

6. Koenigsmann, and E.A. Starke, Jr., "Cavity Nucleation and Growth in an Al-Si-Ge Alloy," Scripta Metallurgica et Materialia, Vol. 35, pp. 1205-1209 (1996).

7. B. Skrotzki, H. Hargarter and E.A. Starke, Jr., "Microstructural Stability Under Creep Conditions of Two Al-Cu-Mg Alloys", Aluminium Alloys, Their Physical and Mechanical Properties - Proceedings ICAA5, July 1-5, 1996, Grenoble, France, p.1245-1250 (1996).

8. H.J. Koenigsmann and E.A. Starke, Jr., "Cavity Nucleation and Fracture in an Al-Si-Ge Alloy", Aluminium Alloys, Their Physical and Mechanical Properties - Proceedings ICAA5, July 1-5, 1996, Grenoble, France, p. 1479-1484 (1996).

APPENDIX II: GRANT PRESENTATIONS (July 1 to December 31, 1996)

1. Haynes and R.P. Gangloff, "Elevated Temperature Fracture Toughness of Al-Cu-Mg-Ag", ASM-TMS Materials Week '96, Cincinnati, OH, October 7-10, 1996.

2. Haynes and R.P. Gangloff, "Localized Deformation and Elevated Temperature Fracture of Submicron Grain Aluminum with Dispersoids", ASM-TMS Materials Week '96, Cincinnati, OH, October 7-10, 1996.

3. T. Lyttle and J. A. Wert, "The Plastic Anisotropy of Aluminum Alloy Extrusions", TMS/ASM Materials Week '96, Cincinnati, Ohio.

4. Hargarter, M.T. Lyttle, E.A. Starke, Jr. "Influence of Precipitate Orientation on the Yield Stress Anisotropy in Al-Cu- and Al-Cu-Mg-Ag-Alloys" , ASM-TMS Materials Week '96, 7 - 10 October 1996, Cincinnati, Ohio.

5. B. Skrotzki, H. Hargarter and E.A. Starke, Jr., "Microstructural Stability Under Creep Conditions of Two Al-Cu-Mg Alloys", Aluminium Alloys, Their Physical and Mechanical Properties - Proceedings ICAA5, July 1-5, 1996, Grenoble, France.

6. H.J. Koenigsmann and E.A. Starke, Jr., "Cavity Nucleation and Fracture in an Al-Si-Ge Alloy", Aluminium Alloys, Their Physical and Mechanical Properties - Proceedings ICAA5, July 1-5, 1996, Grenoble, France.

APPENDIX III: GRANT PROGRESS REPORTS (January, 1988 to December, 1996)

1. R.P. Gangloff, G.E. Stoner and R.E. Swanson, "Environment Assisted Degradation Mechanisms in Al-Li Alloys", University of Virginia, Report No. UVA/528266/MS88/101, January, 1988.

2. R.P. Gangloff, G.E. Stoner and R.E. Swanson, "Environment Assisted Degradation Mechanisms in Advanced Light Metals", University of Virginia, Report No. UVA/528266/MS88/102, June, 1988.

3. R.P. Gangloff, G.E. Stoner and R.E. Swanson, "Environment Assisted Degradation Mechanisms in Advanced Light Metals", University of Virginia, Report No. UVA/528266/MS89/103, January, 1989.

4. T.H. Courtney, R.P. Gangloff, G.E. Stoner and H.G.F. Wilsdorf, "The NASA-UVa Light Alloy Technology Program", University of Virginia, Proposal No. MS NASA/LaRC-3937-88, March, 1988.

5. R.P. Gangloff, "NASA-UVa Light Aerospace Alloy and Structures Technology Program", University of Virginia, Proposal No. MS NASA/LaRC-4278-89, January, 1989.

6. R.P. Gangloff, "NASA-UVa Light Aerospace Alloy and Structures Technology Program", University of Virginia, Report No. UVA/528266/MS90/104, August, 1989.

7. R.P. Gangloff, "NASA-UVa Light Aerospace Alloy and Structures Technology Program", University of Virginia, Report No. UVA/528266/MS90/105, December, 1989.

8. R.P. Gangloff, "NASA-UVa Light Aerospace Alloy and Structures Technology Program", UVa Report No. UVA/528266/MS90/106, June, 1990.

9. R.P. Gangloff, "NASA-UVa Light Aerospace Alloy and Structures Technology Program", UVa Report No. UVA/528266/MS91/107, January, 1991.

10. R.P. Gangloff, "NASA-UVa Light Aerospace Alloy and Structures Technology Program", UVa Report No. UVA/528266/MS91/108, July, 1991.

11. R.P. Gangloff, "NASA-UVa Light Aerospace Alloy and Structures Technology Program", UVa Report No. UVA/528266/MS92/109, January, 1992.

12. R.P. Gangloff, "NASA-UVa Light Aerospace Alloy and Structures Technology Program", UVa Report No. UVA/528266/MS93/111, July, 1992.

13. R.P. Gangloff, "NASA-UVa Light Aerospace Alloy and Structures Technology Program", UVa Report No. UVA/528266/MSE93/112, March, 1993.

14. R.P. Gangloff, "NASA-UVa Light Aerospace Alloy and Structures Technology Program", UVa Report No. UVA/528266/MSE93/113, July, 1993.

15. R.P. Gangloff, "NASA-UVa Light Aerospace Alloy and Structures Technology Program", UVa Report No. UVA/528266/MSE93/114, March, 1994.

16. R. P. Gangloff, "NASA-UVa Light Aerospace Alloy and Structures Technology Program," UVA Report No. UVA/528266/MSE94/116, July, 1994.

17. E.A. Starke, Jr. and R.P. Gangloff, "NASA-UVa Light Aerospace Alloy and Structures Technology Program", UVa Report No. UVA/528266/MSE94/117, March, 1995.

18. R.P. Gangloff, and E.A. Starke, Jr., "NASA-UVa Light Aerospace Alloy and Structures Technology Program", UVa Report No. UVA/528266/MS95/118, July, 1995.

19. R.P. Gangloff, and E.A. Starke, Jr., "NASA-UVa Light Aerospace Alloy and Structures Technology Program", UVa Report No. UVA/528266/MS96/119, January, 1996.

20. R.P. Gangloff and E.A. Starke, Jr., "NASA-UVa Light Aerospace Alloy and Structures Technology Program", UVa Report No. UVA/528266/MS96/120, June, 1996.

DISTRIBUTION LIST

1-4	Mr. D.L. Dicus Contract Monitor Metallic Materials Branch, MS 188A NASA Langley Research Center Hampton, VA 23681-0001
5-6*	NASA Scientific and Technical Information Facility P.O. Box 8757 Baltimore/Washington International Airport Baltimore, MD 21240
7	Mr. Joseph Murray Grants Officer, M/S 126 NASA Langley Research Center Hampton, VA 23681-0001
8	Dr. Darrel R. Tenney Materials Division NASA Langley Research Center Hampton, VA 23681-0001
9	Dr. Charles E. Harris Mechanics of Materials Branch NASA Langley Research Center Hampton, VA 23681-0001
10	Mr. W. Barry Lisagor Metallic Materials Branch NASA Langley Research Center Hampton, VA 23681-0001
11	Mr. T.W. Crooker Code RM NASA Headquarters Washington, DC 20546
12	Dr. Robert S. Piascik Mechanics of Materials Branch NASA Langley Research Center Hampton, VA 23681-0001

13 Mr. W. Brewer
Metallic Materials Branch, MS 188A
NASA Langley Research Center
Hampton, VA 23681-0001

14 Mr. Thomas T. Bales
Metallic Materials Branch, MS 188A
NASA Langley Research Center
Hampton, VA 23681-0001

15 Mr. John Wagner/Ms. Cynthia Lach
Metallic Materials Branch, MS 188A
NASA Langley Research Center
Hampton, VA 23681-0001

16 Dr. William F. Bates
Lockheed Aeronautical Systems Co.
86 South Cobb Drive
Marietta, GA 30063-0648

17 Dr. Alex Cho
Reynolds Metals Co.
4th and Canal Street
Richmond, VA 23261

18 Mr. E.A. Colvin
Alcoa Technical Center
Route 780, 7th Street Road
Alcoa Center, PA 15069

19 Dr. L.M. Karabin
Alcoa Technical Center
Route 780, 7th Street Road
Alcoa Center, PA 15069

20 Dr. Ravi Kahandal
McDonnell Douglas Aerospace
Mail Stop 36-90
3855 Lakewood Boulevard
Long Beach, CA 90846

21 Mr. Fred Casey
Space Transportation Systems Division
Rockwell International
Dept. 289, MC/AC 56
12214 Lakewood Boulevard
Downey,CA 90241

22-23 E.A. Starke, Jr.; MS&E

24-25 R.P. Gangloff; MS&E

26 G.J. Shiflet; MS&E

27 G.E. Stoner; MS&E

28 J.A. Wert; MS&E

29 J.R. Scully; MS&E

30 R.G. Kelly; MS&E

31 Mr. Brian McPherson
Code ED 24
Marshall Space Flight Center
Huntsville, AL 35812

32 Dr. William E. Quist
Boeing Aerospace and Electronics
Aerospace Group
Mail Stop GH-CJ
P.O. Box 3707
Seattle, WA 98124

33 Dr. Howard G. Nelson
NASA-Ames Research Center
EEM: 213-3

34 Dr. R.G. Forman
Mail Code ES-5
NASA-L.B. Johnson Space Flight Center
Houston, TX 77058

35 Professor A.K. Noor
Center for Computational Structures Technology
NASA Langley Research Center
Hampton, VA 23681-0001

36 Professor A.K. Ghosh
Department of Materials Science & Engineering
University of Michigan
2102 Dow Building
Ann Arbor, MI 48109-2136

37 Dr. D. Ferton
Pechiney Centre de Recherches
De Voreppe
B.P. 27 -- 38340 Voreppe
FRANCE

38 Dr. John Papazian
Grumman Aerospace & Electronics
Mail Stop A02-026
Bethpage, NY 11714-3582

39 Dr. Richard Lederick
McDonnel Douglas Aircraft Company
Mail Stop 111-1041
P.O. Box 516
St. Louis, MO 36166

40 Dr. Alan Hopkins
Senior Research Metallurgist
The University of Dayton, Research Institute
300 College Park
Dayton, H 45469-0172

41 Dr. Frances Hurwitz
Ceramic Composites
NASA Lewis Research Cneter
21000 Brookpark Road
Cleveland, OH 44135

42 Dr. Malcolm Ozelton
Manager, Metallic & Ceramic Materials
Northrop Corporation, B-2 Division
8900 E. Washington Boulevard
T241/GK
Pico Rivera, CA 90660-3737

43 Dr. S. Sampath
Technical Center
Federal Aviation Administration
Atlantic City International Airport, NJ 08405

44 Dr. James Staley
Alcoa Laboratories
Alcoa Center, PA 15069

45 Dr. Jeffrey Waldman
Code 6063
Naval Air Development Center
Warminster, PA 18974

46 M. Rodeffer, Clark Hall

47 SEAS Preaward Research Administration

** SEAS Postaward Research Administration

Updated: February, 1997

* One reproducible copy
** cover letter